CHARACTERIZATION OF MICROBES COLONIZING YELLOWING DISEASED COCONUT PLANTS GROWING AT THE KENYAN COAST

FATMA MOHAMED OMAR

MASTER OF SCIENCE

(Biotechnology)

JOMO KENYATTA UNIVERSITY

OF

AGRICULTURE AND TECHNOLOGY

2024

Characterization of Microbes Colonizing Yellowing Diseased Coconut Plants Growing at the Kenyan Coast

Fatma Mohamed Omar

A Thesis Submitted in Partial Fulfillment of the Requirements for the Degree of Master of Science in Biotechnology of the Jomo Kenyatta University of Agriculture and Technology

2024

DECLARATION

This thesis is my original work and has not been presented for a degree in any other university

Signature……Date…….

Fatma Mohamed Omar

This thesis has been submitted for examination with our approval as the University Supervisors

Signature……Date…….

Dr Johnstone Neondo, PhD

JKUAT, Kenya

Signature……Date…….

Dr Cecilia Mweu, PhD

JKUAT, Kenya

DEDICATION

I would like to dedicate this thesis to my beloved parents, Mohamed Omar Matano and Zuweina Ambasa Andalo. They not only raised and nurtured me, but also made many sacrifices over the years to ensure my education and intellectual development. It is hard to put into words how grateful I am to them. Despite the challenges of our cultural society, they persevered and encouraged me to believe in myself and have faith in Allah. I am so proud to call them dad and mom. I extend my dedication to my younger siblings, Omar and Yasmin, whose unwavering love and encouragement have been a driving force behind my academic pursuit. Their mere presence fills me with profound joy and a sense of purpose, making this thesis a heartfelt tribute to our inseparable bond and collective aspirations.

ACKNOWLEDGEMENT

Firstly, I express my gratitude to Allah for giving me life and guiding me throughout this journey. I would also like to extend my appreciation to the administration of Jomo Kenyatta University of Agriculture and Technology for providing me with the opportunity to pursue my master's degree at the Institute of Biotechnology Research (IBR) throughout this period. I am incredibly grateful to Africa-AI-Japan for providing generous financial support for my research, and I also want to express my gratitude to my father once again, Mohamed Omar Matano, for funding my MSc studies.

I am immensely grateful for the invaluable assistance, support, and patience of my supervisors, Dr. Johnstone Neondo and Dr. Cecilia Mweu, throughout the completion of this thesis and MSc studies. Their exceptional academic expertise and unwavering dedication have played a pivotal role in every aspect of my research journey, from coursework completion to proposal preparation, securing research funds, refining my research work, writing my research paper, and compiling the final thesis document. Their guidance and support have been instrumental in my success, and I owe them a heartfelt gratitude for their contributions to my academic achievement.

Finally, I would like to express my appreciation to the technicians at the Institute for Biotechnology Research, Mr. Barasa and Catherine, for their graceful assistance during my laboratory experiments. I would also like to thank my friends; Bryan Aburchery and Bryson Kimemia, for their guidance, corrections, encouragement, and assistance in analyzing my data.

TABLE OF CONTENTS

LIST OF TABLES

LIST OF FIGURES

LIST OF PLATES

LIST OF APPENDICES

ACRONYMS AND ABBREVIATIONS

ASVs	Amplicon Sequence Variants
CASAVA	Consensus Assessment of Sequence And Variation
CLYD	Coconut Lethal Yellowing Disease
CTAB	Cetyl Trimethyl Ammonium Bromide
CYD	Coconut Yellowing Disease
DADA 2	Divisive Amplicon Denoising Algorithm 2
DNA	Deoxyribonucleic acid
EAT	East African Tall
GDP	Gross Domestic Product
HVRs	Hypervariable Regions
H_2O	Water
IPDM	Integrated Pest and Disease Management
KCDA	Kenya Coconut Development Authority
LAMP	Loop-Mediated isothermal Amplification
LYD	Lethal Yellowing Disease
LY/LD	Lethal Yellowing/Lethal Disease
MG-RAST	Metagenome Rapid Annotation using Subsystem Technology

MR	Methyl Red
NA	Nutrient Agar
NCBI	National Center for Biotechnology Information
NGS	Next-Generation Sequencing
OTUs	Operational Taxonomic Units
PERMANOVA	Permutational Multivariate Analysis of Variance
PCoA	Principal Coordinates Analysis
PCR	Polymerase Chain Reaction
PDA	Potato Dextrose Agar
PGM	Personal Genome Machine
QIIME 2	Quantitative Insights Into Microbial Ecology 2
RBA	Rose Bengal Agar
RDP	Ribosomal Database Project
RNA	Ribonucleic Acid
rRNA	Ribosomal Ribonucleic Acid
SPRI	Solid Phase Reverse Immobilization
TSI	Triple Sugar Iron
UNITE	User-friendly Nordic ITS Ectomycorrhiza

ABSTRACT

Coconut is a highly versatile plant with multiple uses for its different parts. Despite its economic importance, there is inadequate scientific documentation of diseases affecting coconuts along the Kenyan coast. This cross-sectional study aimed at identifying microbes occurring in coconut plants with symptoms of yellowing diseases growing along the Kenyan coast, specifically in Kwale, Kilifi, and Lamu counties. A survey study was conducted and out of 1,080 coconut plants surveyed, 162 had symptoms of yellowing disease. This data was used to compute disease prevalence and severity scores. Fifty-four diseased samples were collected using the purposive sampling technique while nine samples were collected from health coconuts making a total of sixty-three samples collected for microbial isolation, morphological and biochemical assays as well as genetic profiling experiments. Total genomic DNA was extracted from leaf samples using CTAB and profiling of the genetic structure of microbial communities using amplicons of 16S rRNA sequences (V4 region) with Illumina MiSeq. The sequence data was analyzed using the QIIME 2 pipeline, and machine learning for prediction of the presence of differential OTU using Random Forest classifier. Nested-PCR using the P1/P7 primers for the first reaction and Phyto3F/R for the second reaction was used to confirm the absence of phytoplasma strains in the samples. From the surveyed areas, the highest disease prevalence and severity were recorded in Kilifi with 16.67% and 72.22%, while the lowest were recorded in Lamu with 13.61% and 59.26%, respectively. Heatmaps were generated utilizing nine morphological descriptors for bacteria and ten morphological descriptors for fungi to discern relationships among the isolates and compare them to presumptive positive controls. The samples yielded a total of 172 bacterial isolates, with the majority being translucent (63.74%), gram-positive (83.63%), and rod-shaped (79.53%), resembling the genera *Erwinia* and *Pseudomonas*. For fungi, 109 isolates were obtained, most of which were grey or black in colour (45.37%), while 76.85% were fluffy, most of the characteristics belonging to the Phylum Ascomycota. A total of 113,330 reads were obtained with sequence clustering, yielding 285 OTUs for bacteria. The most abundant phylum was Actinobacteria (84.87%), while *Streptomyces* was the most prevalent genus (61.24%). The most defining microbial taxon in Kilifi was *Streptomyces*, while in Kwale it was *Agrobacterium* and *Actinocatenispora*, with Lamu having no distinct microbial taxon. Fungi were clustered into 28 OTUs with 1,806 reads. Ascomycota was the dominant phylum (98.56%), while *Cyphellophora* and *Devriesia* were the most prevalent genera at 22.42% and 21.93% respectively. The findings indicate that microbial diversity was higher in Kilifi and Kwale counties as compared to Lamu, which registered the lowest diversity. For both bacteria and fungi, healthy control samples exhibited low diversity with minimal microbial concentration. The results provide a comprehensive understanding of the prevalence, severity, and microbial communities present in yellowing, diseased coconut plants. This will help with future elucidation of the agents exacerbating coconut disease symptoms as well as in the adoption of research findings by stakeholders like KCDA to tackle the challenges encountered by coconut plants, thereby promoting the improvement and conservation of coconut germplasm.

CHAPTER ONE

INTRODUCTION

1.1 Background Information

The Coconut palm tree (*Cocos nucifera* L.) is one of the highly essential perennial crops growing in equatorial and tropical countries (Bila et al., 2015; Pham, 2016). It primarily grows in Kenya's coastal regions because its seeds are often dispersed by ocean currents, hence widely scattered along the tropical coasts (Harries & Clement, 2014). In addition to being grown for food, the plant is also sold commercially in Kenya and other parts of the world (Prades et al., 2016). Since the prehistoric periods, mankind has utilized almost all parts of the coconut palm for a variety of purposes (Venugopal et al., 2017). This broad use has been quite influential in shaping the genetic and phenotypic diversity of the plant (Rasam et al., 2016).

Coconut-based imports into Kenya have been rising over time and now account for sizable amounts. From 3,069.11 tons valued at KES 689.21 million in 2018 to 3,721 tons valued at KES 732.89 million realized in 2019 (Afa-nocd, 2020). This indicates a low level of domestic production and a heavy dependence on foreign sources for these products. Due to the importation, a huge variety of completed coconut-based items are now offered in retail establishments, sparking competition between locally created goods and imports (Afa-nocd, 2020).

Coconut cultivation faces a strong phytopathological constraint as more than 50 diseases, some of which are highly destructive and fast spreading, and this poses a big threat to coconut farming despite the palm's hardy and adaptable nature to varied climatic conditions. (Ramjegathesh et al., 2012; Snehalatharani et al., 2016). The major diseases affecting the palm tree are; lethal yellowing disease, root wilt disease, basal stem rot, bud rot, leaf blight, hartrot, stem bleeding, and leaf rot (Michel et al., 2012). Identification of these diseases is solely based on phenotypic symptoms and this is challenging since they

exhibit similar morphological symptoms despite having different causative agents (Bailey & Meinhardt, 2016).

One of the most damaging diseases caused by *Candidatus phytoplasma*, a parasitic, phloem-restricted, and wall-less prokaryote, is Coconut Lethal Yellowing Disease (CLYD) (Danyo, 2011; Eziashi & Omamor, 2010). Common symptoms of coconut palm yellowing include browning and yellowing of the leaves, early nut loss, darkening of the inflorescence, and ultimately death within 4-6 months of the onset of the first symptoms (Eziashi & Omamor, 2010). The Lethal yellowing disease is a major hinderance to coconut farming in many parts of the world such as Mozambique, East Africa, West Africa and the Caribbean (Mazivele et al., 2018). The greatest effects of the disease have been felt by small scale subsistence farmers that rely on the crop for food and as a source of income. The rest of the coconut industry has also been affected by the disease but there have been little focus and resources devoted into research of the disease (Top & Huanglongbing, 2014).

In addition to pathogens, coconut palms are susceptible to insect pests that attack the terminal bud, fronds, stem, roots, inflorescences, and fruits as well as parasitic fungi such as *Phytophthora katsurae* and *Phytophthora palmivora* that cause rotting of the terminal bud and unripe nuts (Michel et al., 2012). Due to its single meristematic zone, these diseases cause the palm tree to succumb easily once afflicted. An outbreak of coconut necrosis disease along the Indian Ocean coast, which has already wiped out the coconut industry in Mozambique, has created a high alert in Kenya (Gurr et al., 2016). To mitigate the impact, the Kenya Plant and Health Inspectorate Service (KEPHIS) has initiated disease monitoring based on morphological signs along the Kenyan coast (Heya, 2022). However, the genetic erosion of coconut in Kenya remains unchecked due to land fragmentation for industrial or urban expansion in the traditional coconut growing areas and natural calamities like droughts and diseases (Alpex Consulting Africa Ltd, 2013).

Transboundary plant pathogens, including those affecting coconuts, have far-reaching economic implications and can impact global food security because they are difficult to

quickly and effectively detect and prevent, especially if they cause outbreaks of new and invasive plant diseases (Piombo et al., 2021). Pathogens that affect crops before and after harvest contribute to significant losses in potential productivity, affecting food security, quality, and safety as well as the entire food supply chain, either directly or indirectly (Piombo et al., 2021).

Plants harbor complex microbial communities where some are pathogenic and cause diseases while others are not (Dong et al., 2019). The diversity of phyllospheric microbes can be fully analyzed from various types of plant hosts, including agronomic crops, prairie plants, and naturally growing trees (Dong et al., 2019). There has been a lot of research over the past few decades that has been devoted to understanding the microbes connected to plants, though it is still difficult to evaluate the composition, behaviors, and functions of microorganisms that are connected to plants (Azaroual et al., 2022). Therefore, microbial diversity research is vital in determining the microbial flora that exists in plants in their natural environment (Zaynab et al., 2019).

1.2 Statement of the Problem

These diseases with yellowing symptoms have caused substantial losses of coconut palm trees and have threatened global coconut production, especially due to their invisible incubation period (Gurr et al., 2016). The economic consequences of yellowing, diseased coconut palms in Kenya highlight the potential risks to coconut production in African countries. Copra, the dried meat or kernel of the coconut, and its oil are the principal products of the coconut palm. Historically, the quality of copra produced in the coastal region has been poor. Despite the significant potential to produce up to 46,756 tons of copra annually, national production averages have fluctuated between 5,000 and 10,000 tons (Kadere, 2021). Additionally, a survey conducted in 2012 revealed that the average local production of coconuts per plant was only 27 nuts per year, which falls far below the recommended yield of 50-100 nuts per year as per Food and Agriculture Organization (FAO) (Funke et al., 1993). One contributing factor to this discrepancy is the prevalence of diseases affecting coconut plants, particularly yellowing disease. This disease severely

impacts the health and productivity of coconut palms, leading to lower quality and quantity of copra. Addressing yellowing disease is essential to improve copra quality and increase production to meet its full potential (Kadere, 2021).

Previous outbreaks of yellowing diseased coconut in countries like Ivory Coast destroyed over 350 hectares of coconut plantations and resulted in a loss of 12,000 tons of copra per year (Arocha-Rosete et al., 2014). Similarly, in Ghana, about 1 million coconut palms have been destroyed over the last 30 years due to the same disease (Arocha-Rosete et al., 2014). The lack of scientific documentation and quantitative data on diseases affecting coconuts on the Kenyan coast, especially coconut yellowing disease (CYD), presents a significant problem for coconut production in the region. Additionally, the prevalence and severity of yellowing diseased coconut palms have not been adequately studied or quantified (Afa-nocd, 2020). This lack of information hampers the evaluation of the disease's impact on coconut production and the development of effective disease management strategies. Without proper understanding and documentation of the microbes in CYD in Kenya, it is challenging to estimate the extent of yield losses and devise targeted interventions.

The few reports available of estimated yield losses from diseases in Kenya are limited to visual estimates and anecdotal reports, primarily focused on pests associated with the diseases. The low literacy levels among coconut farmers and their limited awareness of the effects of yellowing, diseased coconut palms further compound the challenges (Pole et al., 2014). Improved knowledge and awareness among farmers are crucial for the early detection and management of coconut diseases, which can significantly impact production.

1.3 Justification of the Study

Effective and rapid diagnosis is crucial in the mitigation of the negative economic impact of these diseases on coconut production (Gurr et al., 2016). There is need for reliable detection methods to identify risks to plant health. Although LYD has been studied for a

long time, high throughput sequencing has not been employed to define the microbial population linked to yellowing diseased coconut plants in Kenya. This study combined culture-dependent and culture-independent techniques to comprehensively characterize the microbial communities in yellowing diseased coconut palms as well as determine whether phytoplasma exist. The integration of standard microbiological procedures and Next Generation Sequencing (NGS) enhances accuracy and enables the detection of both culturable and unculturable microbes (Mushtaq et al., 2022). By characterizing these microbes colonizing CYD palms, knowledge gaps regarding coconut diseases are likely to be resolved with high precision with this scientific data that stands the test of time. This research also advances our understanding of microbial diversity and pathogenicity of coconut-associated microbes.

The study provides insights into epidemiology of CYD as well as plant-microbe interactions. This knowledge is essential for developing early detection methods and implementing targeted interventions to prevent wide spread of disease. Moreover, investigating the genetic diversity of the identified microbes pioneers valuable information for future breeding programs and the development of resistant coconut varieties. The outcomes of this research are significant for the KCDA and coconut farmers in developing effective disease management strategies, improving productivity, and ensuring the long-term sustainability of the coconut industry in Kenya.

1.4 Objectives of the Study

1.4.1 General Objective

To characterize microbes colonizing yellowing diseased coconut plants growing at the Kenyan coast.

1.4.2 Specific Objectives

1. To investigate the prevalence and severity of yellowing diseased symptomatic coconut plants at the Kenyan coast.

2. To identify culturable bacterial and fungal microbes from yellowing diseased symptomatic coconut plants.
3. To determine the genetic identity of microbial communities and phytoplasma in coconut plants with yellowing disease symptoms at the Kenyan coast.

1.5 Null Hypotheses

1. There is no observed prevalence or severity of yellowing disease symptoms in coconut plants at the Kenyan coast.
2. There are no cultural bacterial and fungal microbes from yellowing diseased symptomatic coconut plants.
3. No microbial communities or phytoplasma are present in coconut plants exhibiting yellowing disease symptoms at the Kenyan coast.

CHAPTER TWO

LITERATURE REVIEW

2.1 The Coconut Palm Tree

The coconut palm, scientifically identified as *Cocos nucifera* L., belongs to the Arecaceae family, commonly referred to as the Palmaceae family, specifically the Cocoideae subfamily (Verma et al., 2017; Zhou et al., 2020). The Cocoideae subfamily encompasses 27 genera and approximately 600 different species and is the only species of the genus *Cocos* that is still alive today (Zhou et al., 2020). This monoecious plant bears both male and female flowers on the same inflorescence. *Cocos nucifera* exhibits pinnate leaves that can reach a length of 4–6 m (13–20 ft.), with individual leaflets measuring 60–90 cm (2–3 ft.) in length (Zhou et al., 2022).

It is a highly versatile palm that is commonly known as the "Tree of Life" or "Tree of Abundance" since most if not all parts of the tree are utilized, hence it fulfills almost all requirements for a living (Al-Khayri et al., 2016; Wijerathna, 2015). Some products sourced from the palm include coconut oil, coconut milk, coconut cream, coconut chips, coconut jam and desiccated coconut, which comes from the dried endosperm (copra) (Nadun, 2023). Fibres from the mesocarp are widely to manufacture mats, rugs, and ropes. These products form a big part of the economic products of coconut-growing areas (Finyange et al., 2019). In addition to those, the stem can be used as a construction material for furniture and a fuel source. The roots are used in the production of dyes, while the inflorescence is widely used in making alcoholic drinks known as toddy (Finyange et al., 2019; Prades et al., 2016). Coco peat, which is an essential agricultural substrate, is also sourced from coconut. The used coconut shell can be processed into charcoal, activated carbon, and crafted into art. The leaves are used as roofing and brooms while the trunk is a source of wood (Alpex Consulting Africa Ltd, 2013).

In addition, the coconuts' high concentration of beneficial fats, vitamins, dietary fibre and minerals has drawn attention to their nutritional significance (Al-Khayri et al., 2016). The

coconut water in the young green coconuts is a popular thirst-quencher and natural electrolyte-rich beverage. White coconut meat is utilized in various culinary preparations, and coconut oil derived from the copra has gained recognition for its diverse applications in the food, cosmetics, and pharmaceutical industries (Prades et al., 2016).

The coconut palm is classified into three main varieties: Tall, Dwarf and Hybrid. The Hybrid variety comes from the cross-breeding of the dwarf and tall coconut kinds (Rajesh et al., 2013). However, each of these major types has many subvarieties. For instance, the tall variety has roughly 11 sub-varieties, each typically linked with a particular place in Africa (Alpex Consulting Africa Ltd, 2013). Tall varieties can attain heights of up to 100 feet, have a longer lifespan and yield larger fruits later in life. Under favourable conditions, tall palms can produce up to 75 fruits annually, showcasing greater variability. The tall varieties are the most often farmed palms in all of the regions of the world where coconuts are grown because they are resilient and thrive in various environmental circumstances (Rajesh et al., 2014). The dwarf varieties grow to around 30 ft. with a shorter lifespan. They are easier to harvest and exhibit the unique trait of producing small fruits at a young age, sometimes as early as two years. They feature a narrow trunk without a bole or bulging base, closely spaced leaf scars, and they produce a lot of fruits (Rajesh et al., 2014). The colour of their nuts is the primary indicator of dwarf status. They are assumed to have come from tall palms, maybe through inbreeding or mutation. Although less prevalent than the tall kind, dwarf coconuts are typically seen growing near people (Huang et al., 2013). Genetic diversity studies of coconut palms involve a variety of approaches, including morphological, physiological, agronomic, biochemical, and DNA analyses which have been conducted on coconut palms across different regions and islands (Al-Khayri et al., 2016; Pandey & Gupta, 2020).

There are three distinct coconut varieties grown in Kenya; the "East African tall", the "Pemba Dwarf", and a few hybrids (Karun & Niral, 2019). The following hybrids have been introduced to boost coconut yields and quality in Kenya. They include A72, a hybrid of Green Dwarf and West African Tall, and PB 121, a combination of Malayan Yellow

Dwarf and West African Tall. In particular, the hybrid "PB 121" has proven to be highly producing (Alpex Consulting Africa Ltd, 2013; Burns et al., 2020).

Coconut palms can thrive in sandy soil, survive saltwater exposure, and tolerate strong winds in tropical and coastal areas (Harries & Clement, 2014). Their extensive root systems enable the tree to be anchored and to reach subsurface water sources, ensuring its adaptability to many ecological situations. The extensive root system of coconut palms and the breakdown of their leaf litter also contribute to soil conservation, improving soil fertility and promoting the establishment of other plant species nearby (Bila et al., 2015). Additionally, coconut palms' thick foliage helps to shade and cool coastal areas, decreasing the effects of heatwaves and fostering a favorable microclimate for other plant and animal species (Rasam et al., 2016).

2.2 Status of Coconut Farming in Kenya

The coconut palm tree is predominantly cultivated on the Kenyan coast, between 20^0N and 20^0S latitudes. This region's suitable altitudes range from sea level to 1000m, allowing widespread cultivation (Maurice et al., 2015). Adopting various agricultural practices has allowed the plant to be grown in more regions across the country (Oyoo, 2021). Originally from the Indo-Malayan region, the coconut palm tree has been widely distributed across tropics (Gurr et al., 2016). Its introduction to Kenya dates back to the 16th century when the Portuguese brought it to the country (Kadere, 2021). Since then, it has become an integral part of the livelihood of coastal people, with more than 80% of farm households benefiting directly or indirectly (Pole et al., 2014). Coconut farming primarily involves male farmers, while female farmers are less involved, resulting in its perception as a crop associated with male gender roles (Afa-nocd, 2020).

Most coconut farmers in Kenya cultivate the trees on farm sizes ranging from 0.24 to 5 acres, although some opt for larger plots exceeding 15 acres (Pole et al., 2014). Most of the coconut trees (45%) fall within the 30-to-60-year age range, characterized by high nut and palm wine yields. The 5- to 29-year-old trees constitute about 35% of the population,

while those over 60 years have lower nut and palm wine yields (Afa-nocd, 2020). Inheritance from previous generations is the primary source of coconut trees for most farmers, with limited planting of new trees from seedlings (Pole et al., 2014).

A baseline survey conducted by the KCDA indicates a total coconut tree population of 9,907,115 in the country, with Kwale and Kilifi counties having the highest number of coconut palms (James & Josephine, 2022). While research on coconut palm varieties in Kenya is limited, only 16% of coconut trees are of the dwarf form, with the EAT type accounting for slightly more than 84% of the trees. Lamu and Mombasa show some differences between counties, with the two counties reporting higher percentages of these newer hybrid varieties (Alpex Consulting Africa Ltd, 2013). Coconut production in Kenya currently stands at a low average of 30 nuts per tree per year, attributed to various factors including, poor management practices, limited genetic diversity, aging trees, and the prevalence of pests and diseases (Pole et al., 2014). In Kenya, most farmers have reported incidences of pests such as the rhinoceros beetle and diseases like bud-rot to pose significant threats to coconut palms, causing extensive damage, stunted growth, and even death of the trees and nuts (Pole et al., 2014). Farmers even need more technical knowledge to mitigate these challenges, combined with the inadvertent creation of breeding sites by leaving coconut waste heaps unattended (Afa-nocd, 2020).

2.3 Lethal Yellowing and other Coconut Plant Diseases

Numerous pathogenic diseases affect coconut plants, including those brought on by bacteria, fungi, viruses, and phytoplasmas each exhibiting specific symptoms and damage to different parts of the coconut palm (Nampoothiri et al., 2019). These ailments can influence the regular growth of the coconut palm and development in various ways, by manifesting in roots, stem, leaves or inflorescences. Even though coconut palm is hardy and adaptable to varied climatic conditions, it is affected by more than 50 diseases (Ramjegathesh et al., 2012; Snehalatharani et al., 2016). These diseases have detrimental effects on coconut palms' ability to produce crops, leading to economic losses for farmers (Manimekalai et al., 2014). These diseases include lethal yellowing diseases, root wilt

disease, basal stem rot, bud rot, leaf blight, hartrot, stem bleeding, and leaf rot (Michel et al., 2012).

Lethal yellowing diseases are the most notable and diverse diseases affecting coconut palms (Adkins et al., 2020). They are brought on by phytoplasmas which are phloem-inhabiting bacteria with no cell wall. These pathogens are associated with class Mollicutes and transmitted by Hemiptera insects (planthoppers, leafhoppers or psyllids) (Ekhorutomwen et al., 2019). Due to their similarity, they were initially known as Mycoplasma-Like-Organisms but were later assigned the taxonomic name *'Candidatus phytoplasma*' (Gurr et al., 2016). This disease is characterized by darkening of the inflorescence, the leaves of palm tree turning yellow or brown, starting with the oldest and progressing to the youngest hence shedding of the leaves, loss of both ripe and unripe nuts, wilting, retarded growth and ultimately death of the palm trees that occurs within 4-6 months of the first symptoms (Gurr et al., 2016). However, similar symptoms are present in other diseases, making it difficult to precisely identify CYD symptoms (Aidoo et al., 2021). The characteristics and progression of the symptoms are affected by various factors, such as topography, host species, bacteria present or phytoplasma class (Adkins et al., 2020; Wei et al., 2021).

Globally, these diseases have led to significant reductions in coconut productivity, including the obliteration of Mozambican coconut farms (Bila et al., 2016). Other names for the disease LYD include Lethal Declines and LY Type Syndrome (Arocha-Rosete et al., 2014). Other phytoplasmal diseases that bring about LY include; coconut yellow decline, Weligama coconut leaf wilt, oil palm stunting disease, Hainan arecanut yellow leaf, and Al-wajam disease of date palm, have been reported worldwide, affecting various palm tree species (Nair et al., 2016).

Bacterial bud rot caused by *Erwinia spp.* infect the young leaves of coconut and oil palms. When the delicate buds in the middle of the cluster of leaves are broken by wind and rain, bud rot may spread to the young leaves leading to the death of the apical shoots and releasing a powerful odour (Michel et al., 2012). Similarly, bacterial soft rots are caused

by *Erwinia* plus other gram-negative bacteria, such as *Pectobacterium* and *Pseudomonas* being the most frequent culprits. A bacterial soft rot infection can affect a plant in a variety of ways. They infect the coconut plants through direct inoculation into wounds or naturally occurring openings (stomata or lenticels) in adult plants, which is the most common (Decoin et al., 2014). *Ralstonia solanacearum*, a fatal phytopathogenic bacteria, has also been identified in the tropics between Cancer and Capricorn as a cause of bacterial wilt in coconut (Blomme et al., 2017).

Phytophthora bud rot, another significant disease affecting coconut palms, has become a global concern due to its widespread occurrence and the high cost associated with its control. Similar to the LYD, this disease has reached epidemic levels worldwide (Nair et al., 2016). This disease is caused by *Phytophthora palmivora*; however, identifying this pathogen in palms affected by bud rot is challenging due to the rapid emergence of secondary invaders. Among these invaders, the fungus *Thielaviopsis paradoxa* is commonly observed, along with *Fusarium spp*, *Penicillium spp*, *Cylindrocladium spp*, and *Cephalosporium spp* (Michel et al., 2012). Basal stem rot, or wilt or root rot, is another severe coconut plant disease caused by a fungus belonging to the genus *Ganoderma*. The pathogen quickly attacks coconut palms aged 10 to 30 years (Kandan et al., 2010). Symptoms include yellowing, wilting, and drying of the fronds, as well as discolouration and decay of the lower stem and roots. This disease can lead to the collapse and death of the entire palm if left unmanaged (Snehalatharani et al., 2016).

Leaf blight disease is a common airborne infection that occurs predominantly during drought and is caused by *Bipolaris incurvata* (Manamgoda et al., 2014). It has a significant impact on the overall nut yield of coconut palms. In its initial stages, the disease manifests as yellowish-brown spots on the leaflet, gradually progressing to a greyish colour (Michel et al., 2012). As the disease advances, the affected leaves appear burnt, further compromising the health and vitality of the coconut palm (Singh et al., 2021). Stem bleeding disease is another ailment characterized by fluid draining down the trunk and reddish/dark brown patches on the trunk that eventually turn black (Da Costa e Carvalho et al., 2013). The disease is brought on by *Thielaviopsis paradoxa*, a plant-pathogenic

fungus that feeds on plant waste in the soil (Da Costa e Carvalho et al., 2013). It causes permanent harm, kills the tree, and affects neighbouring plants if neglected or undetected. Hartrot, another coconut disease, shares the same symptoms as LYD and is caused by *Phytomonas spp.,* also limited to the phloem (Dollet et al., 2014). The illness often affects fruitful coconut trees, and depending on the population of the disease's vectors, its spread is quick, leading to an almost complete eradication of the plantation (Dos Passos et al., 2019).

The coconut palm is also affected by viruses. The cadang-cadang disease, which affects numerous palm trees, including the coconut palm, is caused by coconut cadang-cadang viroid (CCCVd). It is a single-stranded, tiny, circular microorganism with no cell wall hence totally reliant on a host because they cannot proliferate independently (Michel et al., 2012). Over 30 million coconut palms have been killed since Cadang-cadang was discovered. Orange spotting is a defining characteristic of this illness, and CCCVd directly impacts copra production (Wu et al., 2013). Coconut palms succumb prematurely and die because of this disease. In the Philippines, the CCCVd is pervasive. Due to the unsanitary environment, CCCVd can spread mechanically, primarily through contaminated farm implements like harvesting scythes or machetes (Vadamalai et al., 2017).

2.4 Microbial Diversity of Bacteria and Fungi Associated with Yellowing Diseased Coconuts and Plant-Microbe Interactions

Understanding the microbial diversity of coconut plants is crucial for elucidating their interactions, roles in plant health, and disease development (Trivellone & Dietrich, 2021). In recent years, studies have focused on understanding the role of microbial communities in yellowing diseased coconuts (Nadia et al., 2017).

Previous studies have identified diverse bacterial and fungal species in yellowing diseased coconuts. Bacterial genera from *Bacillus, Burkholderia, Enterobacter, Cryptococcus, Trichoderma, Purpureocillium, Penicillium, Ralstonia, Pseudomonas* and *Streptomyces* are commonly known to be present in yellowing diseased coconut palms (Gurr et al., 2016;

Nadia et al., 2017). They have been isolated previously and are reported to be virulent to other plant species hence can pose a threat to palm trees through horizontal gene transfer (Jaskowska et al., 2015). For instance, *Streptomyces spp* can infect higher plants and cause diseases, including potato scab, while *Leifsonia spp* of the Microbacteriaceae family is known to cause ratoon stunting disease in sugarcane (Lewin et al., 2016). Additionally, beta-proteobacteria belonging to the *Burkholderia* genus causes yellowing in leguminous plants in Africa and South America (Villarreal, 2017). These bacteria flourish in coconuts because they use the organic compounds in the coconut oil produced from the copra as a carbon and energy source (Nadia et al., 2017).

In addition, some fungal moulds and yeast have also been reported to be present in yellowing diseased coconuts. Their genera include *Candida, Saccharomyces, Fusarium, Penicillium, Purpureocillium* and *Aspergillus* (Nadia et al., 2017). Coconuts affected by fungi tend to turn soft on the trunk with a yellow rot and turn dark as they mature. The trunk may also produce fluids of reddish-brown colour that stream down the trunk (Da Costa e Carvalho et al., 2013). The entry points for fungi in coconut palms are through wounds caused by insects and animal bites, mechanical damage and even environmental stress (Nair et al., 2016).

Understanding the interactions between coconut palms and their associated microbial communities is crucial for elucidating the disease mechanisms. Microorganisms associated with coconut plants can positively and negatively affect plant health. Beneficial microorganisms, such as plant growth-promoting bacteria and mycorrhizal fungi, enhance nutrient uptake, promote growth, and confer tolerance to biotic and abiotic stresses (Lee et al., 2021). Conversely, pathogenic microorganisms can cause significant damage to coconut palms, leading to reduced productivity and even plant mortality (Trivellone & Dietrich, 2021).

Some bacteria and fungi found in the ecosystem of palm may not be harmful but endophytic, whose titers are suppressed upon phytoplasma infection leading to competition (Ekhorutomwen et al., 2019). Plant defence response can be induced by

phytoplasmas leading to an increase in endophytic strains that adapt to the new niche (Nadia et al., 2017). Endophytes are organisms that form the normal microbiome within a plant without causing any harm to the plant. They enter the plant systems through active selection or passive diffusion from the rhizosphere (Le Cocq et al., 2017). They can also be introduced to plants by insects, after which they make their way through the vascular system to leaves, roots, tubers and stems (Hardoim et al., 2015). Endophytes develop a symbiotic relationship with the plant where in exchange for nutrients and physical protection, they secrete compounds and metabolites that promote plant growth or protect the plant from pests and pathogens (Golinska et al., 2015).

Some of the most common endophytes belong to the *Enterobacter, Bacillus* and *Pseudomonas* genera. These endophytes have been investigated as possible biocontrol agents in coconut palms (Nadia et al., 2017). Endophytes present in the rhizosphere are also important to plants and aid them through stimulation of root growth, breaking down organic material into fertilizers, reduction of stress in the root system, improving resistance to pests and pathogens as well as outcompeting detrimental microbial species (Compant et al., 2013). There is little research into the use of endophytic organisms in controlling LYD, with a few plants like apples and grapevines being tested (Nadia et al., 2017). Preliminary results indicate that the microbes in the rhizosphere could help reduce the rate of phytoplasma infection (Bulgari et al., 2011).

According to Gurr et al., (2016), highly diverse microbial communities associated with yellowing diseased coconut palms could also be influenced by abiotic factors such as soil type, climatic conditions, and geographical location. Therefore, pathogen invasion, environmental stress, and imbalanced plant-microbe interactions can all contribute to the development of yellowing diseases in coconut palms (Bertrand et al., 2015). Studies employing culture-dependent and culture-independent techniques have revealed the presence of these microbes in diseased plants, which are known to cause disease symptoms and impact the overall health and productivity of coconut palms (Kashyap et al., 2023). Furthermore, environmental stressors, such as drought, flooding, and temperature changes, can impact dynamics of microbial communities and their

interactions with coconut plants, potentially exacerbating disease development or affecting plant resilience (Hasnain et al., 2023).

2.5 Impact of Diseases on Coconut Palm Cultivation and Socioeconomic Factors

Coconut is essential in improving the quality of life and generating income for millions of rural farmers in tropical areas worldwide (Gurr et al., 2016). In 2016, coconut was cultivated by approximately 11 million farmers in 90 countries and territories, producing 61 million tons. The largest producers were Indonesia, the Philippines, and India (Aidoo et al., 2021). Despite its potential, coconut production in Africa remains low, with only 2 million tons produced in 2016 (Aidoo et al., 2021). For instance, the top producer of coconuts in Africa is Tanzania, with 134,068 ha (or 1% of the world's arable land) dedicated to the crop. The sustainability and profitability of the coconut industry are hampered by a number of factors, including poor farming practices, a limited genetic foundation, climate change, pests, and diseases. Diseases, however, remain a substantial barrier. The most severe threat to the coconut business, particularly in Sub-Saharan Africa, is the deadly yellowing disease of coconut (Aidoo et al., 2021).

The diseases affecting coconut not only cause direct losses by affecting the yield and quality of coconuts but also have broader implications for the coconut industry, including the livelihoods of farmers and the economy of coconut-producing regions (Khalfan, 2015). The coconut palm is considered one of the world’s major palms due to its popularity in various aspects, such as food and social customs (Gurr et al., 2016). In Kenya, this crop greatly contributes to the agricultural GDP (1.5%) and national GDP (0.4%) (Alpex Consulting Africa Ltd, 2013). It is regarded as a food and cash crop on the Kenyan coast. As a food crop, coconut provides food security owing to its continuous production of nuts throughout the year, consumed either at their tender stage (*madafu*) or when they are mature (Pole et al., 2014).

With diseases being the major constraint in coconut, LYD is a highly destructive ailment that affects coconut trees, and its presence in any region poses a significant threat to the

coconut industry (Aidoo et al., 2021). An infection of LYD before fruit production necessitates farmers to uproot and replant the coconut trees (Chowdappa et al., 2018). Consequently, a large-scale plant loss brings less income; hence more rural agriculturalists migrate to urban areas intensifying rural poverty (Gurr et al., 2016). Some developing countries benefit greatly both socially and economically from coconut production, creating significant economic upheaval upon any outbreak of disease, particularly LYD (Aidoo et al., 2021).

At the end of the 19th century, LYD was first found in the Caribbean. After that, Florida made follow-up reports, showing its widespread worldwide (Bertaccini, 2022). Over the past thirty years, it has been damaging coconut trees in numerous nations as they have expanded across Africa. This disease has been responsible for causing substantial economic losses, such as 85.54% of coconut trees in Jamaica between 1963 and 1983, 38% of coconut trees in Tanzania, and millions of coconut trees in Ghana, Nigeria, and Togo. An outbreak of LYD in Ivory Coast resulted in the loss of over 350 hectares of planted coconuts (Aidoo et al., 2021). The disease has killed millions of palms worldwide in recent decades, and its devastating effects have endangered the survival of the entire coconut industry (Naderali et al., 2017).

Research in other coastal regions of Tanzania, Mozambique, and Somalia has also reported the occurrence of yellowing diseases in coconut plantations. These highlight the widespread presence of yellowing disorders in East African coastal regions (Aidoo et al., 2021). Studies conducted in Kenya have barely shed light on the prevalence and severity of these diseases in the region, making it challenging to implement effective management strategies to combat yellowing diseases and ensure the sustainable growth of coconut production (Aidoo et al., 2021). The disease has been reported and confirmed in African countries such as Tanzania, Mozambique, Nigeria, Cameroon, Benin, Ghana, and Nigeria. In these countries, the most significant effects of the disease have been felt by small-scale subsistence farmers that rely on the crop for food and as a source of income (Gurr et al., 2016). As a result of widespread crop failure like coconut, and the associated loss of

revenue, more rural agriculturalists relocate to urban regions, thus escalating rural poverty (Gurr et al., 2016).

Factors including illness awareness and education levels of the small-scale subsistence farmers impact agriculture production, food security, and livelihood of farmers (Okereke & Iwezor, 2015). The majority of underprivileged farmers have limited understanding about yellowing diseased coconuts and the existence of preventative methods which cause significant crop losses. In developing countries, farmers often struggle to improve their crop production because they do not have enough knowledge or information on diseases (Mahyao et al., 2016). It is widely known that agricultural intervention would only be successful if the local population were well-informed on the primary disease issues and their effects. For agricultural extension, farmer-led innovation, and adoption of disseminated knowledge, farmer groups offer a particular access point to coconut rural farming communities (Brownhill et al., 2016).

2.6 The Spread of Coconut Yellowing Disease, Management and Control Methodologies

2.6.1 Outspread of the Disease

Several factors contribute to the outbreaks of yellowing diseases in coconut production. First and foremost, the vector responsible for transmitting the phytoplasma, often leafhoppers or planthoppers, plays a crucial role in disease spread (Gurr et al., 2016). Environmental factors including temperature, humidity, and rainfall patterns influence disease prevalence and severity. Additionally, coconut varieties and their genetic susceptibility to specific phytoplasmas can influence the susceptibility of coconut palms to yellowing diseases. Poor agronomic practices, such as inadequate fertilization and irrigation, can further exacerbate the vulnerability of coconut plantations to disease outbreaks. Aidoo et al., (2021) describes that climate change can directly or indirectly contribute to the distribution and abundance of plant pathogens by interfering with host resistance to pathogens and microbial interactions.

Human activities also play a significant role in the distribution of microbes across various regions (Burdon et al., 2006). For instance, in the 1980s, human-mediated movement of grass and species from Florida to Mexico led to the emergence of LYD in Mexico, which later expanded throughout the Central American region (Gurr et al., 2016). The soaring community of vectors and migratory behaviour at greater distances also contributes to high epidemic and dissemination rates (Top & Huanglongbing, 2014). The spread of CYD is primarily through insect vectors but can also be transmitted to embryos and seeds (Gurr et al., 2016). Outbreaks usually start with a few plants before spreading to nearby plants in a 100-meter range, then expanding to distances of up to 100 km. The infection and spread rates are influenced by seasonal changes and geographic hindrances that would impede the movement of vectors (Pacifico et al., 2015). There is a latency period after infection before symptoms appear, attributed to bacterial adaptation to the new plant.

2.6.2 Management and Control Strategies

Controlling and managing CYD is crucial for sustaining coconut palm cultivation, ensuring the industry's long-term viability and overcoming vast outspread (Tanno et al., 2018). Comprehensive disease management strategies may include the identification and utilization of disease-resistant coconut cultivars, implementation of strict quarantine measures to prevent disease introduction and spread, adoption of good agricultural practices to promote palm health and resilience, and timely detection and diagnosis of diseases for effective disease control (Nair et al., 2016).

Various techniques are being used to control and manage yellowing diseases in different parts of the world. The most common approach involves uprooting and eliminating diseased palms or transplanting them with resistant species to slow down the spread of diseases (Eziashi & Omamor, 2010). When coconut trees become infected with LYD, farmers are compelled to migrate or replant with other crops, as coconut palms don't begin to produce nuts for many years after being replanted (Arocha-Rosete et al., 2014). Quarantine protocols can also be implemented to prevent human-assisted disease transmission, where the plants infected with yellowing diseases are secluded from the rest

of the healthy ones (Gurr et al., 2016). Long-lasting insecticides are also viable for preventing infections by killing the insect vectors before they spread. The lingering effects of the insecticides can protect the palms through their long lifespans and productive years. However, using insecticides is faulty and can negatively affect the environment and human health, but this has not discouraged their use as control agents (Dusfour et al., 2019). Some countries, such as Jamaica, burn the felled palms making the plant lose turgidity, becoming unattractive to adult vectors making the plant less prone to infestation by insect vectors, leading to reduced infection (Bianco et al., 2019; Thomas et al., 2019).

Antibiotics like tetracycline have been used to control CYD infections in valuable ornamental palms, but they have been deemed inappropriate in many European countries due to agricultural practice bans (Dusfour et al., 2019; Gurr et al., 2016). While oils, extracts, native and artificial proteins, and organic fertilizers have been used in controlling yellowing infections in tobacco plants, they have not been tested in coconuts (Nadia et al., 2017). Moreover, as insect vectors transmit CYD, managing vector populations using IPDM has demonstrated the potential to limit disease spread (Dusfour et al., 2019). This approach encompasses integrating diverse management practices to effectively control vector populations and diseases, thereby reducing disease transmission (Bianco et al., 2019). It preserves a wholesome environment for the benefit of the following generation while ensuring that the incidence of pests and diseases is minimal. Adopting this practice enables ecosystem sustainability, which is crucial for agricultural economic production (Chowdappa et al., 2018).

Research efforts have also focused on breeding coconut varieties with enhanced resistance to specific phytoplasmas. Moreover, rapid and accurate diagnostic tools, such as PCR-based assays, have facilitated early detection and timely management of yellowing diseases. The lack of genotypes showing significant resistance to phytoplasma-mediated LYD in coconuts has hindered research efforts into effective disease control (Top & Huanglongbing, 2014). Thus, understanding existing pathogen diversity is crucial in developing more effective management strategies. Maintaining healthy plants is gaining more attention as a national priority, resulting in implementing these monitoring systems

to improve prevention and management strategies for plant diseases (Top & Huanglongbing, 2014). All in all, of all the strategies being utilized, yellowing diseases have not yet been managed effectively (Aidoo et al., 2021).

2.7 Diagnostic Techniques for Coconut Plant Diseases

Implementing efficient disease control techniques and ensuring sustainable coconut agriculture depends on promptly and accurately detecting illnesses affecting coconut plants (Bianco et al., 2019). In the past, diagnosing diseases relied on conventional diagnostic techniques, including symptomatology and visual inspection (Noble et al., 2022). These techniques were helpful but frequently lacked specificity and sensitivity, resulting in incorrect diagnoses and ineffective control measures. The diagnostic methods for diseases of coconut plants have changed dramatically as due to advances in science and technology (Nadia et al., 2017; Nair & Manimekalai, 2021). The various diagnostic techniques used for coconut plant diseases include traditional culture methods, PCR-based assays, DNA sequencing, and the latest advances in NGS technologies (Nair & Manimekalai, 2021). By understanding the strengths and limitations of these techniques, researchers and plant health professionals can make informed decisions to enhance disease surveillance, management, and ultimately, safeguard global coconut production (Sharma & Sharma, 2016).

2.7.1 Coconut Plant Microbial Identification - Culture-based Techniques

Culture methods have been widely used to isolate and identify the bacterial and fungal pathogens linked to coconut diseases. Robert Koch developed the first method for detecting microorganisms using the culture media method for microbial growth, traditionally employed for pathogen detection (Kim & Kim, 2021). He proposed that the cornerstone of all studies into infectious diseases is a pure culture (Lagier et al., 2015). Therefore, traditional microbiological investigations of plant microbiota involve isolating and cultivating single strains, followed by morphological and biochemical characterization (Coughlan et al., 2015).

The isolating procedures involve growing the microbes on agar-based media in petri dishes (Bodour et al., 2020). These microbes are cultured in vitro with conditions such as incubation time, nutrients, environment, and temperature usually considered to enable growth (Jufri, 2020). In the culturing of bacteria, the serial dilution method is used to lower the concentration of bacteria for analysis. It involves making a series of dilutions with decreasing concentrations, typically using precise ratios like 1:10 or 1:100. By plating the diluted samples on agar plates; scientists can determine the number of viable microorganisms by counting the resulting colonies (Thomas et al., 2015). This method accurately estimates bacterial cell counts in a sample and is crucial for microbial analysis and experimentation (Jufri, 2020). Solid media, predominantly nutrient agar and blood agar are commonly employed to isolate bacteria as pure cultures (Bonnet et al., 2020). These media types support the growth of a wide range of bacteria without requiring additional enrichment. The standard procedures used in solid media are spread plating and streaking methods (Aladdin, 2021). In spread plate, a glass, plastic, or steel spreader is used to apply the bacterial sample to an agar-gelled nutrient medium; the spreader is typically thought of as merely a tool to disseminate the inoculum over the agar surface (Thomas et al., 2015).

Conversely, the streaking method employs a sterile inoculating loop to spread a small mixed culture sample onto the agar plate surface in a pattern that thins out the bacteria (Thomas et al., 2015). On the other hand, culturing fungi involves using specific media such as PDA and RBA. PDA provides essential nutrients from potato extract and dextrose, promoting fungal development, while RBA is selective for fungi and inhibits bacterial growth. Moreover, adding antibiotics ensures the suppression of any potential bacterial contaminants, enabling the fungi to thrive undisturbed (Bhargava & Tandon, 2015).

Once pure cultures have been obtained, their colony and cell morphology is determined and observed under a microscope (Petersen & Mclaughlin, 2016). Biochemical and serological tests are also performed to help characterize the microbes. However, these techniques are limited in accurately identifying the pathogen, especially if it cannot be

cultured or observed under a light microscope. For example, viruses and phytoplasmas require an electron microscope for identification (Sharma & Sharma, 2016).

Although the culture-based detection approach is inexpensive and straightforward, only a small percentage of bacteria cells are identified, with many microorganisms still uncultivated (Bodour et al., 2020; Steen et al., 2019). Additionally, the traditional culture-based approach is labour-intensive, time-intensive and has low selectivity (Kim & Kim, 2021). Despite numerous attempts, establishing pure phytoplasma cultures in vitro has proven challenging due to their unique characteristics. As bacteria without cell walls, phytoplasmas cannot survive independently and must inhabit a host organism to thrive (Wei et al., 2021). Numerous other detection techniques have been reported in these regards. Recent research on PCR, isothermal amplification and sequencing are examples of this. While culture methods may still be useful and relevant in some circumstances, their use in high-throughput diagnostics may be constrained by their time and labour requirements (Bodour et al., 2020).

2.7.2 Coconut Plant Microbial Identification - Culture-independent Techniques

Information obtained from traditional culturing methods only provides about 0.1 to 10% of the overall estimated microbial population in a particular sample (Coughlan et al., 2015; Lennon et al., 2018). Molecular techniques being culture-independent, present a powerful tool to study the diversity of both culturable and unculturable microbes by analyzing their DNA and better characterizing the microbial flora of plants. Various molecular techniques are currently being used to rapidly detect plant pathogens and vectors, forming an integral part of plant pathology research (Buja et al., 2021).

2.7.2.1 Polymerase Chain Reaction (PCR) Technology

This technology has revolutionized the field of plant pathology in diagnosing various plant pathogens. It has proven to be the gold standard procedure for molecular detection of bacterial and fungal infections (Delic, 2012). The technique has gained much traction in the previous decades due to its high reliability and sensitivity compared to DNA hybridization and serological assays (Sharma & Sharma, 2016). PCR-based diagnostic techniques primarily focus on specific DNA regions, such as ribosomal DNA (rDNA), found in all organisms with a high copy number. The inter-transcribed spacers (ITS) region is also utilized to create DNA barcodes for identifying fungal species (Nair & Manimekalai, 2021). PCR targets the DNA sequence of interest by flanking forward and reverse primers that allow for its amplification. The primers are usually synthetically designed in silico from various databases and are complementary to the DNA sequences of the microbe to be detected (Warokka et al., 2020). Therefore, this leads to multiple copies of the DNA strands observed using electrophoresis in an agarose gel stained with ethidium bromide. The detection of a particular DNA band of the anticipated size confirms the presence of the target pathogen in the sample (Nair & Manimekalai, 2021). Phytoplasma sequences are analyzed using the 16S rRNA sequences and comparing the *Candidatus phytoplasma* sequence, where a new species is classified when the sequences have less than 97.5% of a similarity score (Abeysinghe et al., 2016).

To improve the sensitivity of PCR, various methods have been developed, such as nested PCR. Nested PCR is a two-step, sequential PCR process in which the first round's PCR results are amplified again using more specific primers (Nair & Manimekalai, 2021). The initial primer pair may have amplified from non-target regions when creating PCR products. A second PCR uses the first PCR's results as a template (Sharma & Sharma, 2016). Amplification of the 16S rDNA using phytoplasma-specific universal and group-specific primers is more reliable than conventional PCR. The universal primer pair for phytoplasma are P1/P6, P1/P7 and F2n/R2 that can detect at least 28 types of phytoplasma, targets a conserved gene and nested PCR may be required due to the low concentration of phytoplasma in the phloem of woody plants like coconuts (Mazivele et al., 2018). Strain-

specific primers such as LY-F/LY-R for the Caribbean LYD, Phyto14F/R and Phyto3F/R specific for CLYD as well as RhodeF/R for the Tanzanian LYD exist, but their sequences must be optimized to changes in other strains in order to work (Ekhorutomwen et al., 2019).

Quantitative polymerase chain reaction (qPCR), also known as real-time PCR, is a diagnostic assay for detecting phytoplasma and other microbes, enhancing accuracy and dependability (Nair & Manimekalai, 2021). As its name suggests, it enables us to keep track of the PCR reaction's development in real time. The method enables the simultaneous measurement of the target DNA in a sample (Nair & Manimekalai, 2021). Additionally, Trivellone et al., (2021) discovered six previously unidentified phytoplasma strains by screening 227 leafhopper specimens from various natural environments worldwide using qPCR.

With multiplex PCR, different DNA targets can be simultaneously and sensitively detected in a single reaction, cutting down on time and expense without compromising the usefulness of the experiment (Sharma & Sharma, 2016). It is helpful in plant pathology because several microorganisms frequently infect a single host, necessitating sensitive detection and lowering the number of tests necessary. Multiple target sequences are amplified in a single PCR experiment and recognized based on the sizes of the molecules on agarose gels, but care must be taken to optimize the conditions so that the corresponding amplicons may be produced successfully (Ekhorutomwen et al., 2019). Because numerous phytoplasma strains cause yellowing diseases in coconut, this method makes it simple to detect in a single trial.

2.7.2.2 Loop-mediated Isothermal Amplification (LAMP) Assay and DNA Sequencing

LAMP is another diagnostic technique gaining favour over conventional PCR especially in impoverished regions (Sharma & Sharma, 2016). It is a DNA amplification method that amplifies DNA under isothermal conditions with great specificity, efficiency, and speed

taking approximately an hour or less (Nair et al., 2016). Based on primers targeting the small subunit rRNA gene, the LAMP assay has been used to precisely identify *Ganoderma lucidum* linked with the basal stem rot disease of coconut (Siddiqui et al., 2021). Of all the amplification techniques, nested PCR is the most sensitive phytoplasma detection technique (Nair et al., 2016).

DNA sequencing, conversely, has brought about a revolutionary shift in microbial ecology, particularly in phylogenetic studies. It has been used to detect phytoplasma and revealed that the diversity of prokaryotes was previously underestimated using cultivation-based techniques hence becoming more and more significant in identifying species. (Gilbert & Dupont, 2011; Rajendhran & Gunasekaran, 2011; Sharma & Sharma, 2016). Furthermore, metagenomic projects in the past used Sanger sequencing to sequence the entire 16S rRNA gene, but it was a time-consuming, expensive and limited method that didn't allow for a deep understanding of the microbial diversity in a complex environment (Gürsoy & Can, 2020). With the era of modern DNA sequencing, the successful completion of the first draft of the human genome led to further innovation and development of advanced high-throughput DNA sequencing strategies (Nikolaki & Tsiamis, 2013). These strategies are collectively known as next-generation sequencing (NGS). Metagenomic projects have been combined with NGS technologies, significantly boosting microbial ecology in recent years. For the last decade, NGS has been a vital tool in plant pathogen detection, especially for causal agents of plant diseases like bacteria, fungi, viruses and phytoplasmas (Gedil et al., 2016). These technologies provide a much higher throughput than traditional Sanger sequencing, making them a hot topic in biological sciences (Goodwin et al., 2016). Metagenomics and high-throughput sequencing have allowed scientists to explore the life of still uncultured microorganisms and discover new genes and genome sequences, especially for low to medium-complex ecosystems (Rajendhran & Gunasekaran, 2011).

2.8 Advancements in NGS Technologies in Coconut Plant Microbiomes

Advancements in NGS technologies have made it possible to extensively study the microbial population. A huge number of recent research using NGS technologies have uncovered more microorganisms and taxa than were previously unknown (Fukuda et al., 2016). NGS allows for high-throughput, cost-effective, and rapid sequencing of DNA and RNA, providing valuable insights into the complex microbial communities associated with coconut plants (Arumugam & Hatta, 2022). It is a powerful sequencing technology that can comprehensively view an entire genome or specific regions of interest. It can simultaneously confirm multiple DNA sequences and identify genetic variations, mutations, or pathogens in a sample (Hu et al., 2021). NGS is particularly useful for identifying unknown or novel DNA sequences, providing a deeper understanding of genetic composition and diversity (Buermans & Dunnen, 2014). With NGS, researchers can comprehensively analyze microbial communities, providing in-depth information on the overall microbial population within a sample (Gupta et al., 2014).

2.8.1 Illumina Sequencing

Illumina sequencing, also known as Solexa sequencing, is one of the most widely used NGS platforms due to its reliability, accuracy, and versatility (Serrano Cardona & Muñoz Mata, 2013). It uses a method called sequencing by synthesis, which involves capturing individual DNA molecules onto a solid glass surface and amplifying them into clusters using bridge PCR (Illumina Inc, 2013). These clusters are then sequenced using dye-labelled terminators, where only one nucleotide is incorporated in each step, allowing for high-accuracy sequencing (Slatko et al., 2018). Illumina sequencing has much higher throughput and accuracy than other NGS technologies like 454 sequencing, with less than 1% error rates, but sacrifices longer read lengths for this increased capacity (Nikolaki & Tsiamis, 2013). Illumina sequencing has detected both culturable and non-culturable organisms while providing details on the plant microbiome (Lewis et al., 2020; Piombo et al., 2021).

Illumina offers several variants of its sequencing platforms, each tailored to different research needs. The MiSeq platform stands out for its adaptability and widespread use in diverse research areas, including metagenomics studies (Azaroual et al., 2022; D'Amore et al., 2016). Its compact benchtop design makes it suitable for small-scale projects and targeted sequencing applications. Researchers often employ the MiSeq for amplicon sequencing, targeted gene panels, and small RNA sequencing. The MiSeq system offers various read lengths, ranging from 2x36 bp to 2x300 bp, allowing flexibility in the sequencing depth and data output. For example, with 2x300 bp reads, the MiSeq can perform up to 25 million reads per run, resulting in approximately 15 Gb of data output (Stoler & Nekrutenko, 2021). The versatility and cost-effectiveness of the MiSeq platform make it a popular choice for researchers studying coconut plant microbiomes.

In contrast, the HiSeq platform is designed for high-throughput sequencing and is ideal for large-scale projects, such as whole-genome sequencing, transcriptomics, and epigenomics. It can produce up to 600 Gb of data per run, with a maximum of 3 billion reads and read lengths of up to 2x150 bp (Stoler & Nekrutenko, 2021). The HiSeq is suitable for projects requiring substantial sequencing depth and comprehensive genome coverage. Illumina offers the NovaSeq platform for ultra-high throughput applications, capable of generating up to 6 Tb of data per run. The NovaSeq is commonly used for large-scale population studies, whole-genome sequencing, and metagenomics research. It can produce up to 6 billion reads with read lengths of up to 2x150 bp, making it an ideal choice for extensive sequencing studies (Slatko et al., 2018; Stoler & Nekrutenko, 2021). The NextSeq platform provides a balance between flexibility and throughput. It is suitable for various applications, including gene expression analysis and single-cell sequencing. With 400 million reads at a length of 2x150 bp, the NextSeq can deliver up to 120 Gb of data per run, making it a versatile option for researchers with diverse sequencing needs (Stoler & Nekrutenko, 2021). Lastly, the iSeq platform is a compact and budget-friendly sequencer for targeted sequencing, small RNA, and microbial genomics. It can produce a maximum of 8 million reads, with up to 1.8 Gb of data and read lengths of up to 2x150

bp. The iSeq is suitable for smaller-scale projects, especially those with limited resources (Slatko et al., 2018).

This diverse range of Illumina platforms, including the MiSeq variant, has revolutionized the study of coconut plant microbiomes and pathogen detection. The MiSeq's adaptability and reliability have made it a favoured choice for researchers studying microbiomes in different plants. In samples from fruit trees and grapevines, the Illumina MiSeq platform was used to detect viruses, viroids, and phytoplasmas. The technology made it possible to simultaneously detect several pathogens from a single sample and low-titre tissue infections (Nair & Manimekalai, 2021). According to Chalupowicz et al., (2019), applying this technique is useful to distinguish plants that were infected with *Candidatus phytoplasma* from *Catharanthus roseus*. As NGS technologies evolve, researchers can expect even more efficient and cost-effective methods to deepen our understanding of coconut plant health, plant pathogens detection, disease resistance, and ecological dynamics. These advancements hold promise for developing sustainable coconut farming practices and improved agricultural outcomes and global food security.

2.8.2 16S rRNA Gene Targeting

Amplicon sequencing methods targeting the 16S rRNA gene are widely used for microbiome analysis with NGS platforms (D'Amore et al., 2016). This gene has been the focus of most investigations of microbial communities in environments ranging from plants and soil to the human gut (Poretsky et al., 2014). The 16S rRNA gene is a universal marker for bacteria and archaebacteria, containing conserved and hypervariable regions that enable taxonomical classification and differentiation (Fukuda et al., 2016). Therefore, the focus shifted to sequencing short HVRs of the 16S rRNA gene at greater depth instead of sequencing the whole gene (Mizrahi-Man et al., 2013). Metabarcoding using 16S rRNA marker is therefore used for studying complex microbial communities, making it a reliable tool for detailed microbial classification through phylogenetic analysis (Nikolaki & Tsiamis, 2013). This gene is commonly used to classify and identify microbes as it is present in most types and displays reliable variations. 16S rRNA is a useful genetic marker

due to the presence of nine HVRs (V1-V9). Also, the number of gene sequences registered in public databases is significantly rising, providing crucial information on identifying and classifying bacterial taxonomic investigations (Fukuda et al., 2016). These regions are surrounded by conserved regions that allow universal primers to amplify the target sequences (Miranda et al., 2020). In microbial diversity studies, the V3 and V4 HVRs of the 16S rRNA gene are predominantly sequenced and analyzed using Illumina platforms (Jeong et al., 2021; Santos et al., 2020). Additionally, multiple primer combinations have been developed to amplify the HVRs and generate amplicons of variable lengths suitable for sequencing with different NGS platforms. The Illumina MiSeq approach is suitable since the lengths of HVRs of the 16S rRNA gene are usually 100-300 bp, readily covered using short paired-end reads produced by common NGS technologies (Zhang et al., 2014).

Although analyzing the highly HVRs of the 16S gene is an effective technique for studying bacterial taxonomy, it struggles to distinguish between closely related species (Větrovský & Baldrian, 2013). For instance, certain species within families like Enterobacteriaceae, Clostridiaceae, and Peptostreptococcaceae can share up to 99% sequence similarity across the entire 16S gene (Jovel et al., 2016). Therefore, V4 sequences may differ by only a few nucleotides, resulting in reference databases being unable to accurately classify these bacteria at lower taxonomic levels (Jovel et al., 2016). This limited analysis of select HVRs may also cause these studies to miss differences between closely related taxa, resulting in them being grouped into a single taxonomic unit and underestimating the total diversity of the sample (Větrovský & Baldrian, 2013). Other possible reasons could be DNA extraction process and its efficiency or biases brought about by PCR. Although this method may not be the most precise way to classify bacterial species, analyzing the HVRs remains one of the most beneficial tools for bacterial community studies (Větrovský & Baldrian, 2013). Furthermore, assessing biodiversity to the species level is possible if there is an increased read size, such as amplifying a longer stretch of the 16S rRNA gene (Degois et al., 2017).

While the traditional approach is still necessary for isolating specific strains, NGS molecular techniques have gained widespread use for profiling microbial communities and their dynamics in different plants and plant compartments (Fadiji & Babalola, 2020).

2.9 Taxonomic Classification of 16S rRNA Gene Sequences for Diversity Studies

Classifying DNA sequences taxonomically is a crucial step in comprehending the dynamics of microbial communities as well as how organisms may affect or be affected by their host or environment (Poretsky et al., 2014). Numerous 16S rRNA gene-specific taxonomic categorization pipelines, including MOTHUR, QIIME 2, DADA 2 and MG-RAST, have been devised (Bolyen et al., 2019; Callahan et al., 2016; Miranda et al., 2020). At a threshold of 97% sequence similarity, sequences are grouped into OTUs. As an alternative to OTUs, ASVs or zero-radius OTUs (zOTUs) have been proposed. Sequences are grouped using OTU clustering based on similarity, striking a balance between computational efficiency and resolution, particularly useful when sequences are variable and one aims to capture all reads. In contrast, ASV clustering differentiates unique sequences to offer finer resolution but often excludes low-abundance or rare reads (Brandt et al., 2021; Santos et al., 2020). For taxonomy assignment, sequences with the fewest mismatches to other sequences in a cluster are referred to as sequence representatives (Edgar, 2018).

The 16S rRNA gene sequence for most bacteria and archaea is accessible on public databases like NCBI (Lee et al., 2017; Yoon et al., 2017). Consequently, several secondary databases have been established that collect 16S rRNA sequences and are widely used. The most commonly used databases that provide taxonomic annotations for bacteria include SILVA, RDP and GreenGenes (Chaudhary et al., 2015). These databases utilize algorithms that provide the taxonomy of microbial sequences. Several methods are employed, such as Naive Bayesian classifier (Liu & Wong, 2013), 16S classifier (Bengtsson-Palme et al., 2015; Chaudhary et al., 2015) and microclass (Liland et al., 2017). The choice of reference database depends on the type of sample and research

question though SILVA ensures consistent and standardized taxonomy assignments across different studies and samples (Almeida et al., 2018).

The demand for precise and computationally effective classifiers has risen dramatically in the dynamic field of microbiology (Li et al., 2022). Investigating different data mining and machine learning techniques might be useful in creating reliable classifiers for microbiological data analysis. QIIME 2 also implements several supervised learning methods like Random Forest, Support Vector Machines, and Gradient Boosting from scikit-learn (Bokulich et al., 2018). When these methods are used in conjunction with sample data, such as microbiota composition, supervised learning approaches can predict sample data, such as metadata values. In classification or regression tasks, these anticipated outcomes may manifest as either distinct sample categories or continuous numerical values (Bae et al., 2021).

Another curated database is UNITE, which provides standardized and updated references for fungal DNA sequences. It is widely used in fungal community analysis and taxonomic assignments based on high-throughput sequencing data, including data obtained from 16S rRNA sequencing for fungal identification and diversity studies (Nilsson et al., 2019). The UNITE database includes fungal species information, reference sequences, and various tools and resources for researchers in the field of mycology and environmental studies. By utilizing UNITE, researchers can confidently navigate fungal sequence data and gain deeper insights into the composition and dynamics of fungal communities in various ecosystems (Tedersoo et al., 2022).

CHAPTER THREE

MATERIALS AND METHODS

3.1 Disease Surveillance and Sample Collection

A cross-sectional study design was adopted in the counties of Kwale (4.1816° S, 39.4606° E), Kilifi (3.5107° S, 39.9093° E), and Lamu (2.2696° S, 40.9006° E). These are the major coconut-growing areas in coastal Kenya, with a high coconut tree population (Afa-nocd, 2020). Disease surveillance was conducted to determine the prevalence and severity of yellowing diseased coconut palms in the three counties. This exercise of area identification was done with the help of KCDA officials with fields chosen at random, spaced 5-20 kilometres apart. (**Figure 3.1**). A structured checklist detailing information on identifying diseased-coconut plants, scoring disease severity, and capturing each sampling site's Global positioning system (GPS) coordinates was developed and used to undertake surveillance exercise (**Appendix I, II & III**). The coordinates were recorded and used to generate a spatial surveillance map of the sampled region using ArcGIS Desktop version 10.5 software (**Figure 3.1**).

A total of 1,080 coconut plants were surveyed in this study, out of which 162 had symptoms of CYD. During sample collection, visual inspection was used to distinguish between pathogen-induced yellowing and senescence. Pathogen-induced yellowing was identified by localized patches or irregular patterns on the leaves, rapid spread, damaged inflorescence, yellowing and damaged leaves, and prematurely damaged fruits. In contrast, senescence was recognized by a uniform and gradual process that began with older leaves at the base and progressed upwards. From this sample data, disease prevalence and severity scores were computed. Prevalence was recorded as the percentage number of plants with CYD symptoms divided by the total number of plants surveyed. (Chowdhury et al., 2015), while severity was recorded using a modified scale of i to iii according to Ries et al., (2003), where i= <10% of plant showing symptoms; ii= 10-50% of plant showing symptoms; iii= >50% of plant showing symptoms.

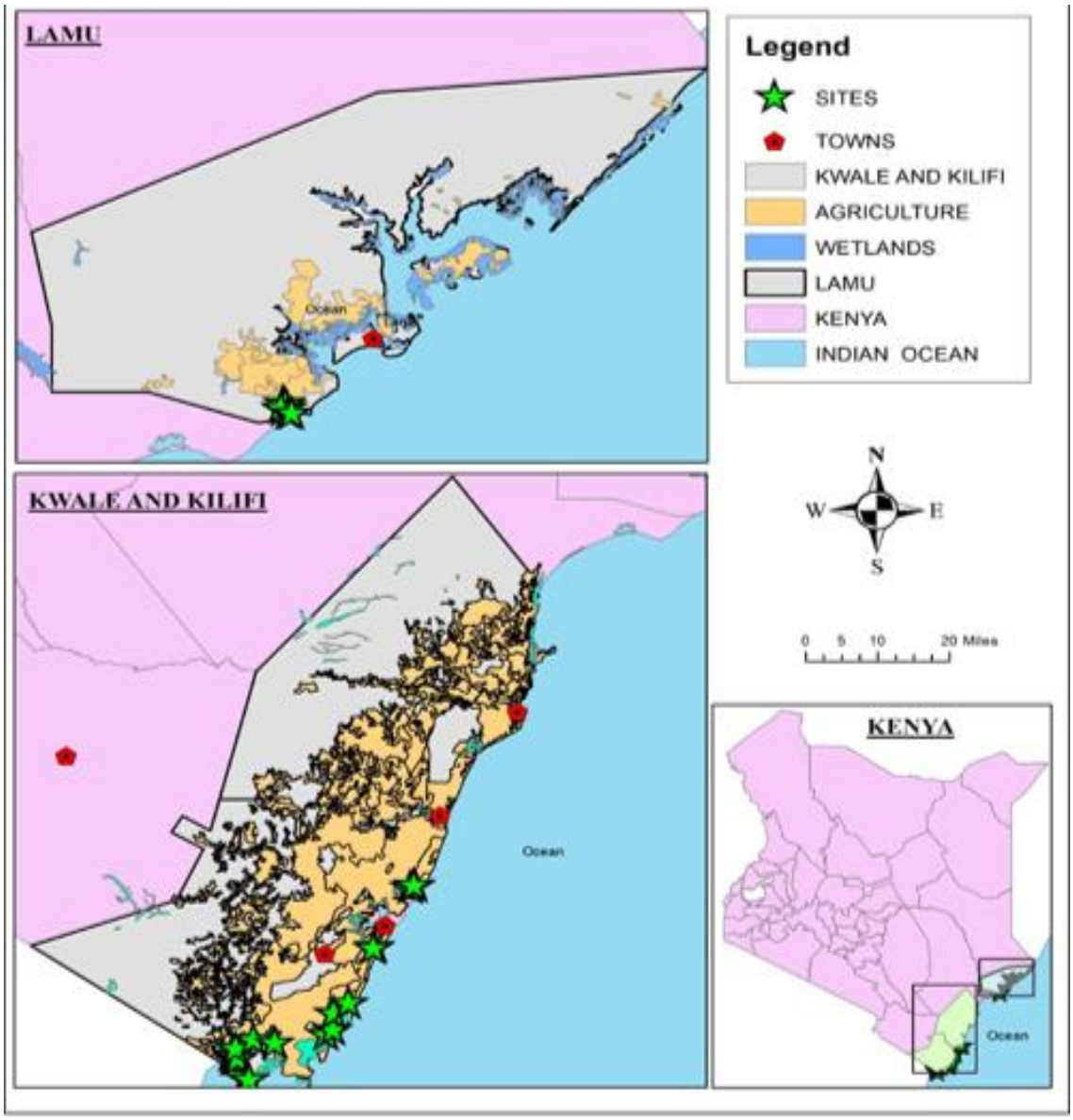

Figure 3.1: Geospatial Analytical Map of Sites where Survey Study was done and Yellowing Diseased Coconut Leaves were Collected

The sample size determination process in this study followed the Cochran's formula for sample size calculation for cross-sectional studies and surveys (Charan & Biswas, 2013; Sapra, 2021). The formula is depicted as:

$$\boldsymbol{n} = \left[\frac{Z_{1-\frac{a}{2}}{}^2 p(1-p)}{e^2}\right] = \left[\frac{1.96^2 0.15(1-0.15)}{0.1^2}\right] = 49$$

Where *n* represents the sample size, *Z* is the Z score (standard normal variate), *p* denotes the population proportion based on previous studies or pilot studies, and *e* signifies the standard error or precision level. For this study, a significance level of $P<0.05$ was used, corresponding to a Z score of 1.96. Since there are no previous studies on CYD in Kenya, thus no available estimate for the population proportion, the utilization of prevalence data is appropriate, as described by (Sapra, 2021). Upon surveying 1,080 coconut plants, with 162 displaying symptoms of CYD, the necessary data was available to estimate the disease prevalence. The total prevalence was 0.15 (15%), which was used as the value *p*. A precision level of 0.1 (10%) was chosen to ensure robustness (Naing et al., 2022).

The resulting calculation yielded a sample size of 49, but for practical reasons, the number was rounded up to 54, a close multiple of 3 due to the three counties involved in the study. To achieve this, purposive sampling technique (Palinkas et al., 2015) was used to collect symptomatic leaves from diseased coconut plants based on the symptoms of CYD, alongside non-symptomatic leaves from healthy coconut plants (controls) (**Figure 3.2**). These healthy leaves were chosen based on visual inspection, ensuring they exhibited no symptoms of yellowing at all. The sample allocation was evenly distributed among the three counties: Kwale, Kilifi, and Lamu, with 18 samples collected from each, totaling fifty-four diseased leaf samples. Additionally, 3 healthy leaf samples were collected from each county, resulting in a total of nine healthy control samples. All samples were collected aseptically and stored in sterile falcon tubes containing autoclaved silica gel to preserve their integrity (**Figure 3.2**). Diseased samples were appropriately labelled based on the prevalence per 20 plants and the severity of the disease rating, as outlined in the tables (**Appendix I, II & III**). For example, KW01Di indicates that it was the first sample from Kwale, and in the sampled farm/area, 4 out of 20 plants were symptomatic, with less than 10% of the plant showing symptoms while healthy coconut leaf samples were labelled as E. The details of sampled diseased coconut plants were recorded in a hardcopy

checklist and later entered into an Excel sheet for analysis (**Appendix IV**). The samples were then transported to the molecular biology laboratory at the Institute for Biotechnology Research (IBR) at JKUAT, Kenya.

Figure 3.2: Sampling Exercise of Yellowing Diseased Coconut Leaves.

3.2 Screening for Culturable Bacterial and Fungal Isolates from Sampled Coconut Plants

3.2.1 Culture Isolation of Bacteria and Fungi

Isolation of bacteria from the leaf samples was conducted using the serial dilution method as described by Thomas et al., (2015). The plant tissues were cut into small pieces (2 cm* 2cm) and transferred into sterile test-tube containing 10ml of sterilized distilled water. An aliquot of both 30µl from dilution 10^0 and plant pieces were cultured according to (Hartman, 2011) on nutrient agar (HiMedia Laboratories LLC, USA) with a concentration of 28g/l and spread using a sterile glass spreader till dry (Thomas et al., 2015). The media was prepared in conical flasks covered by an aluminium foil, autoclaved for 15 minutes at 121 ℃ and left to cool to about 50 ℃ then supplemented with amphotericin B (0.05

g/l). The plates were then secured with parafilm, inverted, and incubated at 37 ℃ for 24 hours. The representative colony types for bacteria were further purified by subculturing on fresh NA plates using the streak plate method as described by Sue Katz et al., (2012) to obtain pure colonies. Pure cultures were characterized both morphologically and biochemically then cryopreserved at -20 °C in nutrient broth supplemented by 20% (v/v) glycerol.

For fungal isolation, the leaf samples were cut into small pieces (2 cm* 2cm) and plated on potato dextrose agar (HiMedia Laboratories LLC, USA) with a concentration of 39 g/l. The media was prepared in conical flasks that were covered by an aluminum foil, autoclaved for 15 minutes at 121 ℃ and left to cool to about 50 ℃ before the addition of 0.1 g/L of streptomycin. The mixture was stirred by gently swirling the flask before pouring into sterile petri dishes. The medium was allowed to solidify before inoculation (Bechem & Afanga, 2018). The plates were then secured with parafilm, inverted and incubated at 25 ℃ for 7 days. To obtain pure cultures, new PDA plates were prepared, and separate fungal colonies from the primary cultures were cut off using a sterile blade. Parafilm was used to seal inoculated plates, which were incubated for 7 days at 25 °C. Pure cultures were also characterized morphologically and then cryopreserved at -20 °C in 50% glycerol.

3.2.1.1 Nomenclature of the Bacterial and Fungal Isolates

During the bacterial and fungal isolation processes, 63 individual samples (54 diseased samples plus the 9 healthy controls) were inoculated on culture media, yielding multiple pure isolates. A labelling system was implemented for the pure isolates to differentiate between the various isolates from the same original sample. For instance, a sample labelled as "KW01Di" after the first isolation would be further designated as KW01Di (1), KW01Di (2), and KW01Di (3) for the subsequent isolates derived from it. In cases where an isolate originated from KW01Di (1), it would be further labelled as KW01Di (1a), KW01Di (1b), and KW01Di (1c) to distinguish between different isolates obtained from the same source. This labelling scheme ensured clear identification and categorization of

the multiple isolates originating from individual samples, enabling precise tracking and analysis throughout the study.

3.2.2. Morphological Characterization of Bacterial and Fungal Isolates

Colony morphology of the pure cultures was observed under a dissecting microscope using seven morphological descriptors: form (circular, irregular, filamentous, rhizoid or spreading), elevation (flat, convex, umbonate, crateriform or raised), margin (entire, filiform, curled, lobate or undulate), size (measured as diameter in millimetres - pinpoint is ≤ 1 mm, small is 2-3 mm, medium is 4-5 mm, and large is > 5 mm), colour (cream, yellow, white, orange or colourless), surface (rough, smooth or glistening), opacity (opaque, translucent or transparent) (Kandi, 2015; Reynolds, 2021).

The gram staining technique examined the cell morphology of fresh, pure isolates (Smith & Hussey, 2005). A sterile loop was used to fix the isolates on clean slides, and the smear was heat-fixed to attach the cells. The slides were stained with crystal violet, washed with water, and treated with gram's iodine as a mordant. After washing with ethanol, the slides were counterstained with safranin. Finally, the stained slides were examined under oil immersion with a light microscope at X100 magnification to characterize the cell morphology using two descriptors: cell shape (rods, cocci, spiral or vibrio) and gram status (gram-negative or positive).

On the other hand, fungal colonies on each media plate were differentiated based on the following characteristics: appearance (fluffy, wavy, cottony, velvety, less fluffy or mucoid), surface (dry, wrinkled, concentric rings or moist), type of mycelium (thick or thin), elevation (raised, convex, flat, umbonate, crateriform), margin (entire, curled, undulate, lobate or filiform), bottom colour and top colour (grey, white, cream, black, yellow, red, brown, green, purple, orange or pink). The microscopic characteristics were carried out using tape touch mounts preparation to determine the type hyphae (septate, aseptate, pseudoseptate) and the presence (+) or absence (-) of spores (Ezeonuegbu et al., 2015). In preparing tape touch mounts, a 3-inch piece of tape was taken from a roll and

gently pressed onto the pure mycelial colonies in a culture dish. The tape flag containing fungal elements from the colony was then carefully placed onto a drop of lactophenol cotton blue stain on a clean slide. Subsequently, the slides with the mounted samples were observed under oil immersion using a microscope to examine their microscopic characteristics (Alsohaili & Bani-Hasan, 2018; Harris, 2000).

The morphological characteristics were assessed using the Bergeys Manual (Osborne, 2008), Methuen Handbook of Colour Chart to select colony colours (Kornerup & Wanscher, 1981). The description of colony morphology was based on both a laboratory manual, a pictorial atlas for fungal identification authored by Watanabe, (2010) and novel neural network application for bacterial colony classification authored by Huang & Wu, (2018).

3.2.3. Biochemical Characterization of Bacterial Isolates

Various biochemical tests, including the methyl red test, citrate utilization test, motility indole urease (MIU) test, catalase test, triple sugar iron (TSI) test, and oxidase test, were performed on the obtained pure culture isolates (Gopireddy, 2011). All tests were conducted in triplicate where the outcome, whether positive or negative, was determined based on the majority result among the triplicates.

3.2.3.1 Citrate Utilization Test

Using an inoculating needle, freshly prepared pure isolates were inoculated on slanted Simmons's citrate agar to pick a single colony and incubated at 37°C for 48 hours. *Escherichia coli* culture was employed as a negative control, and *Klebsiella pneumoniae* culture was used as a positive control. While a negative reaction revealed no growth and no colour change along the slants, a positive reaction revealed a green tint that transitioned to an intense blue colour. (National Institute of Open Schooling, 2012).

3.2.3.2 Methyl Red (MR) Test

The tubes containing sterile Methyl red (MR) broth were inoculated with freshly prepared pure isolates (24 hours old) and incubated at 37°C for 24 hours, after which 3 drops of MR indicator were added. *Escherichia coli* culture was employed as a negative control, and *Klebsiella pneumoniae* culture was used as a positive control. A red colour denoted a positive test after about 10 minutes, while a yellow colour indicated a negative result (Mcdevitt, 2009).

3.2.3.3 Motility Indole Urease (MIU) Test

This test was done using Motility Indole Urea agar according to Liofilchem, (2007). The isolates' freshly made colonies (24 hours old) were inoculated into the test tubes containing the Motility Indole Urea agar by selecting one colony and inserting/stubbing it two-thirds into the media using a sterile loop, then incubated for 24 hours at 37 °C. *Escherichia coli* culture was employed as a negative control, and *Klebsiella pneumoniae* culture was used as a positive control. The tubes were observed for urease test through a change of colour from yellow-orange to pink-red for a positive reaction and no colour change for a negative reaction. For indole production, 5 drops of Kovac's reagent were added after incubation, where a positive indole test was indicated by a red colour layer on top of the medium or a yellow layer for indole negative. Motility was identified by the diffusion of the injected isolate or clouding of the media, while a negative reaction showed growth solely along the stabbing line.

3.2.3.4 Catalase Test

Freshly isolated colonies (24 hours old) were placed onto a sterile microscope slide, and then one drop of 3% hydrogen peroxide was added. The slide was then observed for immediate bubble formation (positive result) and no bubbles for negative result. *Enterococcus faecalis* culture was employed as a negative control, and *Salmonella* culture was used as a positive control.

3.2.3.5 Triple Iron Sugar (TSI) Agar Test

This test was used to check for lactose, sucrose and glucose sugar fermentation and production of Carbon (IV)oxide and Hydrogen Sulphide. The TSI agar was prepared by dissolving 65.524g of this agar in 1000 ml of distilled water. It was distributed into test tubes, sterilized in an autoclave at 121 ℃ for 15 minutes, and left to solidify in a slanted position to give a 2.5 cm butt and a 3.8 cm slant in the safety cabinet. A sterile wire loop was used to touch the top of a colony (24 hours old), then stabbing the butt through the middle of the agar to the bottom of the tube and then streaking the slant. The test tubes were loosely closed with sterile cotton wool and incubated at 37 °C for 48 hours. The yellow colour of both the butt and the slant indicated lactose and sucrose fermentation. A red slant and a yellow butt indicated glucose fermentation. The slant and butt remained red in some tests indicating lactose, sucrose, and glucose non-fermenters. A black precipitate in the butt showed the production of Hydrogen Sulphide gas. The presence of bubbles, cracks or lifting of the media indicated the production of Carbon (IV)oxide gas.

3.2.3.6 Oxidase Test

This test was done using oxidative discs. First, the discs were moistened with sterile water. Then, the freshly cultured bacteria were applied onto the oxidase discs using a sterile loop. The discs were observed for approximately 2 minutes to check for colour changes. The formation of purple colour indicated a positive test, whereas no colour changes show a negative test.

3.3 Molecular Characterization

3.3.1 Total Genomic DNA Extraction of Sampled Coconut Plant Leaves

Genomic DNA extraction was done using a modified CTAB protocol, as described by Ray & Sinha, (2012). First, 5 g of the leaf samples were frozen in liquid nitrogen and ground into a fine powder using a mortar and pestle. 0.4 g of the grounded samples was put in 2 ml microcentrifuge tubes, then 600 µl of CTAB buffer (containing 0.2% β-

mercaptoethanol) was added, vortexed and incubated for 65 ℃ for 30 minutes in a water bath. The homogenate was centrifuged at 13,000 rpm using the Eppendorf 5415D Digital Centrifuge (Eppendorf, Hamburg, Germany) for 5 mins. The supernatant was transferred to clean 2 ml microcentrifuge tubes, and 25 µl of RNase A, 20 mg/ml lysozyme, and Proteinase K were added and incubated at 37 ℃ for 20 mins. Following the incubation, equal volumes of chloroform/isoamyl alcohol (24:1) were added and centrifuged. The aqueous phase was separated in clean 1.5 ml microcentrifuge tubes, and 0.7 volume of cold isopropanol was added and then incubated at 4 ℃ overnight to allow precipitation of DNA. The DNA was then pelleted by centrifugation at 13,000 rpm for 35 minutes, washed with 600 µl ice-cold 70% ethanol, and dried at 25 ℃ for 2 hours by inverting the tubes on dried, clean laboratory tissue paper on a desk. The DNA was resuspended in 30 µl nuclease free water and stored at -20 ℃.

The extracted DNA from each sample was mixed with 1.0 µl of 6X DNA loading dye (Sigma-Aldrich® Solutions, USA) and checked on 0.8% agarose gel electrophoresis stained with 2.0 µl ethidium bromide in 1X TAE (22.5mM Tris-acetate, 1mM EDTA; pH 8.0) buffer at 80 volts for 30 minutes.

3.3.1.1 Genomic DNA Pooling

The genomic DNA obtained from the leaf samples in the three counties was pooled into fifteen samples for NGS and PCR analysis. These samples corresponded to farms visited in Kwale (1A, 1B, 1C, and 1D), Kilifi (2A, 2B, 2C, and 2D), and Lamu (3A, 3B, 3C, and 3D). Additionally, samples 1E, 2E, and 3E were compiled from the healthy plants from the respective counties. For the diseased samples, which totaled 54 (18 from each county), 5 samples were utilized to create samples A and B, while 4 samples were used to create samples C and D. From each of the 5 samples in A and B, 12 µl was taken to create a new composite sample containing 60 µl. Similarly, from each of the 4 samples in C and D, 15 µl was taken to create a composite sample containing 60 µl. Similarly, for the healthy samples, which consisted of nine samples in total, 20 µl of DNA extract were collected from each of the three samples per county. This volume was selected to account for the

smaller number of healthy samples while still ensuring an adequate representation of each sample within the pooled sample. By combining 20 µl from each of the three samples per county, a new composite sample containing 60 µl was created for each healthy sample. The volume was chosen because it complied with the specifications set by the sequencing facility; they explicitly stated that at least 60 µl should be provided. In addition, the decision to adjust the volume and number of samples for pooling was driven by practical considerations and the need to achieve sufficient DNA yield for analysis, rather than following a rigid protocol of uniformity.

3.3.1.2 Sequencing and Preparation of PCR amplicons for Illumina MiSeq

The bacterial and Archaeal Tag-Encoded FLX Amplicon Pyrosequencing (bTEFAP) process, originally described by Dowd et al., (2008), was used to target the V4 hypervariable region of the 16S rRNA gene using PCR primers 515 F/806 R with a barcode on the forward primer and reverse primer. The HotStarTaq Plus Master Mix Kit (Qiagen, USA) was used for PCR amplification under the following thermocycling conditions: Denaturation was carried out at 95 °C for the first five minutes, then 30 cycles of 95 °C for 30 seconds, 53 °C for 40 seconds, and 72 °C for one minute, followed by a final elongation step at 72 °C for ten minutes. Using 2% agarose gel electrophoresis, the PCR products that were produced were validated (Whitfield-Cargile et al., 2015).

Subsequently, using calibrated SPRI beads, 16S rRNA amplicons were purified based on molecular weight and DNA concentrations. These pooled and purified PCR products generated DNA libraries using the Illumina TruSeq DNA library preparation protocol. The sequencing process employed a paired-end (PE) configuration (2x300 bp), and the MiSeq instrument's embedded MiSeq Control Software (MCS) conducted image analysis and base calling. Sequencing was conducted at MR DNA (www.mrdalab.com, Shallowater, TX, USA) on an Illumina MiSeq sequencing platform, adhering to the manufacturer's guidelines.

3.3.1.3 PCR-based Detection Approach for Phytoplasma

This reaction was aimed to amplify any trace of phytoplasma-specific DNA fragments in the yellowing diseased coconut samples and healthy controls. All PCR reactions (25 µL) were performed with 5X MyTaq Reaction Buffer (Bioline®, USA) with 20 µM final primer concentrations. Nested PCR was conducted using two pairs of oligonucleotides, phytoplasma universal primers pair P1 [5'-AAGAGTTTGATCCTGGCTCAGGAT T-3'] and P7 [5'CGTCCTTCATCGGCTCTT-3'] (Invitrogen, USA) in the first PCR reaction, with an amplicon size of 1800 bp while Phyto3F [5'- GCACGAAAGCGTGGGGAGCA-3'] and Phyto3R [5'- CCCCACCTTCCGGTAGGGAT-3'] (Invitrogen, USA) in the second PCR specific for Coconut Lethal Yellowing Disease (CLYD), with an amplicon size of 763 bp (Mazivele et al., 2018).

The reaction mixture in the first PCR for each sample contained 1.0 µl of template DNA, 1.0 µl of both P1 and P7 primers, 0.25 µl of MyTaq DNA Polymerase (Bioline®, USA), 2.5 µl of with 5X MyTaq Reaction Buffer and 20.25 µl of Nuclease free water. The PCR reaction mixture was vortexed for 10 seconds to mix, and 24 µl of the mixture was added to PCR tubes containing 1.0 µl of the 15 pooled DNA templates. The thermocycler conditions for this reaction were as follows: an initial denaturation of the template at 94°C for 3 minutes, followed by 35 cycles: 94°C for 40 seconds, 54°C annealing for 40 seconds, 72°C extension for 1 minute 40 seconds, and a final 10 minutes extension at 72°C (Nadia et al., 2017).

The second amplification reaction was performed using 0.5 µl of the first PCR amplicons where each sample contained 1.0 µl of both Phyto3F/R primers, 0.25 µl of MyTaq DNA Polymerase, 2.5 µl of with 5X MyTaq Reaction Buffer and 20.75 µl of Nuclease free water. The PCR reaction mixture was vortexed for 10 seconds to mix, and 24.5 µl of the mixture was added to PCR tubes containing 0.5 µl of each DNA template. The nested PCR protocol followed 35 cycles of initial denaturation of the template at 94°C for 3 minutes, 94°C for 40 seconds; 53°C annealing for 40 seconds; 72°C extension for 1 minute, and a final 10 minutes extension at 72°C. From each of the second PCR

amplicons, 5.0 µl of the DNA was mixed with 1.0 µl of 6X DNA loading dye before loading into the gel wells. A negative control with no DNA template, as well as a 100 bp DNA ladder (Solis BioDyne, Estonia) covering the range from 100 bp to 3000 bp were also loaded onto the gel. Electrophoresis was carried out at 70 volts for 40 minutes on 1.0% agarose gel containing 2.0 µl ethidium bromide in 1X TAE (22.5mM Tris-acetate 1mM EDTA; pH 8.0) buffer. The gels were observed under a UV transilluminator to visualize the bands.

3.4 Data Analysis

3.4.1 Analysis of Morphological and Biochemical Data

The prevalence was determined by calculating the percentage of infected plants out of the total number of plants assessed, as described by Alexander et al., (2015). As outlined by Bock et al., (2020) and Chiang et al., (2017), severity was calculated as a percentage derived from the sum of total ratings divided by the product of the sum of disease ratings and the maximum disease grade, as detailed in Appendix IV. The number of disease ratings is the number of samples that appear in a particular rating. Total rating is the product of the number of disease ratings and the specific disease grade (i.e., 1, 2, 3), where the maximum disease grade was 3 (**Appendix IV**). The graph illustrating prevalence and severity scores in the three counties was generated using R version 4.3.1, and a correlation matrix was subsequently derived.

An assessment of both morphological and biochemical traits exhibited by bacterial and fungal isolates was undertaken, utilizing Python version 3.10.8 for comparative analysis. Initially, comprehensive morphological and biochemical data extracted from literature sources (Nadia et al., 2017; Ogugua & Salome, 2015; Shao et al., 2020), outlining the traits of microbes known to colonize yellowing diseased coconuts, were compiled into Excel spreadsheets. This dataset from literature was referred to as "positive controls," serving as a benchmark for comparison with the isolates. Since Python does not directly support categorical data, I needed to convert these categorical variables into numerical values to ensure compatibility with my analysis tools. I decided to manually code these

categories in Excel, a process known as encoding categorical data (Potdar et al., 2017). In Excel, I assigned unique numerical values to each category, converting qualitative characteristics into a quantitative format. This approach is straightforward and allows for an easy transition to Python or any other data analysis software. By coding the categorical data manually, I ensured that the data was prepared in a format suitable for computational analysis while maintaining control over how each category was represented. To create the hierarchical clustergrams, I used the Seaborn library's sns.clustermap function in my code that utilizes the Ward's linkage method and Euclidean distance as the distance metric (Randriamihamison et al., 2021).

Leveraging the software's analytical capabilities, a comparison was conducted between the morphological/biochemical characteristics observed in the isolates and those documented in the positive controls. Hierarchical clustergrams were generated to depict the characteristic relationships among the bacterial and fungal isolates, highlighting their shared traits with the positive controls. This approach enabled the determination of the morphological/biochemical resemblance of the isolates to known microbial species associated with yellowing diseased coconuts.

3.4.2 Analysis of Sequencing Data

These raw sequences received from the sequencing facility were first converted from fasta and qual files into fastq format using the FASTA Qual & FASTq Conversion software. After that, they were subjected to joining the corresponding forward and reverse reads before assigning samples based on barcode and later truncated by cutting off the barcode and primer sequence using FASTq Processor. The sequence data, already demultiplexed in Consensus Assessment of Sequence And Variation (CASAVA) 1.8 format, underwent substantial quality assessment. The data was then processed using QIIME 2 version 2021.4 software to determine the presence of phytoplasma and the diversity of other microbial contigs in the samples (Bolyen et al., 2019). The analysis pipeline employed the following packages: q2-core for basic functionality and data importation, q2-dada2 for denoising and quality filtering, q2-cutadapt for adapter removal. Metadata management

was supported by q2-metadata, and diversity analysis was conducted using q2-diversity. For interactive data visualization q2-emperor was used while q2-feature-classifier for assigning taxonomy to amplicon sequence variants (ASVs). q2-taxa for visualizing taxonomic assignments, while q2-sample-classifier was employed for machine learning-based sample classification and prediction (Jiménez, 2021).

Interactive quality plots were generated by importing the sequences into QIIME 2 and analyzing their Phred scores. The sequences were further subjected to quality control using Divisive Amplicon Denoising Algorithm 2 (DADA 2), a denoising tool designed for Illumina amplicon sequence data. This step involved filtering the sequences to a read length of 220 bp while removing chimeric sequences. The resulting sequences, showing a similarity of over 97%, were clustered into OTUs.

3.4.2.1 Diversity Analysis, Taxonomic Assignment & Statistical Analysis of Sequencing Data

The samples were first rarefied to a sampling depth of 25,000 for bacteria and 150 for fungi to ensure comprehensive diversity analysis. Alpha diversity was estimated using Faith Phylogenetic Diversity (a measure of community richness) and Pielou's evenness metric (a measure of community evenness), while beta diversity was estimated by the weighted UniFrac and unweighted UniFrac methods. Dimension reduction on the data was then done and graphically represented as PCoA emperor plots. All two beta diversity measurements produced similar results, and were used to compare beta diversity due to its previous success in distinguishing microbial communities with a small sample size (Lozupone et al., 2011).

Bacterial taxonomy was determined by assigning classifications at a similarity threshold of 97% where a Naïve Bayes classifier was trained using the SILVA 138-99 Reference Database. The same was applied for taxonomic assignment of fungi but using the UNITE (v.8.0) Reference Database (Su et al., 2022). The sequences were screened against the reference sequence and generated interactive bar plots to show the relative abundances of

organisms at different taxonomic levels. These plots formed the basis for determinations and comparisons of community structure.

PERMANOVA was used to determine beta group significance in QIIME 2. It unbiasedly assessed the multivariate data by comparing the microbial communities in the three counties and generating group significance plots with 999 permutations.

3.4.2.2 Machine Learning Predictions for Differential OTU Presence

Using the QIIME 2 pipeline, machine learning classifiers, specifically the Random Forest algorithm, were employed to assess the predictive ability of microbiome composition for sample characteristics. This approach aimed to determine if the microbiome's composition could serve as a reliable indicator of specific sample attributes, utilizing advanced computational techniques for analysis and prediction.

CHAPTER FOUR

RESULTS

4.1 Prevalence and Severity of Yellowing Diseased Symptoms in the Three Counties

The occurrence or prevalence of the disease varied in different counties, as observed in the study. Kilifi had the highest prevalence rate (16.67%), followed closely by Kwale (14.72%) while Lamu county recorded the lowest prevalence at 13.61% (**Figure 4.1**). The overall disease prevalence rate for all the counties was 15.0%. Additionally, the severity of the disease was also observed to vary across different counties, with Kilifi recording the highest severity score of 72.22%. Kwale followed with a severity score of 62.96%, and Lamu scored 59.26% (**Figure 4.1**). The overall disease severity score for all the counties was 64.81%. These results imply that the prevalence and severity of the disease vary by county, with some having a higher prevalence and severity than others.

Furthermore, the severity of yellowing disease in the three counties exceeded the prevalence scores. To examine the relationship between prevalence and severity, a correlation matrix was generated (**Table 4.1**). The resulting correlation coefficient obtained from this analysis was 0.98, signifying a strong positive correlation between these two factors.

Table 4.1: Pearson Correlation Matrix between Prevalence and Severity

	Severity	**Prevalence**
Prevalence	0.9763366	1.000000
Severity	1.000000	0.9763366

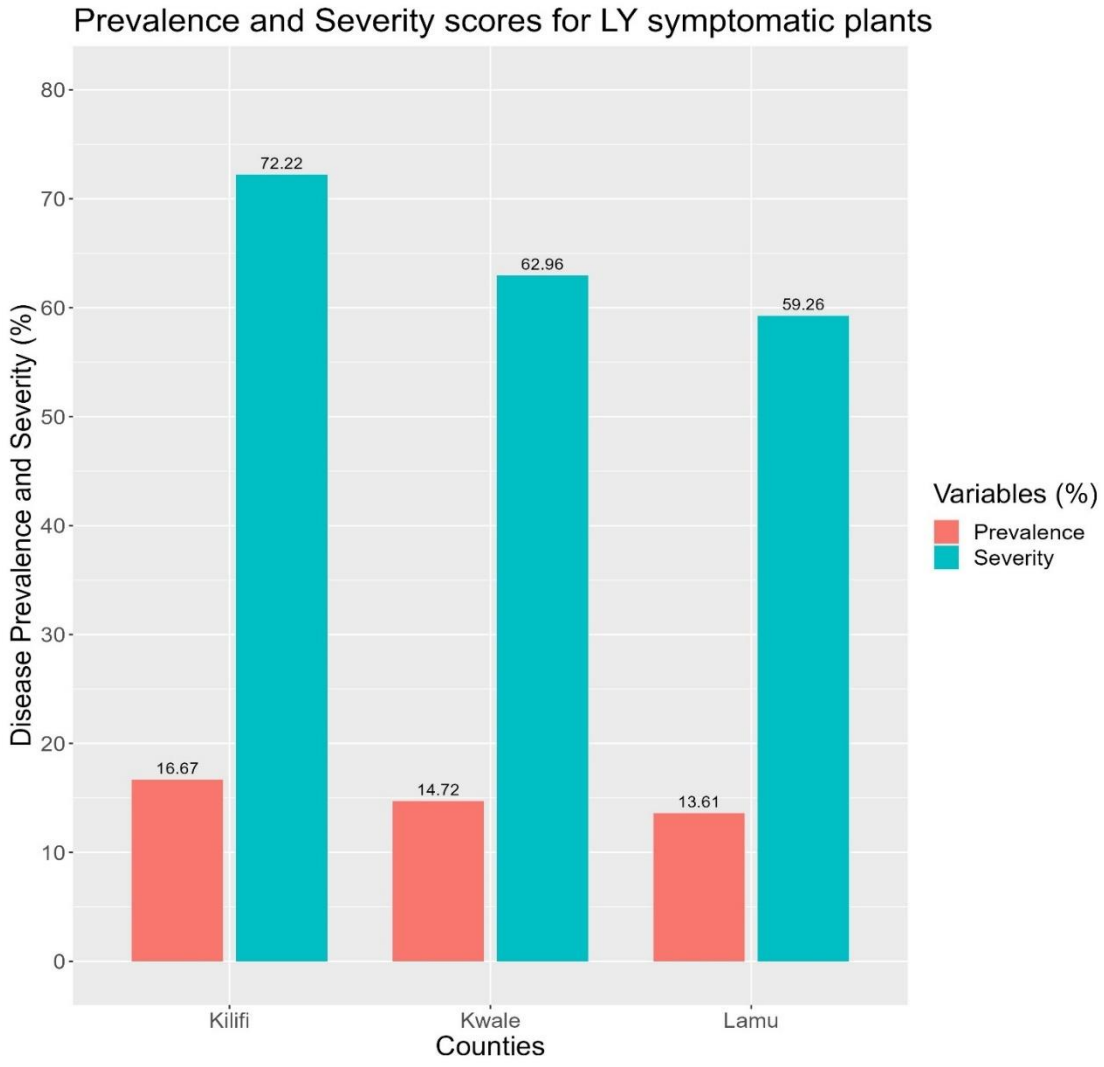

Figure 4.1: Graph Representing Prevalence and Severity Scores for the Three Counties

4.2 Morphological Characterization of Bacterial and Fungal Isolates

4.2.1 Colony Morphology and Microscopic Characterization of Isolated Bacteria

A total of 172 bacterial isolates were obtained from the leaf samples collected from the three counties: 53 from Kwale, 73 from Kilifi, and 46 from Lamu (**Appendix V**). The bacterial isolates were characterized using nine morphological descriptors, both macroscopically and microscopically. While some morphological characteristics were

common among many isolates, others showed distinct variations. The majority of bacterial isolates were translucent (63.74%), gram-positive (83.63%), and rod-shaped (79.53%) (**Plate 4.1**). Regarding the surface descriptor, 43.27% were glistening, 56.14% were rough, and only 0.58% were smooth. On the other hand, the descriptors related to form, colour, margin, and elevation exhibited significant variations, with isolates distributed across different variables for each descriptor. Regarding size, 2.34% of the isolates were pinpoint, 53.80% were small, 35.67% were medium-sized, and 8.19% were large. Additionally, all healthy leaf samples yielded a single isolate, whereas most diseased samples yielded more than one isolate (**Appendix V**).

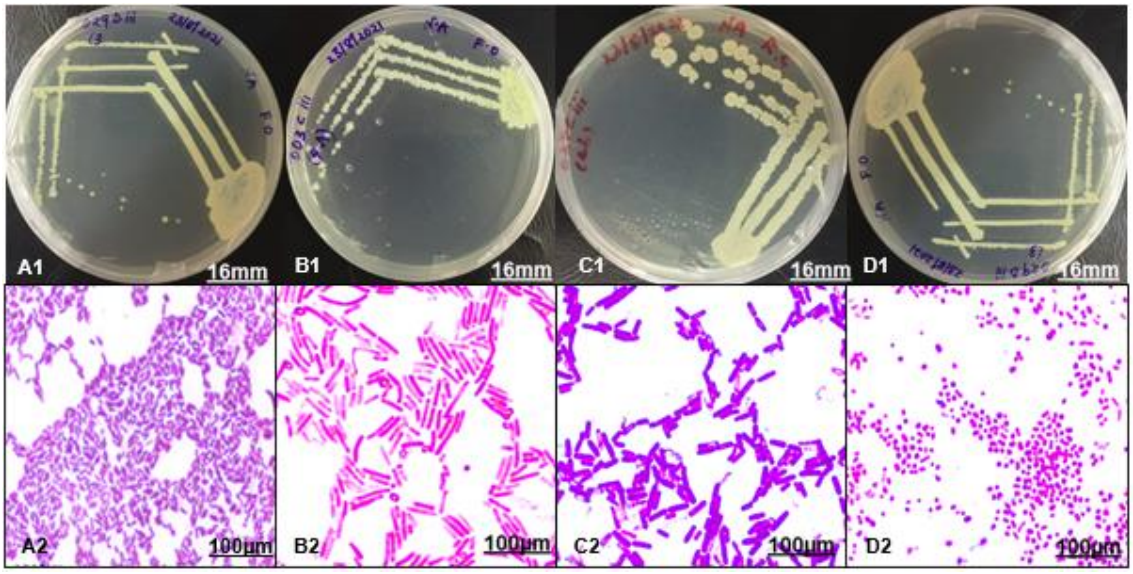

Plate 4.1: Bacterial Isolates on Culture Media and their Respective Microscopic Images

Legend

(A) KL08Diii (2), (**B**) KW03Di (1), (**C**) LA15Ai (1), (**D**) KL04Cii (2b). The Arabic numerals 1 and 2 refers to macroscopic and microscopic images, respectively.

The cluster analysis was conducted to group the isolates based on their morphological attributes, and the clustergram colour-coded the descriptors for each isolate. Warmer

colours (red to light red) indicated higher values, while cooler colours (blue to light blue) represented lower values. The relatedness between the isolates was observed across all counties, rather than isolates from specific counties forming distinct clusters. Most bacterial isolates exhibited high colour intensity in elevation and colour descriptors, indicating their significance in distinguishing the isolates (**Appendix XII**). Microscopic descriptors such as gram staining and cell shape clustered together, indicating similar patterns among the isolates. Conversely, descriptors like surface and opacity had lower colour intensity, suggesting their lesser significance in differentiation. The prevalence of specific descriptors was evident from the cooler colours observed in numerous cells, highlighting the predominance of gram staining, cell shape, surface, and opacity descriptors in the dataset (**Appendix XII**).

The bacterial isolates were examined along with positive controls, which consisted of bacteria that colonize yellowing diseased coconut plants. These positives controls will provide information on how the isolates could be close relatives or microbes of the same species. Based on the clustermap, certain isolates, namely KL19E, LA16Bi (2a), and KW07Aii (3a), showed resemblances in morphological characteristics to *Erwinia psidii* (**Figure 4.2**). These isolates were grouped together due to their similarities in margin (entire), form (circular), and cell shape (rods). Similarly, *Burkholderia nodosa* clustered with isolate KL08Diii (3a) due to shared characteristics like a circular form, an entire margin, a yellow colour, and rod-shaped cells. *Leifsonia sp.* exhibited similarities in morphological characteristics with LA07E, KL15Diii (1), and KW14Di (1), particularly in terms of a raised elevation and being gram-positive rods (**Figure 4.2**). Additionally, *Streptomyces fradiae* shared similar morphological traits with KL09Dii (2), as both displayed a glistening surface and were gram-positive. *Pantoea agglomerans* were in the same cluster with isolate KW03Di (1), KL16E (1), and KL12Biii (1), as they exhibited resemblances in terms of irregular form, umbonate elevation, undulate margin, and rod-shaped cells (**Figure 4.2**). The clustermap revealed these interesting associations among the bacterial isolates and positive controls based on their shared morphological characteristics. Another clustermap was also generated for the cultured isolates alone. The

clustering of specific isolates was attributed to their shared morphological traits, and certain isolates grouped together due to the presence of multiple common descriptors, as depicted in Appendix XII.

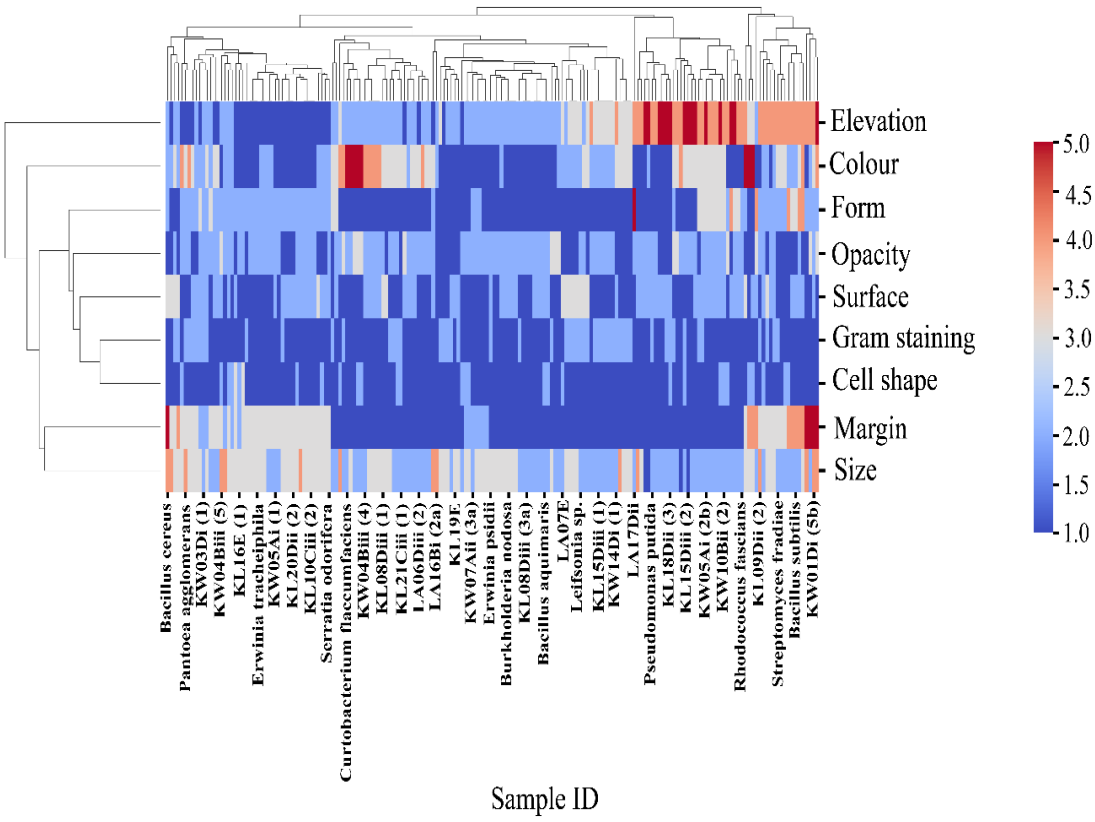

Figure 4.2: Hierarchical Clustergram of Morphological Relationship of the Bacterial Isolates and Positive Controls

Legend

The clustergram depicts the morphological relationship among bacterial isolates and positive controls. The descriptors used include colour, elevation, gram staining, cell shape, opacity, form, surface, margin and size. The colour scale represents the intensity of each descriptor, with higher values indicating stronger characteristics while lower values indicate a weaker characteristic.

4.2.2 Colony Morphology and Microscopic Characterization of Isolated Fungi.

A total of 109 fungal isolates were collected from symptomatic leaf samples across three counties: 35 from Kwale, 42 from Kilifi, and 32 from Lamu **(Appendix VI)**. These fungal isolates underwent macroscopic and microscopic characterization based on ten morphological descriptors.

The analysis revealed both shared and distinct morphological traits among the fungal isolates. Most of the isolates appeared fluffy (76.85%) and black/grey (45.37%), while a smaller proportion exhibited wavy, cottony, velvety, or less fluffy appearances (**Plate 4.2**). Furthermore, 87.04% of the fungal isolates displayed a dry surface, whereas only 11.11% showed a wrinkled appearance, and a mere 1.85% had concentric rings. Additionally, a large portion of the isolates exhibited thick mycelium (81.48%) and a circular form (87.04%), with fewer isolates having thin mycelium (18.52%) and an irregular form (12.96%) (**Appendix VI**). Regarding hyphal characteristics, 67.59% of the fungal isolates had septate hyphae, 24.07% were aseptate, and only 8.33% were pseudoseptate (**Plate 4.2**). Moreover, most of the isolates had a raised elevation (74.07%), while a smaller portion appeared flat (21.30%) or convex (4.63%). In 7 days, some isolates exhibited spores (27.78%), while others did not (72.22%) (**Plate 4.2**).

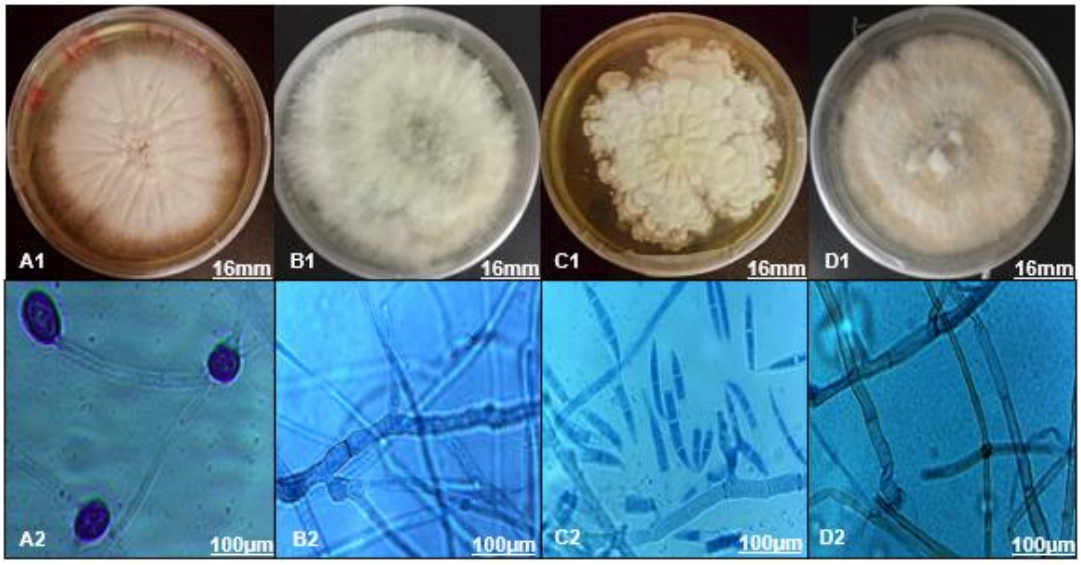

Plate 4.2: Fungal Isolates on Culture Media and their Respective Microscopic Images

Legend

(A) KW20Ciii (2), (**B**) KW02Cii, (**C**) KL09Dii (3), (**D**) KL12Biii (2). The Arabic numerals 1 and 2 refers to macroscopic and their microscopic images when stained with lactophenol cotton blue, respectively.

From the heatmap analysis of the fungal isolates (**Appendix XII**), two major clusters were identified. The relatedness between the isolates was observed across all counties, rather than isolates from specific counties forming distinct clusters. The clustering of certain isolates was attributed to shared morphological characteristics, where warmer colours indicated higher values and cooler colours represented lower values. The prevalence of certain descriptors was evident from the cooler colours (blue to light blue) observed in numerous cells, highlighting the predominance of form, margin, mycelium, surface, and elevation descriptors in the dataset (**Appendix XII**). The top colour and bottom colour descriptors displayed the highest colour intensity and were found to be the most significant in clustering isolates compared to other morphological attributes. These two descriptors formed a distinct cluster and showed the least relation to the rest of the descriptors, which were grouped in another clade (**Appendix XII**).

The fungal isolates were examined alongside positive controls, which consisted of fungi that colonize yellowing diseased coconut plants. The clustermap analysis revealed several noteworthy findings. Isolate LA08Biii (2) shared similar morphological characteristics with *Phytophthora palmivora*, displaying a fluffy appearance, a dry surface, and thick mycelium. *Ganoderma tornatum* and *Aspergillus nomius* were observed in the same clade with isolates KL04Cii (1), KL21Ciii (1), and KL15Diii (2) (**Figure 4.3**). The clustering of these isolates was attributed to their shared traits, which are an entire margin, a circular form, and a flat elevation with a wrinkled surface. Furthermore, *Gibberella fujikuroi* was grouped together with isolate LA20E due to their common characteristics, such as a fluffy appearance, a dry surface, and septate hyphae (**Figure 4.3**). Lastly, *Drechslera halodes* exhibited similarities in morphological characteristics with isolates KW06Cii (2), KL17Di (2), KW11Dii (1), KL05Dii (2), LA02Di (1), LA10Ai, and KW14Di (1). These isolates shared traits such as a fluffy appearance, a dry surface, thick mycelium, a circular form, and a black bottom colour (**Figure 4.3**). The clustermap revealed these interesting associations among the fungal isolates and positive controls based on their shared morphological characteristics.

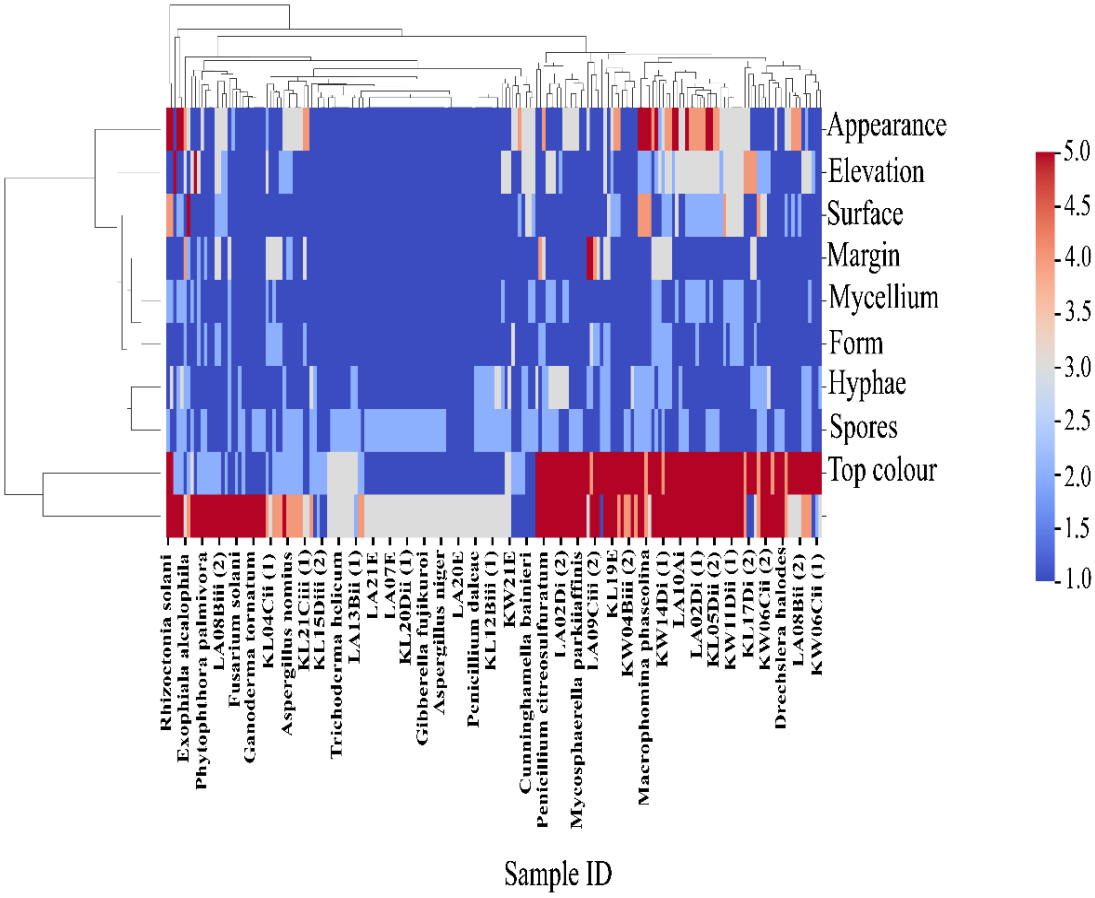

Figure 4.3: Hierarchical Clustergram of Morphological Relationship of the Fungal Isolates and Positive Controls

Legend

The clustergram depicts the morphological relationship among fungal isolates. The descriptors used include bottom and top colour, appearance, elevation, type of hyphae, type of mycelium, presence of spores, form, surface, and margin. The colour scale represents the intensity of each descriptor, with higher values indicating stronger characteristics.

4.2.3 Biochemical Characterization of Bacterial Isolates

The bacteria isolates exhibited diverse results in the biochemical analysis, demonstrating independent variations in their utilization of various substrates and production of different products, which were crucial for their characterization. Among the tests conducted, glucose fermentation and catalase tests emerged as the most significant descriptors for identifying the isolates. In contrast, H_2S gas production, Indole tests, as well as lactose and sucrose fermentation tests proved to be the least effective in distinguishing the isolates. It is worth noting that none of the isolates produced CO_2 gas (**Figure 4.4**). Based on the clustergram analysis, the tests for oxidase, glucose, citrate, and catalase were clustered together, while the remaining tests, including urease test, methyl red, indole test, H_2S, CO_2, motility, sucrose, and lactose fermentation, formed a separate cluster (**Appendix XII**).

The ability of isolates to utilize different substrates was equally convenient in studying the relationship between bacterial isolates and positive controls. According to biochemical characterization, *Burkholderia anthina* shares biochemical characteristics with LA18Dii, LA19Cii (1) and LA19Cii (2), while *Pantoea dispersa* shares with KW09Ci (2) (**Figure 4.4**). These samples were grouped based on their similarities since they had negative results in their sucrose and lactose fermentation tests as well as positive results for oxidase and catalase. For *Pantoea dispersa* and KW09Ci (2), they were catalase positive, motile, lactose and sucrose negative (**Figure 4.4**). *Streptomyces fradiae* was also in a similar clade with KW03Di (1) and KL06Ciii (3a) since they had positive results for glucose fermentation as well as negative results for indole test, sucrose, and lactose fermentation tests. Isolates KW02Cii (2b) and KL08Diii (1) share similar biochemical characteristics (glucose, sucrose and catalase had positive results while indole test was negative) with *Erwinia tracheiphilia* (**Figure 4.4**).

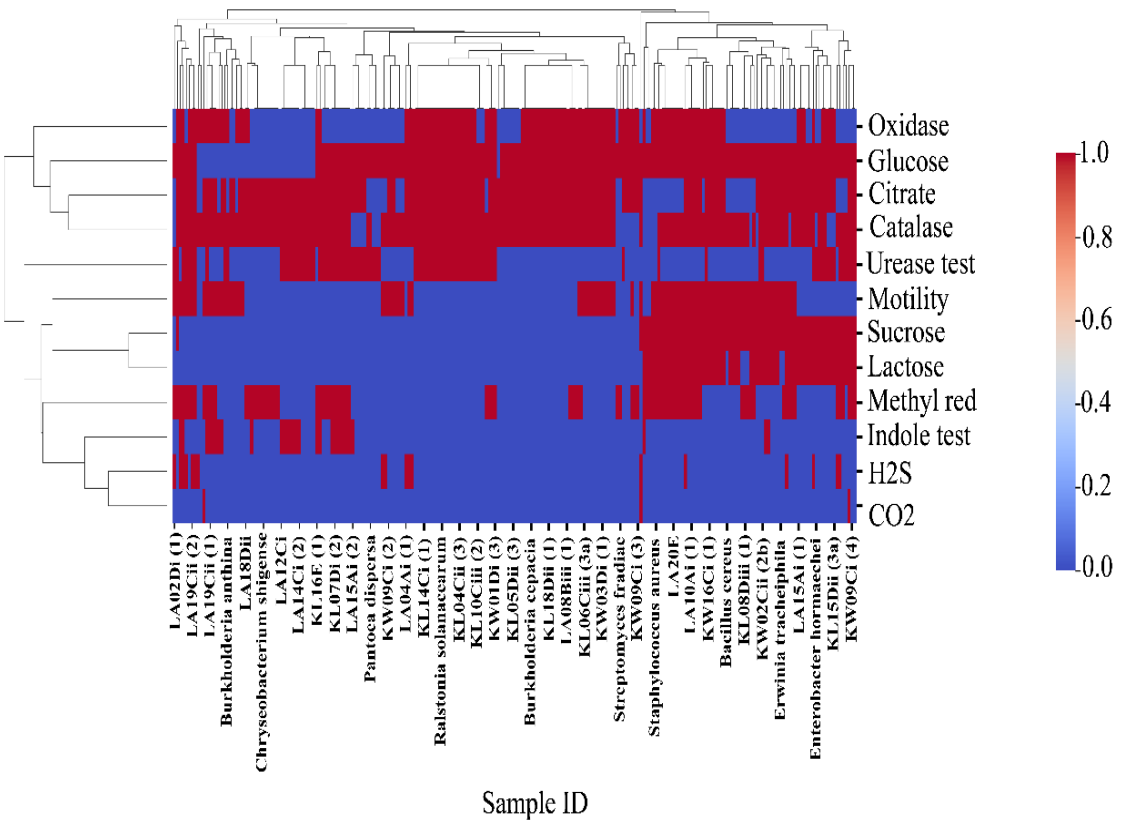

Figure 4.4: Hierarchical Clustergram of Biochemical Relationship among the Bacterial Isolates and Positive Controls

Legend

This map provides a visual representation of the biochemical profiles of the bacterial isolates and positive controls, allowing for easy comparison and identification of shared traits or distinct patterns. The colour intensity in the heat map indicates the presence or absence of biochemical traits, with the warm colour (red) representing positive results and the cool colour (blue) representing negative results.

4.3 The Genetic Identity of Microbial Communities and Phytoplasma in Sampled Coconut Plants

4.3.1 Molecular Characterization using NGS

NGS analysis of the 16S rRNA gene was conducted to characterize microbial communities in the sampled coconut plant leaves as well as determine whether phytoplasma exist. Despite comprehensive sequencing efforts, no sequences corresponding to phytoplasma were identified, illustrating the absence of phytoplasma in the sampled leaves. However, analysis of the sequencing data revealed a diverse array of microbial communities present in the sampled coconut leaves.

4.3.1.1 Characterizing Bacterial Communities in the Sequencing Data

In this study, the fifteen pooled samples were processed for high-throughput sequencing and analysis. Illumina sequencing of bacterial 16S rRNA genes yielded 510,954 valid sequences. After quality trimming, 468,132 trimmed sequences were obtained. The primer pair 515F/806R could amplify bacterial and plant chloroplast DNA under the PCR conditions. After removing reads assigned to the taxonomic kingdom Plantae, 113,330 sequences remained. These sequences were clustered into 285 OTUs at a threshold of 97% sequence similarity (**Appendix VIII and IX**). All reads with less than 97% similarity with the known organisms in the SILVA database were not considered for further analysis. Kilifi samples exhibited the greatest diversity of OTUs, with a count of 265, followed closely by Kwale with 261, whereas Lamu displayed the lowest count at 59 (**Figure 4.5**). Kilifi also had the highest proportion of unique OTUs at 8.4%, Kwale at 6.7%, while Lamu did not record any unique OTUs. Of the total OTUs, 20.4% were common among all the three counties 59 (**Figure 4.5**). Among the 113,100 reads obtained from the diseased samples, Kilifi exhibited a significantly higher proportion of reads at 73.23%, followed by Kwale at 26.08%, while Lamu had the lowest representation at just 0.7% (**Appendix VIII**). On the other hand, out of the 230 reads from the healthy samples, Kilifi had the largest share with 61.74%, Lamu followed at 21.30%, and Kwale had the smallest percentage at 16.96% (**Appendix VIII**).

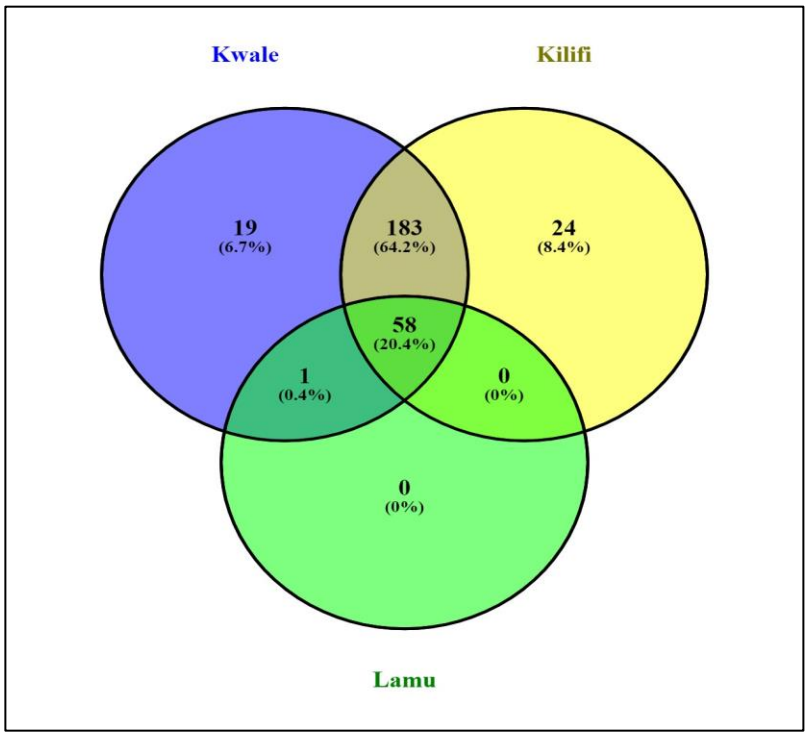

Figure 4.5: Venn Diagram to Compare Bacterial Microbes either Common in all, Two or Specific for only One Geolocation. Venn diagram was done using VENNY (http://bioinfogp.cnb.csic.es/tools/venny/index.html**).**

The rarefaction curve levelled off at a sequencing depth of 25,000, suggesting that the microbial communities were reasonably well characterized with our sampling effort and most of the microbial community diversities captured (**Figure 4.6**). Kilifi samples showed higher saturation than Kwale and Lamu (**Figure 4.6**). Additionally, when comparing the curves representing diseased and healthy samples, it became evident that there was greater diversity within the diseased samples in comparison to the healthy samples (**Figure 4.7**). Further sequencing is unlikely to reveal more OTUs as all the curves ended in plateaus (**Figure 4.6 & 4.7**).

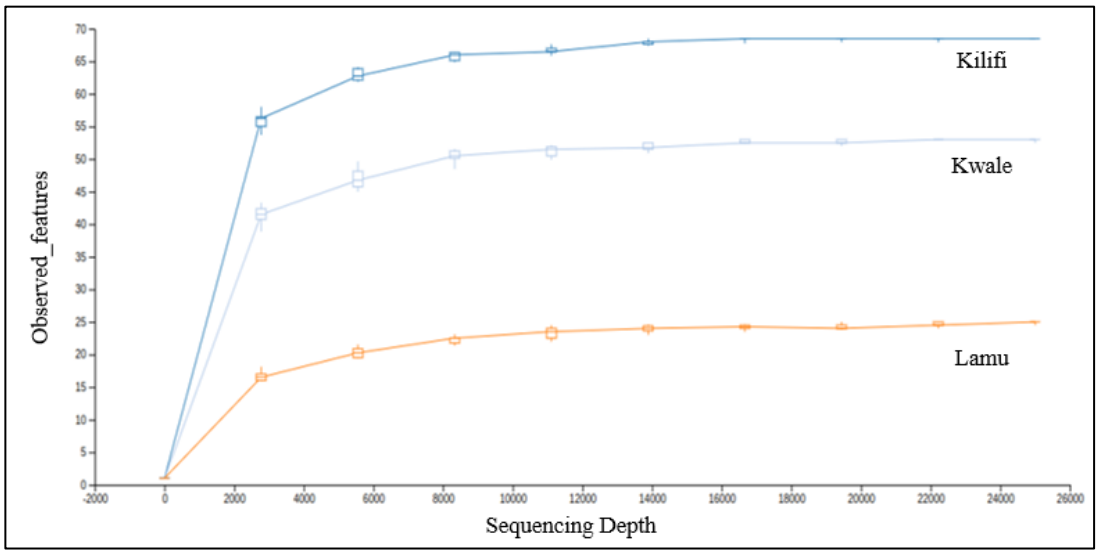

Figure 4.6: Alpha Rarefaction Curve Shows Sample Diversity with Increasing Sequencing Depth Based on the Counties

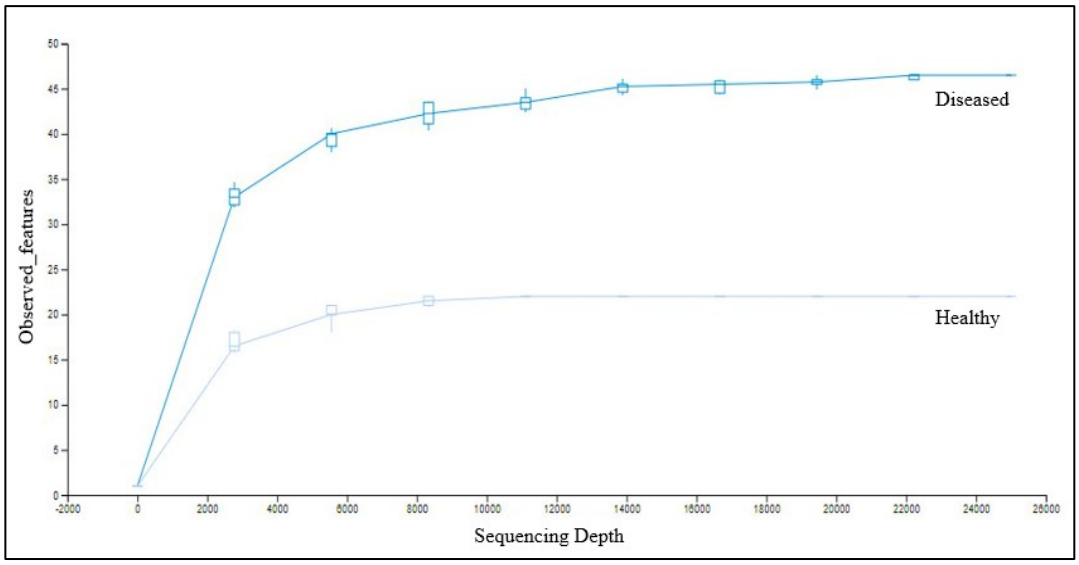

Figure 4.7: Alpha Rarefaction Curve Shows Sample Diversity with Increasing Sequencing Depth Based on the Condition

4.3.1.2 Diversity of Bacterial Communities

Faith's PD and Pielou's evenness metrics were utilized to assess bacterial community diversity in the samples based on two variables of metadata columns: Counties (Kilifi, Kwale, and Lamu) and condition (diseased and healthy states). Regarding counties, the Kruskal-Wallis test-calculated p-values, showed no statistically significant differences in bacterial richness and species distribution among samples within the different counties (Faith's PD, p-value= 0.07; Pielou's evenness, p-value= 0.06) (**Table 4.2**). Kilifi demonstrated the highest richness and evenness, followed by Kwale and Lamu (**Figure 4.8**). Similarly, in terms of condition, there were no substantial variations in terms of bacterial richness and species distribution among samples within the different conditions (Faith's PD, p-value= 0.11; Pielou's evenness, p-value= 0.25) (**Table 4.2**). This analysis revealed that diseased samples exhibited higher richness and evenness compared to healthy ones (**Figure 4.9**). This indicates that there are no statistically significant differences in bacterial diversity detected in either of the two observed variables.

Table 4.2: Kruskal-Wallis Test Results for Bacterial Diversity

Observed variables		Faith's PD	Pielou's evenness
Counties	**H**	5.213620071684595	5.780000000000001
	p-value	0.07376949085918948	0.05557621261148303
Condition	**H**	2.5298685782556847	1.3333333333333428
	p-value	0.11170951995956525	0.24821307898991857

Note: The Kruskal-Wallis test was not significant at the significance level of 0.05, no statistical difference among samples in the different counties and conditions.

Unweighted and Weighted UniFrac distances, commonly used in contemporary bacterial community sequencing studies, were chosen as phylogenetic measures to assess the dissimilarity coefficient between the samples. The PCoA emperor plots revealed a distinct clustering pattern primarily based on the counties rather than condition of samples. This distinction was particularly pronounced in the case of samples originating from Lamu

county, as observed in the Weighted Unifrac analysis (**Figure 4.10**). However, it's worth noting that in both plots, sample 2D (from Kilifi) clustered alongside Kwale samples, while sample 1D (from Kwale) clustered with Kilifi samples (**Figure 4.10**). Moreover, there was a tendency for the three healthy samples to cluster together with the diseased samples from Lamu. In addition, Principal Component (PC) 1, PC 2, and PC 3 of Unweighted Unifrac accounted for 34.50%, 17.07%, and 10.21% of the total changes, respectively while PC 1, PC 2, and PC 3 of Weighted Unifrac accounted for 85.98%, 9.03%, and 3.45% of the total changes, respectively (**Figure 4.10**).

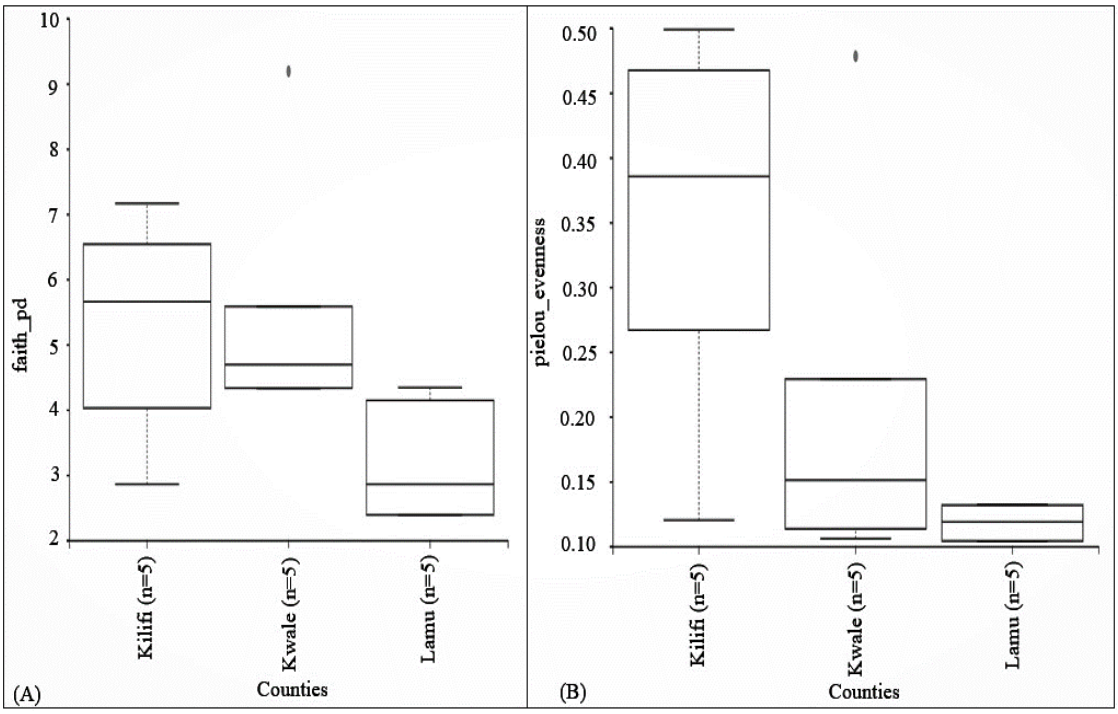

Figure 4.8: Boxplot of Faith's Phylogenetic and Pielou's Evenness Bacterial Diversity Indices in the Three Counties

Legend

The boxplots display the comparison of bacterial diversity indices in Kilifi, Kwale, and Lamu counties. Both boxplots, A for Faith's PD index and B for Pielou's evenness diversity, show no significant difference ($p > 0.05$) among the three counties.

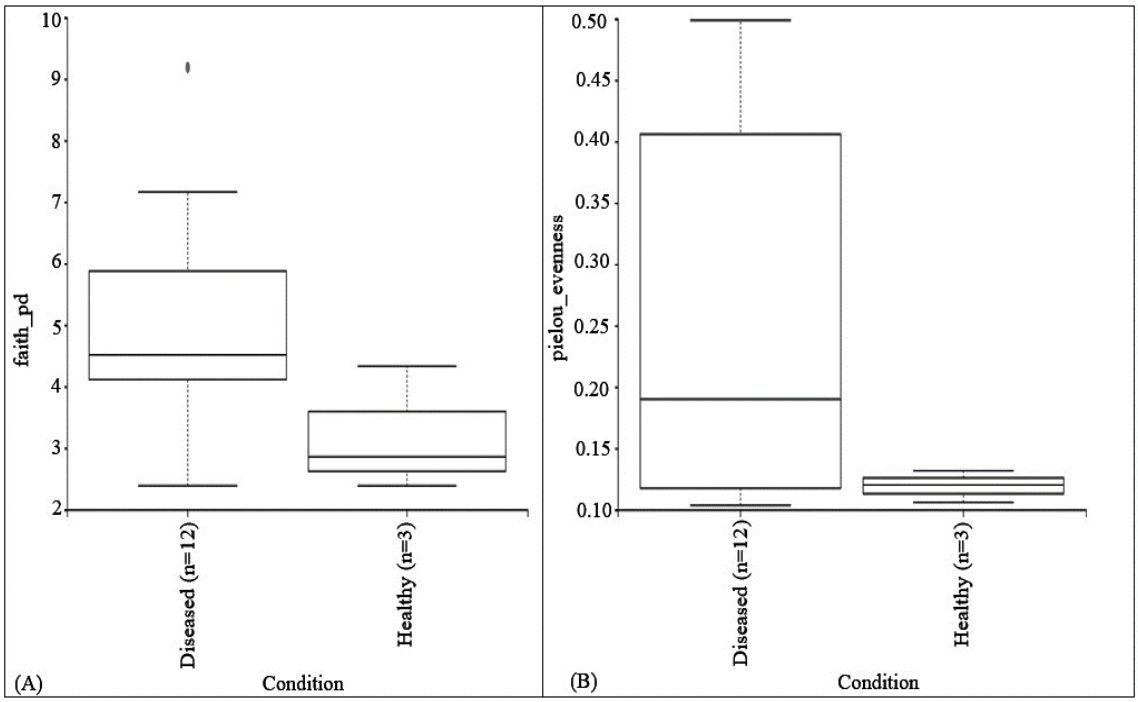

Figure 4.9: Boxplot of Faith's Phylogenetic and Pielou's Evenness Bacterial Diversity Indices in the Two Conditions

Legend

The boxplots display the comparison of bacterial diversity indices in diseased and healthy samples. Both boxplots, A for Faith's PD index and Boxplot B for Pielou's evenness diversity, show no significant difference ($p > 0.05$) between the two conditions.

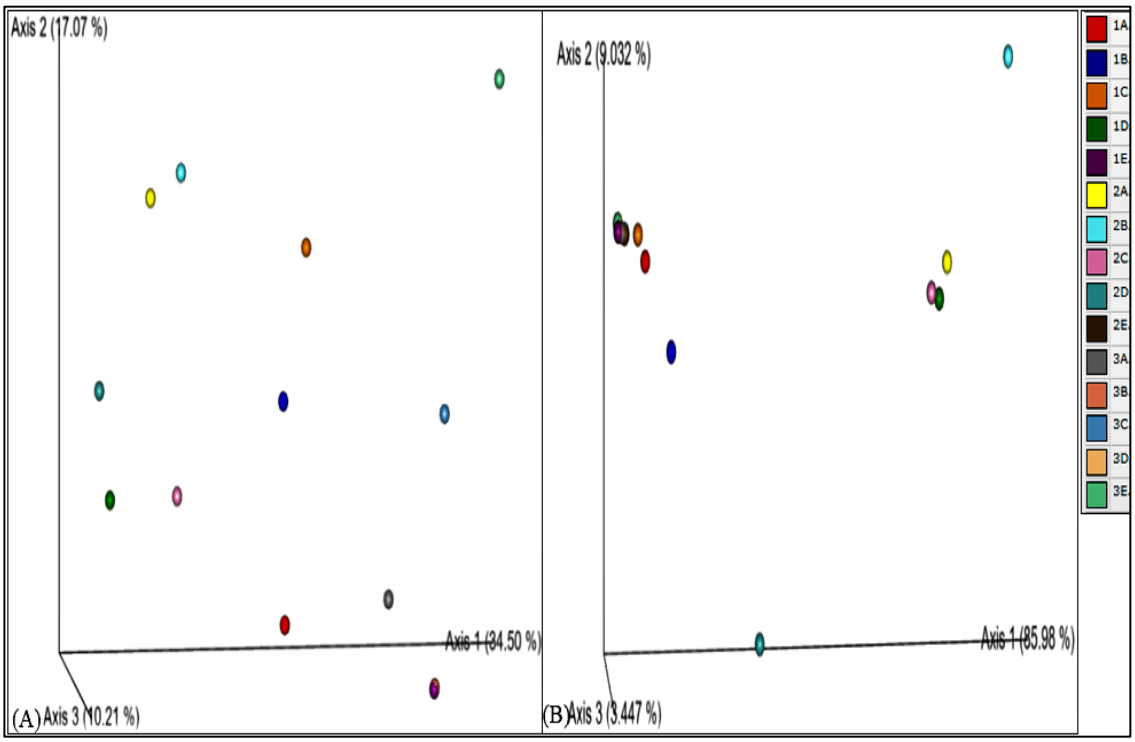

Figure 4.10: PCoA Plots of Beta Diversity of Bacterial Microbial Communities

Legend

The emperor plots illustrate the beta diversity of bacteria where A is the Unweighted UniFrac and B is Weighted UniFrac. They capture the overall dissimilarity among samples and phylogenetic relatedness. The plots provide insights into the spatial distribution and clustering patterns of bacterial communities across the samples.

4.3.1.3 Statistical Analysis of Sequencing Data

PERMANOVA analysis of the microbial community profiles for unweighted group significance revealed that the three counties significantly drove differences in the bacterial community profiles with p-value of 0.019 (**Figure 4.11**). The boxplot showing distances to Kilifi indicates that samples from Kilifi have a greater variability. Also, it suggests that samples from Kilifi are more similar to Kwale than Lamu (**Figure 4.11**). The boxplot showing distances to Kwale indicates that samples from Kwale and Kilifi are relatively

consistent and exhibit almost similar microbial community profiles with Lamu being different. The boxplot showing distances to Lamu are quite different in size indicating that samples from Lamu are not quite similar to samples from the other two counties (**Figure 4.11**). In regards to condition, unweighted group significance demonstrated that the two conditions did not exert a substantial influence on the variations observed in bacterial community profiles, as evidenced by a p-value of 0.171 **(Figure 4.12)**. Examining the distances to the diseased boxplot, it's apparent that both diseased and healthy samples displayed a degree of consistency, showcasing nearly identical microbial community profiles. The boxplot showing distances to healthy indicates that healthy samples exhibited lower variability **(Figure 4.12)**.

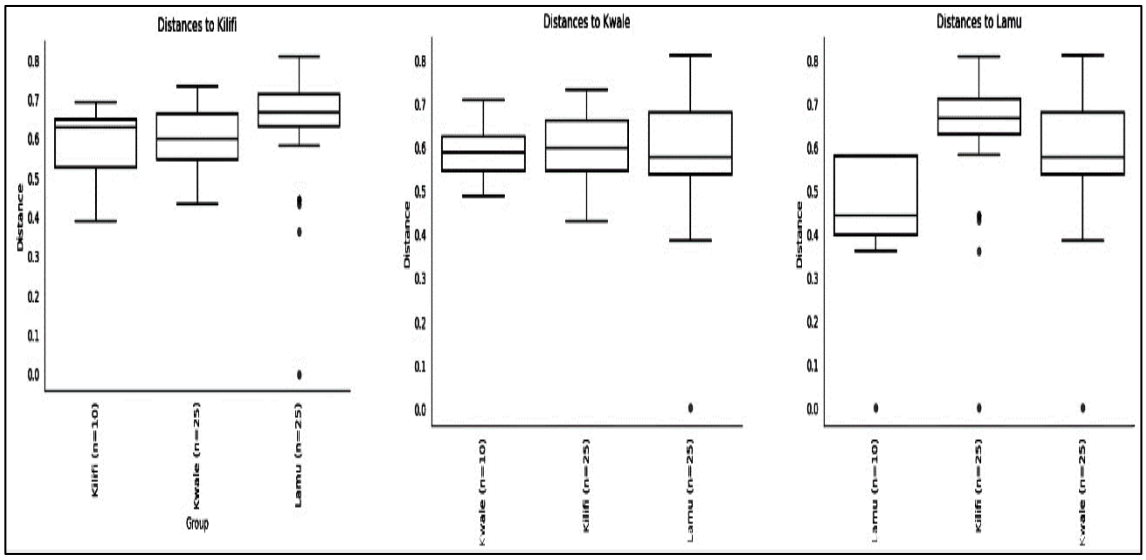

Figure 4.11: Unweighted Unifrac Significance Plots of the Bacterial Microbial Communities' Samples from the Three Counties

Legend

The group significance plots display the dissimilarity between within-group distances and the between-group distance for the samples. The first plot represents the distances to Kilifi, second plot represents the distances to Kwale, and third plot represents the distances

to Lamu. The plots highlight the variations in bacterial community composition and the significance of between-group dissimilarities among the different locations.

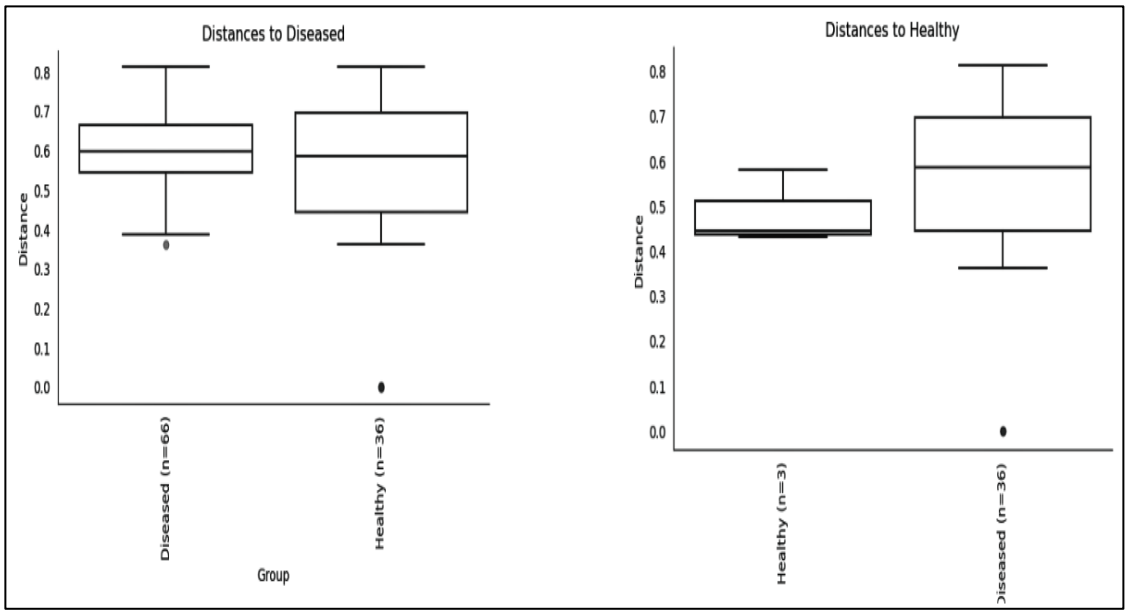

Figure 4.12: Unweighted Unifrac Significance Plots of the Bacterial Microbial Communities' Samples in the Two Conditions

Legend

The group significance plots display the dissimilarity between within-group distances and the between-group distance for the samples. The first plot represents the distances to diseased, and second plot represents the distances to healthy. The plots highlight the variations in bacterial community composition and the significance of between-group dissimilarities among the different conditions.

4.3.1.4 Taxonomic Analysis of Bacteria

The taxonomic classification for bacteria was performed using consensus blast against the SILVA reference sequence database. The identified sequences generated interactive bar plots displaying each sample's relative abundances or organisms at specified taxonomic levels. Regarding the diseased samples, the sequences were classified into 12 phyla.

Actinobacteria emerged as the predominant phylum, constituting 84.87% of the sequences, followed by Proteobacteria (8.40%), Bacteriodota (3.96%), Firmicutes (0.03%), and Chloroflexi (0.018%). Other phyla such as Acidobacteriota, Deinococcota, Verrucomicrobiota, Planctomycetota, Myxococcota, Nitrospirota, and Fusobacteriota were present in negligible proportions (**Figure 4.13**). In the individual counties, the same order of phyla was also followed. The samples with the highest number of reads were 2B, 2C and 1D, with most being Actinobacteria (**Appendix VIII**). Conversely, the healthy samples exhibited a more limited diversity, with only 5 observed phyla. Actinobacteria remained dominant at 58.26%, followed by Proteobacteria at 20.87%, Firmicutes at 17.83%, Chloroflexi at 2.61%, and Bacteriodota at 0.43% (**Figure 4.13**).

At the genus level, the sequence reads were classified into 76 genera, most of which were present in Kilifi samples. There was a high abundance of *Streptomyces*, but it was not detected in sample 3D (**Figure 4.14**). A total of 69,273 (61.24%) sequence reads represented the *Streptomyces* genera (**Appendix VIII & IX**). *Nonomuraea* was the next abundant bacteria at 9.68%, followed by *Promicromonospora* (6.41%) and *Olivibacter* (2.91%). The genera *Actinomycetospora, Pseudonocardia, Methylobacterium* and *Sphingomonas* though not so high in amounts, were detected in all the samples (**Figure 4.14 & Appendix VIII**). Samples from Kilifi and Kwale have shown to drive the abundance of sequences present. For example, *Streptomyces* and *Nonomuraea* were the most abundant genera in Kilifi and Kwale, accounting for 70.96% of the total reads (**Figure 4.14 & Appendix VIII**). However, *Actinomycetospora* and *Sphingomonas* were predominant in Lamu but only accounted for 0.3% of the total reads (**Appendix VIII & IX**). In contrast, the healthy samples demonstrated reduced diversity, featuring a total of 25 observed genera. *Streptomyces* and *Nonomuraea* still emerged as the predominant bacterial genera in the healthy samples, constituting 19.57% and 17.82% of the population, respectively. However, the bacterial read counts in the healthy samples were notably lower when compared to the diseased samples (**Figure 4.14 & Appendix VIII**).

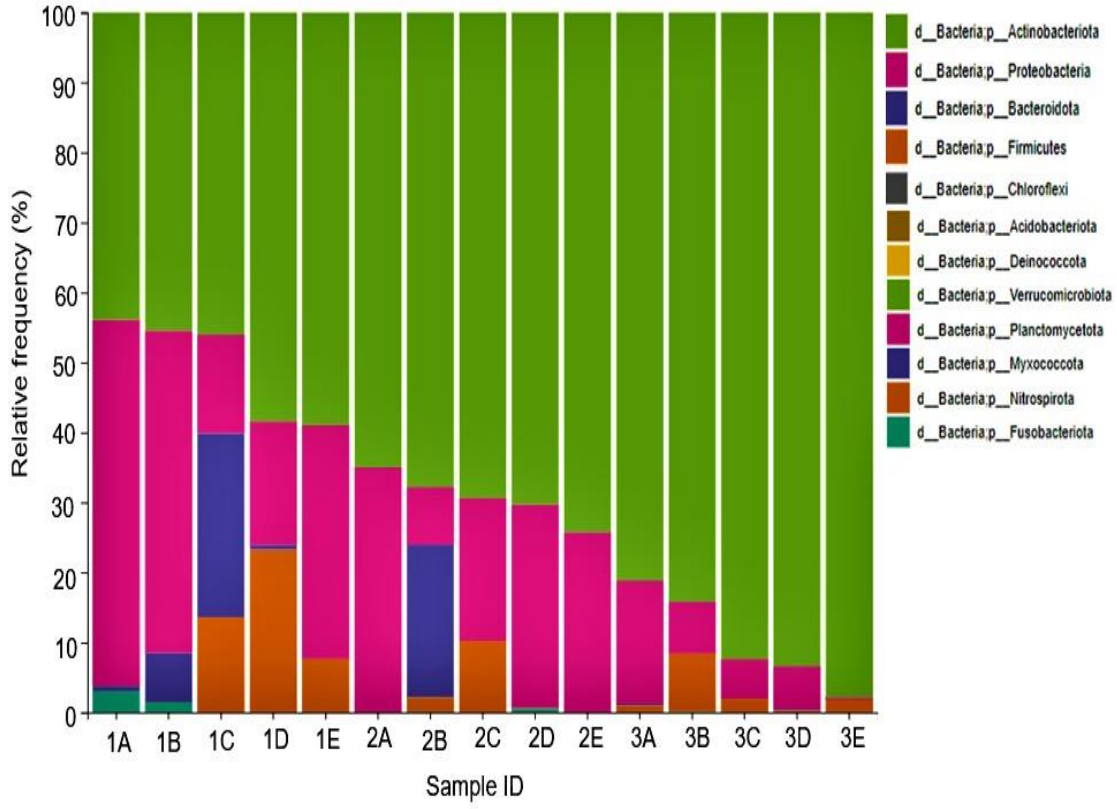

Figure 4.13: Taxonomic Bar-Plots of Bacterial Phyla

Legend

Relative abundance of OTUs in the samples showing the distribution of bacterial phyla at the taxonomic level, providing insights into the composition and prevalence of microbial communities.

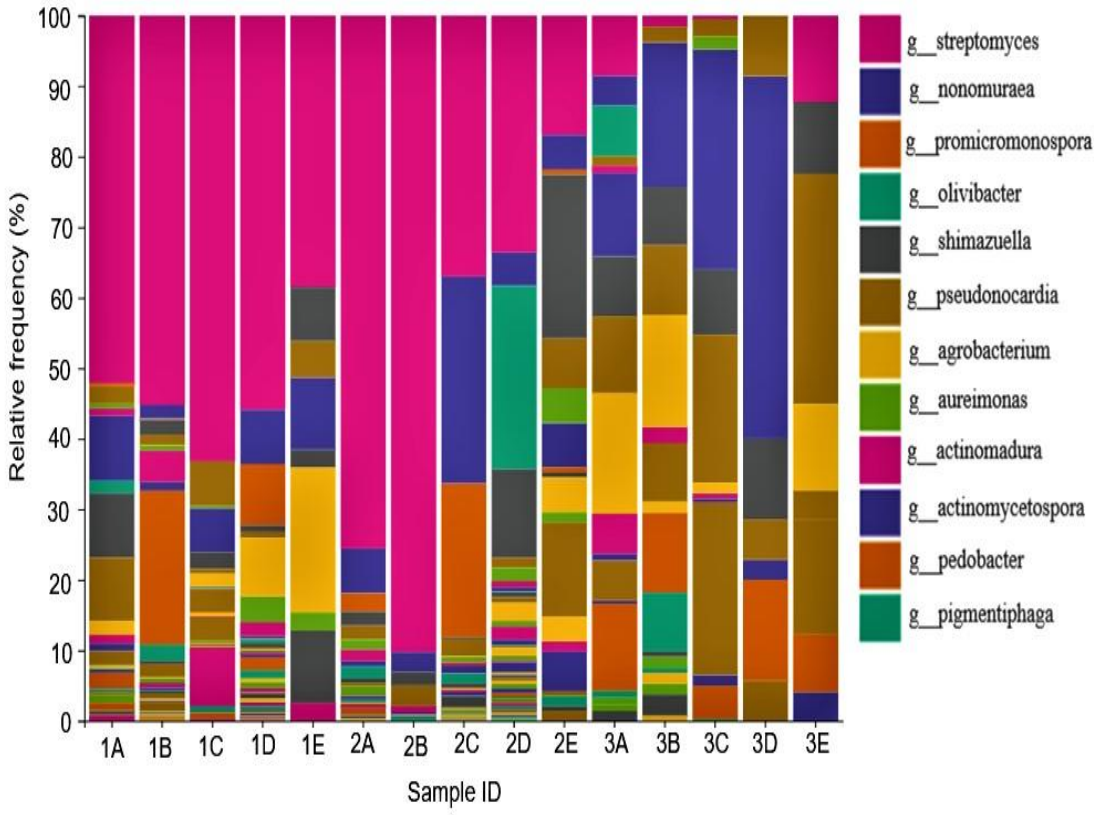

Figure 4.14: Taxonomic Bar-Plots of Bacterial Genera

Legend

Relative abundance of OTUs in the samples showing the distribution of bacterial genera at the taxonomic level, providing insights into the composition and prevalence of microbial communities.

4.3.1.5 Machine Learning Predictions for Differential OTU Presence

From the observed taxa-bar-plot patterns, the categorical sample data (counties) were predicted via machine-learning classifiers (Random Forest algorithm) in QIIME 2. The prediction was used in clustering sequences to reveal OTUs prevalent in a particular county with frequencies above 200 but absent or available in extremely low frequencies in another (**Figure 4.15**). For instance, Kwale had high means for *Agrobacterium,*

Actinocatenispora, and *Neorhizobium,* all completely absent in Kilifi and Lamu counties (**Figure 4.15 & Table 4.3**). In Kilifi, *Streptomyces* and *Pseudonocardia* were the defining microbial taxa (**Figure 4.15 & Table 4.3**). On the contrary, in Lamu, none of the OTUs had frequencies above 100 hence no distinct or defining microbial taxa were observed (**Figure 4.15**).

Ultimately, the performance of the machine learning classifier was assessed using the receiver-operating characteristic (ROC) curve for both micro-average and macro-average that exhibited strong overall performance (**Figure 4.16**). Micro-averaging computes metrics by averaging across all individual samples, which makes it susceptible to the influence of class imbalances within the dataset while macro-averaging treats each class equally, providing a more balanced perspective of classifier performance. The area under the curve (AUC) for micro-average was 0.72, while the AUC for the macro-average notably higher at 0.92 (**Figure 4.16**). This indicates that the Random Forest classifier exhibited strong overall performance in distinguishing between classes, particularly when considering each class equally in the macro-average.

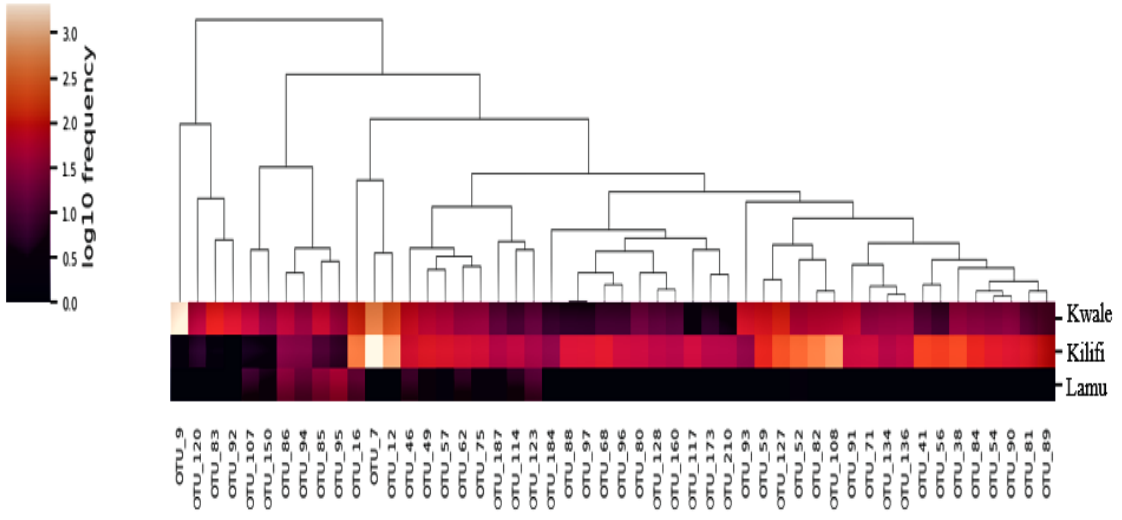

Figure 4.15: Heatmap of OTUs Prediction

Legend

Heatmap displaying the top 50 OTUs for county prediction. The darker colour indicates the absence of the specific OTU, while varying colours represent their presence. The scale represents $\log_{10}$ frequency, with darker shades indicating low or no occurrence and changing colours indicating OTU presence.

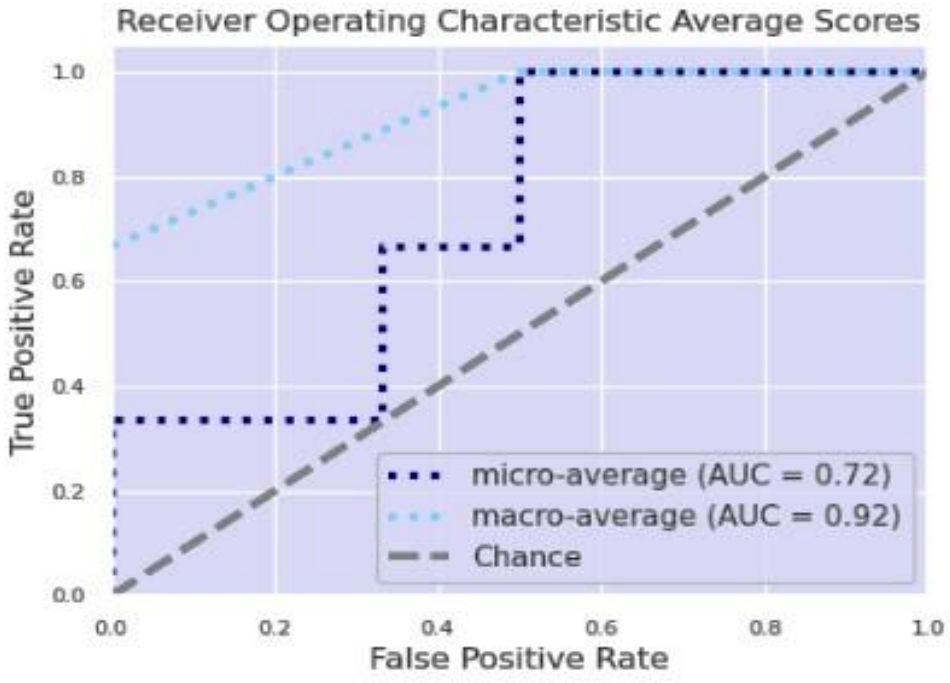

Figure 4.16: Receiver Operating Characteristic (ROC) Curve Showing Performance with the Random Forest Classifier.

Legend

This graphical representation compares sensitivity with "1-specificity." Sensitivity refers to the true positive rate, while "1-specificity" represents the false positive rate. The area under the ROC curve, falling within the range of 0.5 to 1, serves as a reliable metric for assessing classifier performance efficiency.

Table 4.3: Predominant Location-specific OTU's Defining Unique Microbiome Niche

Kwale		Kilifi	
OTU ID	**Genus's name**	**OTU ID**	**Genus's name**
OTU_9	*Agrobacterium*	OTU_117	*Streptomyces*
OTU_92	*Actinocatenispora*	OTU_108	*Streptomyces*
OTU_83	*Rhizobium*	OTU_210	*Pseudonocardia*
OTU_120	*Pigmentiphaga*	OTU_41	*Pseudonocardia*
OTU_107	*Sphingomonas*	OTU_173	*Streptomyces*
OTU_150	*Ochrobactrum*	OTU_56	*Streptomyces*

Note: The top three OTUs in each county were present with frequencies above 200 but occur in low frequencies or absent in the other counties

4.3.1.6 Characterizing Fungal Communities in the Sequencing Data

The incidental detection of fungal sequences in our 16S rRNA sequencing results is worth noting. Although our study primarily focused on bacterial identification for phytoplasma detection, the sequencing approach employed also captured fungal sequences within the dataset. However, it's essential to acknowledge the limitations inherent in using 16S rRNA sequencing for fungal identification. This method is less specific for fungal sequences compared to bacterial ones, leading to a relatively lower abundance and diversity of fungal sequences observed in our dataset. Nonetheless, reporting on these findings allows for a more holistic characterization of the microbial community present in the samples.

A total of 1,806 fungal sequences were obtained, clustered into 28 OTUs at a threshold of 97% sequence similarity (**Appendix X & XI**). All reads with less than 97% similarity with the known organisms in UNITE database were not considered for further analysis. Kilifi samples had the highest number of OTUs (26), followed by Kwale (22), and Lamu had the least at 10 (**Figure 4.17**). Kilifi also had the highest proportion of unique OTUs at 21.4%, compared to 3.6% for Kwale, with Lamu not recording any unique OTUs. Of the total OTUs, 32.1% were common among all the three counties (**Figure 4.17**). In addition, Kilifi had an excessive number of reads at 1,362 (75.41%), followed by Kwale

at 287 (15.89%), with Lamu at the extreme lowest at 157 reads (8.69%). Among the individual samples, sample 2A exhibited the highest read count, accounting for 54.65% of the total reads, while sample 3E had the lowest, comprising only 0.28% of the total reads (**Appendix X**).

The rarefaction curve plateaued at a sequencing depth of 150, indicating adequate characterization of microbial communities at this sampling depth (**Figure 4.18 & 4.19**). Kilifi samples exhibited greater saturation compared to Kwale and Lamu (**Figure 4.18**). Moreover, a comparison of curves between diseased and healthy samples revealed higher diversity within the diseased samples than the healthy ones (**Figure 4.19**).

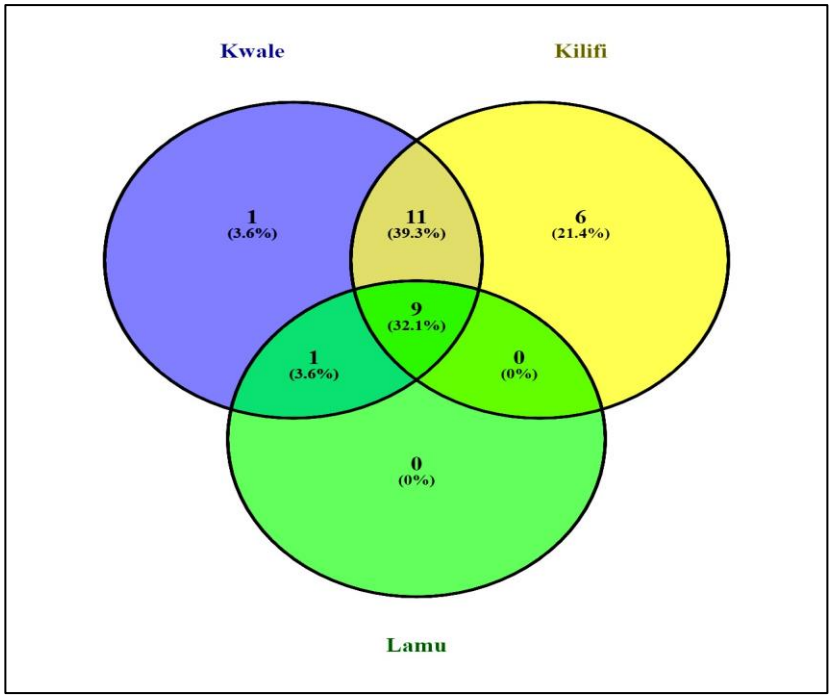

Figure 4.17: Venn Diagram to Compare Fungal Microbes either Common in all, Two or Specific for only One Geolocation. Venn diagram was done using VENNY

Source: (http://bioinfogp.cnb.csic.es/tools/venny/index.html).

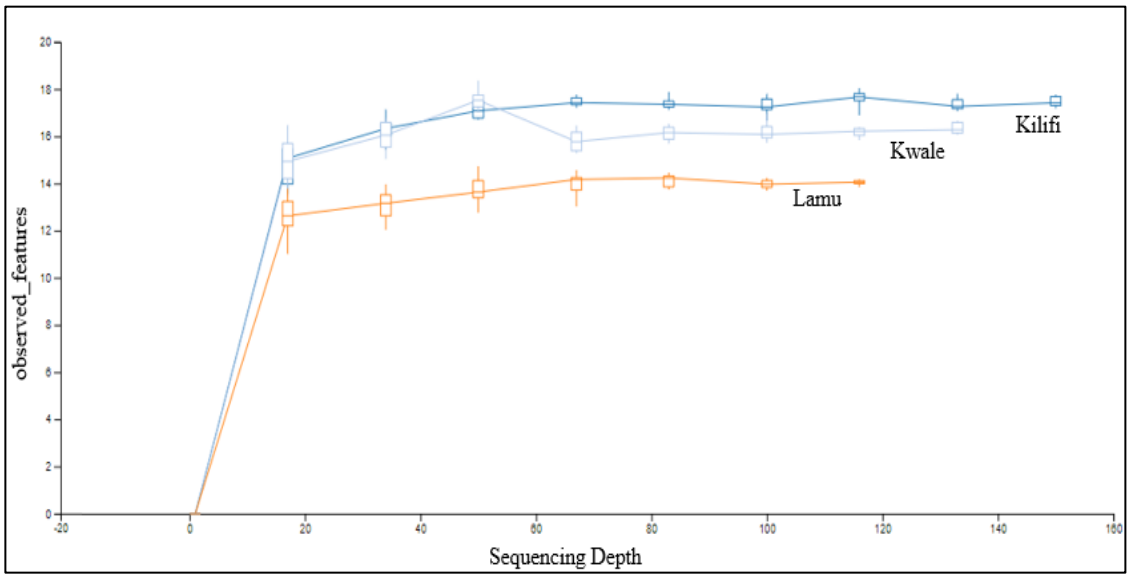

Figure 4.18: Alpha Rarefaction Curve Shows Sample Diversity with Increasing Sequencing Depth Based on the Counties.

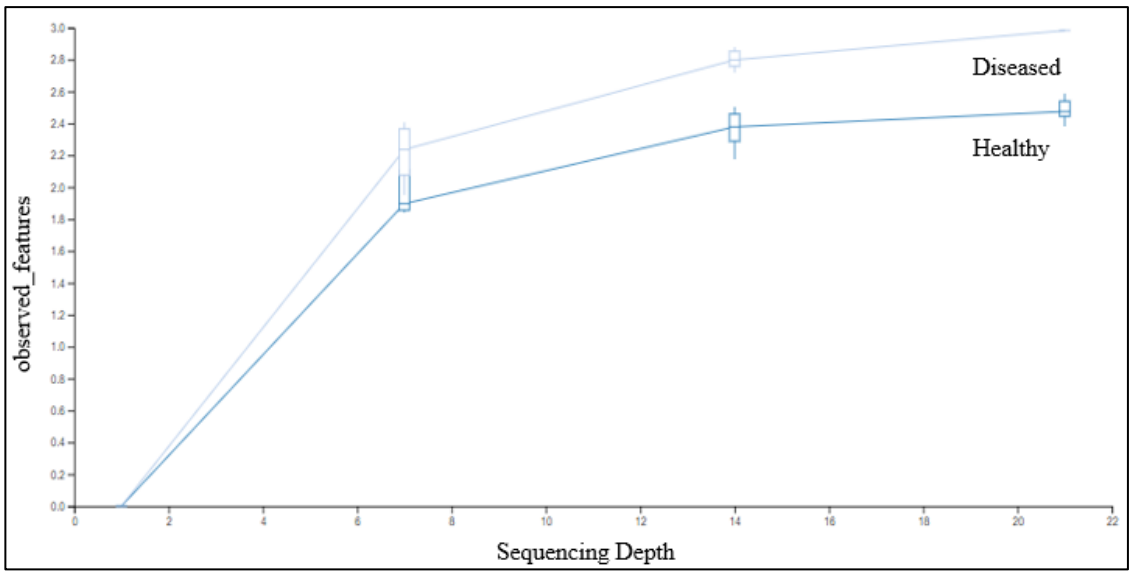

Figure 4.19: Alpha Rarefaction Curve Shows Sample Diversity with Increasing Sequencing Depth Based on the Condition

4.3.1.7 Diversity of Fungal Communities

Faith's PD and Pielou's evenness metrics were employed to evaluate fungal community diversity across the samples based on two metadata variables: counties and condition. For the counties, the Kruskal-Wallis test-derived p-values indicated no statistically significant differences in fungal richness and species distribution among samples across different counties (Faith's PD, p-value= 0.16; Pielou's evenness, p-value= 0.59) (**Table 4.4**). Kilifi exhibited the highest richness and evenness, followed by Kwale and Lamu (**Figure 4.20**). Similarly, regarding condition, there were no significant differences in fungal richness and evenness among samples across various conditions (Faith's PD, p-value= 0.25; Pielou's evenness, p-value= 0.23) (**Table 4.4**). Diseased samples demonstrated higher richness and evenness compared to healthy ones (**Figure 4.21**). Overall, this analysis indicates the absence of statistically significant differences in fungal diversity across the observed variables.

Table 4.4: Kruskal-Wallis Test Results for Fungal Diversity

Observed variables		Faith's PD	Pielou's evenness
Counties	**H**	3.6929729729729766	1.056140350877201
	p-value	0.157790592888845	0.589741970759238
Condition	**H**	1.3453453453453548	1.4391447368421053
	p-value	0.24609350106407027	0.23027779075066712

Note: The Kruskal-Wallis test was not significant at the significance level of 0.05, suggesting no statistical difference among samples in the different counties and conditions.

The beta diversity metrices, Unweighted and Weighted UniFrac distances, were employed to evaluate dissimilarity coefficients among the samples. In the Unweighted UniFrac analysis, the PCoA plot did not exhibit clear clustering, suggesting a lack of distinct separation based on the variables considered, although some clustering tendency was observed in terms of counties (**Figure 4.22**). However, the Weighted UniFrac analysis

revealed a distinct clustering pattern primarily attributed to the counties rather than the condition of the samples. Kwale and Lamu samples exhibited a distinctive clustering pattern, as evidenced in the Weighted UniFrac analysis. However, the clustering was not entirely distinct, as certain samples, such as 2B from Kilifi, clustered alongside Kwale samples, while samples 1D and 1E from Kwale clustered with Kilifi samples (**Figure 4.22**). Principal Component (PC) analysis further elucidated these findings, with PC 1, PC 2, and PC 3 of Unweighted UniFrac explaining 39.28%, 26.99%, and 18.66% of the total changes, respectively. Similarly, PC 1, PC 2, and PC 3 of Weighted UniFrac accounted for 48.32%, 25.06%, and 17.14% of the total changes, respectively (**Figure 4.22**).

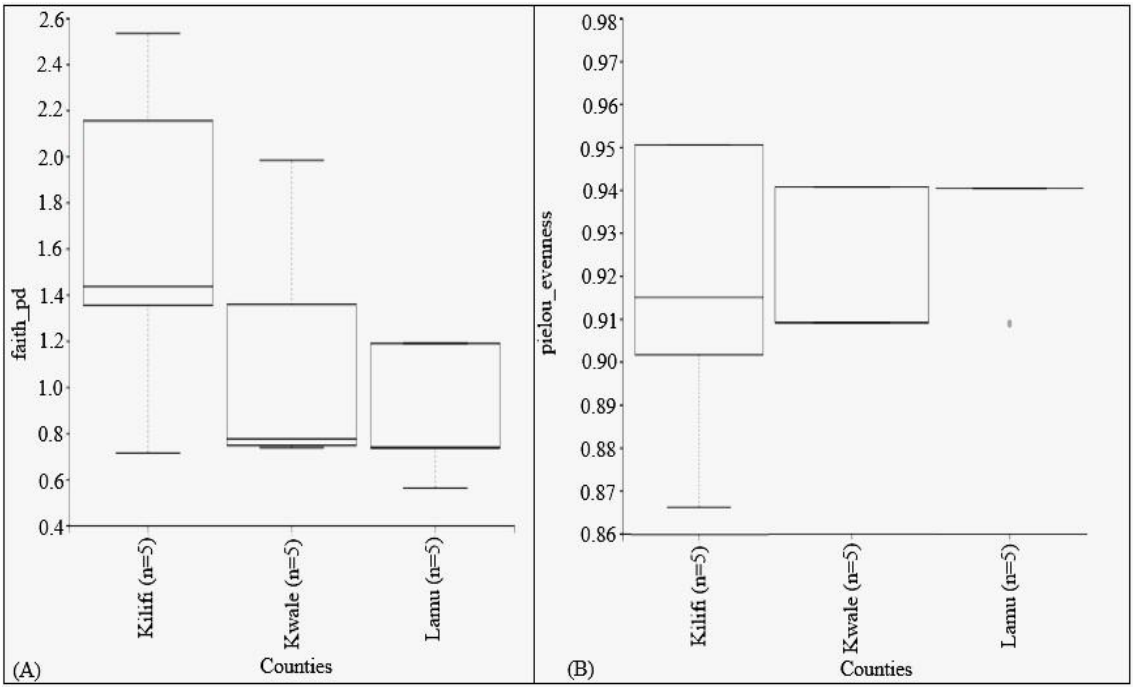

Figure 4.20: Boxplot of Faith's Phylogenetic and Pielou's Evenness Fungal Diversity Indices in the Three Counties.

Legend

The boxplots display the comparison of fungal diversity indices in Kilifi, Kwale, and Lamu counties. Both boxplots, A for Faith's PD index and B for Pielou's evenness diversity, show no significant difference ($p > 0.05$) among the three counties.

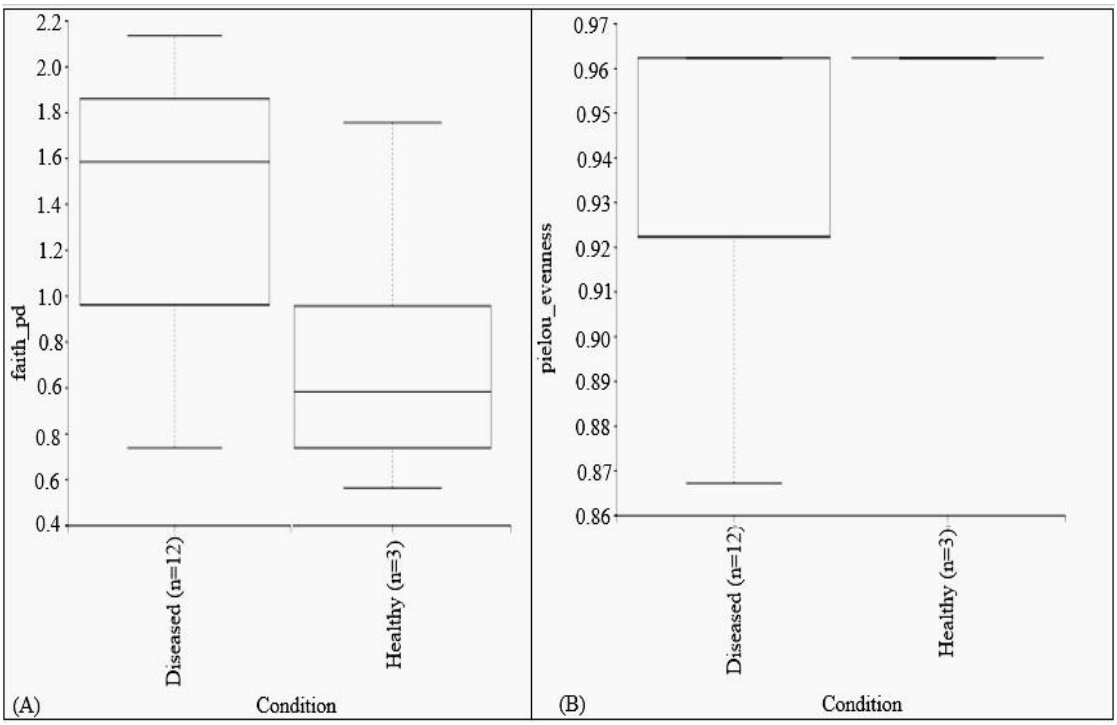

Figure 4.21: Boxplot of Faith's Phylogenetic and Pielou's Evenness Fungal Diversity Indices in the Two Conditions.

Legend

The boxplots display the comparison of fungal diversity indices in diseased and healthy samples. Both boxplots, A for Faith's PD index and Boxplot B for Pielou's evenness diversity, show no significant difference ($p > 0.05$) between the two conditions.

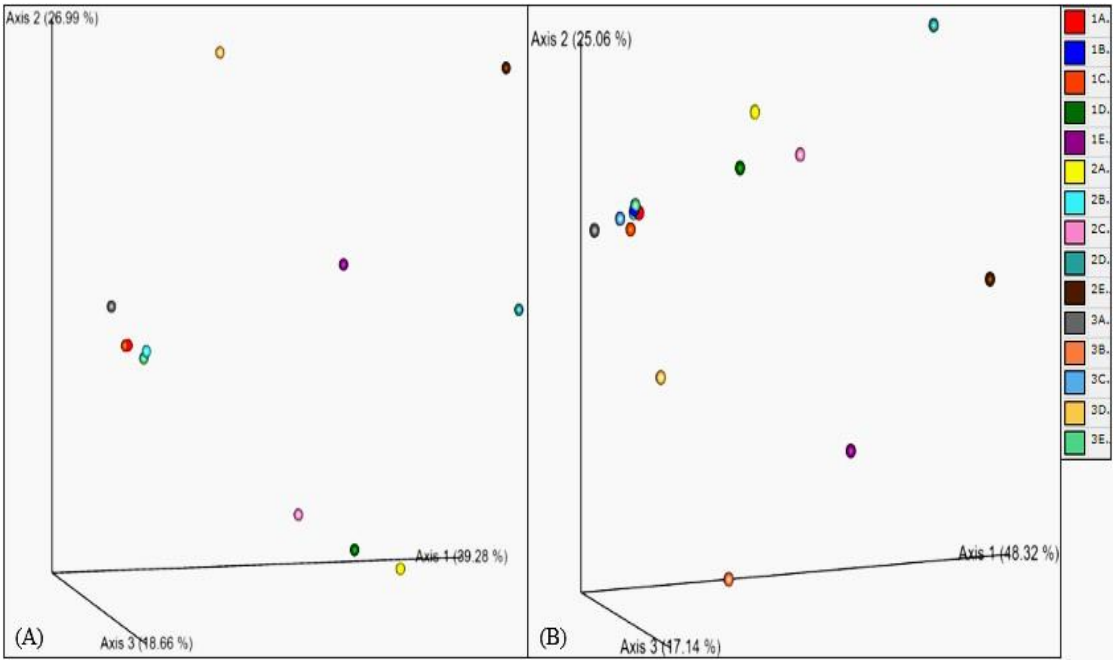

Figure 4.22: PCoA Plots of Beta Diversity of Fungal Microbial Communities

Legend

The emperor plots illustrate the beta diversity of fungi where A is the Unweighted UniFrac and B is Weighted UniFrac. They capture the overall dissimilarity among samples and phylogenetic relatedness. The plots provide insights into the spatial distribution and clustering patterns of fungal communities across the samples.

4.3.1.8 Statistical Analysis of Sequencing Data

The PERMANOVA analysis conducted on the fungal community profiles, for unweighted group significance showed differences driven by the three counties, yielding a p-value of 0.064 (**Figure 4.23**). The boxplot illustrating distances to Kilifi suggested a greater variability among samples from Kilifi, indicating a closer similarity to Kwale than Lamu (**Figure 4.23**). Distances to Kwale exhibited relatively consistent samples with almost identical fungal community profiles to Kilifi and Lamu. Distances to Lamu depicted varying sizes of boxplots, indicating a partial similarity to Kwale samples but a distinct difference from Kilifi (**Figure 4.23**). In terms of condition, unweighted group significance

demonstrated minimal influence of the two conditions on variations in fungal community profiles, evidenced by a p-value of 0.519 (**Figure 4.24**). Analysis of distances to the diseased boxplot revealed a degree of consistency between diseased and healthy samples, with nearly identical microbial community profiles. The boxplot illustrating distances to healthy samples highlighted higher variability among diseased samples (**Figure 4.24**).

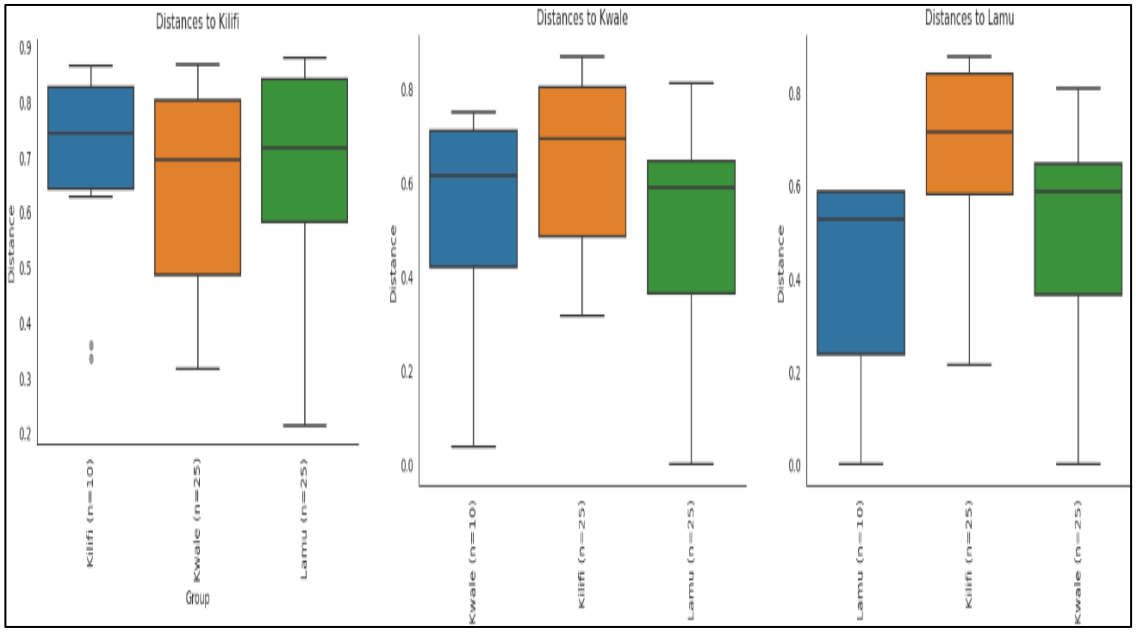

Figure 4.23: Unweighted Unifrac Significance Plots of the Fungal Microbial Communities' Samples from the Three Counties

Legend

The group significance plots display the dissimilarity between within-group distances and the between-group distance for the samples. The first plot represents the distances to Kilifi, second plot represents the distances to Kwale, and third plot represents the distances to Lamu. The plots highlight the variations in fungal community composition and the significance of between-group dissimilarities among the different locations.

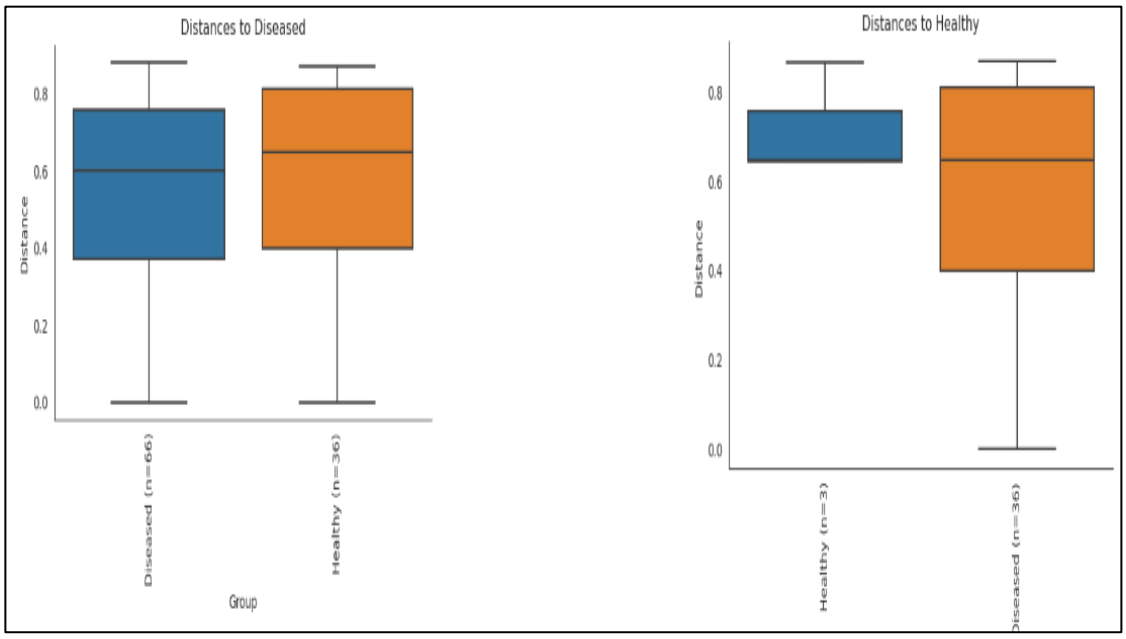

Figure 4.24: Unweighted Unifrac Significance Plots of the Fungal Microbial Communities' Samples in the Two Conditions

Legend

The group significance plots display the dissimilarity between within-group distances and the between-group distance for the samples. The first plot represents the distances to diseased, and second plot represents the distances to healthy. The plots highlight the variations in fungal community composition and the significance of between-group dissimilarities among the different conditions.

4.3.1.9 Taxonomic Analysis of Fungi

The fungal reference sequences from UNITE were utilized to create interactive bar plots, showcasing the relative abundances of organisms at specific taxonomic levels in each sample. The identified sequences were divided into two phyla, with Ascomycota being the dominant phylum, accounting for 98.56% of the sequences, while Basidiomycota represented only a tiny proportion at 1.44% **(Figure 4.25)**. Notably, among the 28 OTUs, only one belonged to the Basidiomycota phylum **(Appendix X & XI)**.

The sequence reads were classified into 17 separate taxa at the genus level, most of which were found in Kilifi samples. **(Figure 4.26)**. The most prevalent genus was *Cyphellophora*, accounting for 22.42% of the total reads, closely followed by Devriesia at 21.93% and Lepidosphaeria at 14.56%. While not dominant, other genera like *Clonostachys*, *Bipolaris*, *Microxyphium*, *Acremonium* and *Fusarium* were still present in significant proportions, comprising 8.69%, 6.47%, 4.98%, 3.77% and 3.49%, respectively **(Appendix X)**. Notably, samples from Kilifi, particularly sample 2A, exhibited the highest abundance of sequences at 54.65%. *Cyphellophora* and *Devriesia* were the most abundant genera in Kilifi, collectively representing 44.35% of the total reads **(Figure 4.26 & Appendix X)**. On the other hand, Lamu had the fewest sequences, with sample 3C only accounting for 0.28% of the total reads. Additionally, *Devriesia* was also prominent in the Lamu samples, with 97 reads **(Appendix X)**.

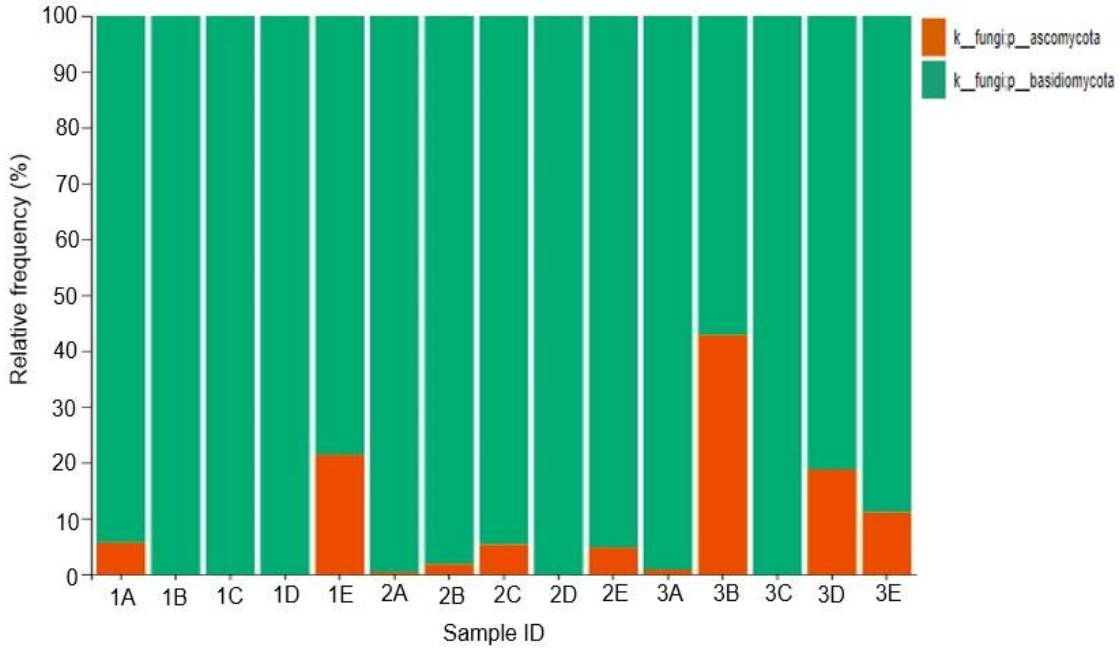

Figure 4.25: Taxonomic Bar-Plots of Fungal Phyla

Legend

Relative abundance of OTUs in the samples from the three different counties showing the distribution of fungal phyla at the taxonomic level, providing insights into the composition and prevalence of microbial communities among the counties.

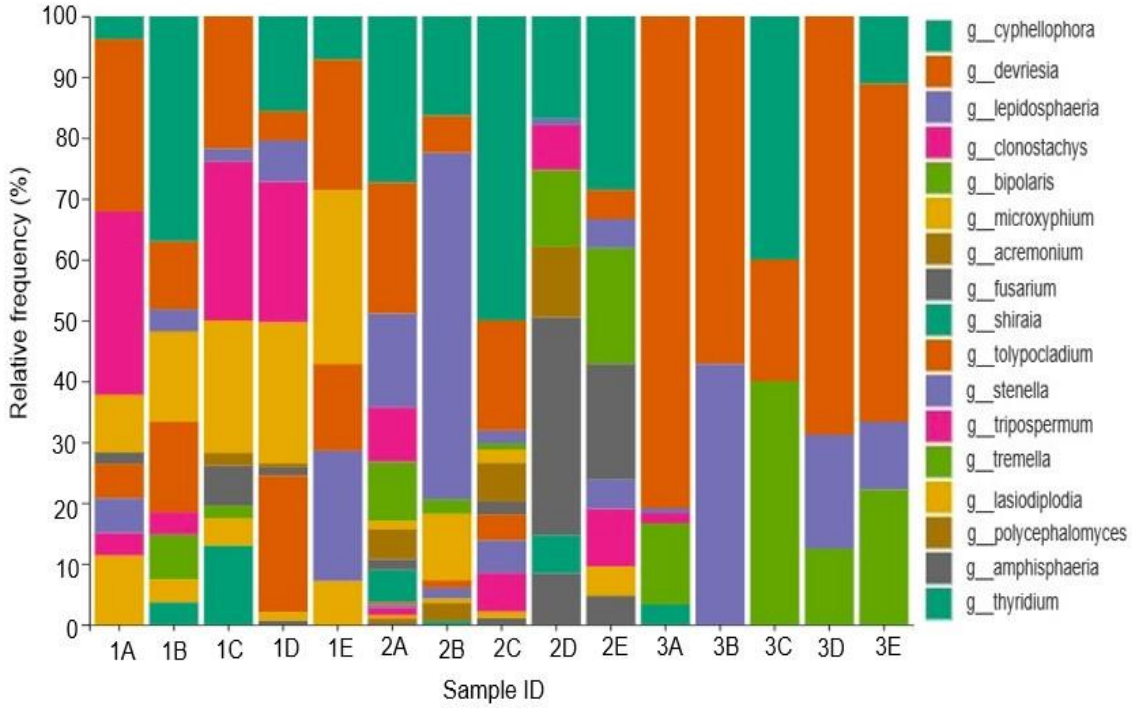

Figure 4.26: Taxonomic Bar-Plots of Fungal Genera

Legend

Relative abundance of OTUs in the samples from the three different counties showing the distribution of fungal genera at the taxonomic level, providing insights into the composition and prevalence of microbial communities among the counties.

4.3.2 Screening for Phytoplasma using PCR Technique

The total DNA from symptomatic and healthy leaves was subjected to nested PCR to detect phytoplasma strains. Despite using universal primers in the first amplification and

specific primers in the second amplification, nested PCR analysis revealed the absence of target bands in the expected size range therefore no bands corresponding to the anticipated amplicon sizes (1800 bp and 763 bp) were observed on the gel (**Plate 4.3**). This confirms the lack of amplification for the targeted phytoplasma DNA fragments. This provided corroborating evidence of the absence of phytoplasma, thus aligning with the findings obtained from NGS analysis.

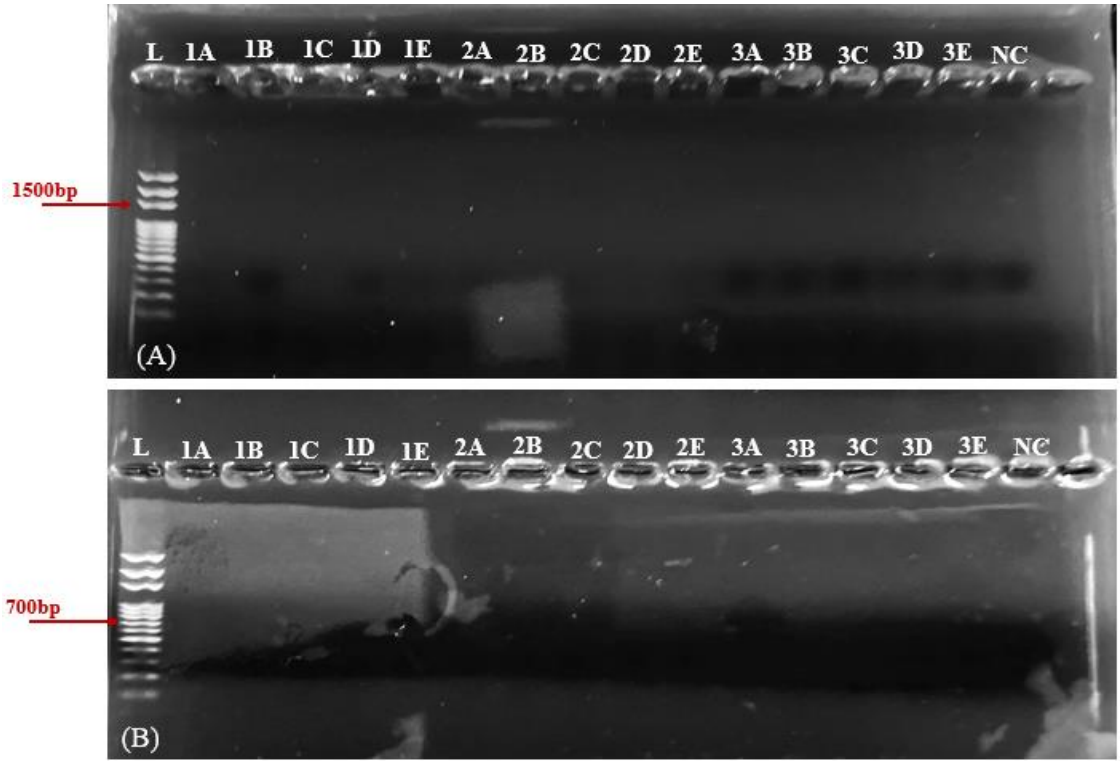

Plate 4.3: Gel Photograph Showing Absence of Phytoplasma Strains

Legend

L) Molecular marker (100 bp DNA Ladder), Diseased samples; 1A, 1B, 1C, 1D, 2A, 2B, 2C, 2D, 3A, 3B, 3C, and 3D, while the healthy controls were 1E, 2E, and 3E. NC is for negative control. Photograph A represents the first PCR reaction using universal primers for phytoplasma, while Photograph B represents the second PCR reaction specific to CLYD.

CHAPTER FIVE

DISCUSSION, CONCLUSION AND RECOMMENDATIONS

5.1 Discussion

This study is the first to quantitatively assess the prevalence and severity of yellowing diseased coconut plants along the Kenyan coast. While previous survey studies have mentioned diseases as constraints to coconut production in the region (Afa-nocd, 2020), they did not provide quantitative data on disease prevalence and severity, making it challenging to assess the relative importance of this disease. A descriptive cross-sectional survey was conducted, allowing accurate information to be collected from a larger sample group, as also described by Wang & Cheng, (2020). This approach was particularly suitable for exploring the microbial communities associated with yellowing diseased coconut plants in the region. Studying the microbial diversity of diseased plants is a quick way to understand the structure and functioning of microbial communities, and it could contribute to the isolation and detection of new microbes (Mushtaq et al., 2022). The study employed culture-dependent and culture-independent techniques to characterize and explore the diversity and composition of microbial communities in coconut leaves affected by yellowing symptoms. While previous research in Kenya has reported the presence of pathogens in coconut palms (Pole et al., 2014), this study provides the first molecular evidence of their presence in coconut plants exhibiting yellowing symptoms.

5.1.1 Prevalence and Severity of Yellowing Diseased Symptoms in the Three Counties

The survey included three counties on the Kenyan coast, and yellowing diseased symptoms were prevalent in all the surveyed regions but with varying intensity. Kilifi had the highest score of prevalence and severity, indicating that it was the most affected county in terms of the symptoms observed, while Lamu had the least score (**Figure 4.1**). The variations in these scores could be attributed to the diverse farming techniques and agricultural practices employed, as well as the unique environmental factors present in

each specific area. Intercropping practices were observed on some of the farms visited in Kilifi, where coconut was grown in close proximity to other crops, thereby facilitating microbial spread through horizontal gene transfer. In Lamu, most of the coconuts belong to the Dwarf variety, while Kilifi has a significant presence of EAT (Alpex Consulting Africa Ltd, 2013). According to Kadere, (2021), dwarf varieties demonstrate greater resilience and can withstand harsh conditions better than tall types.

Kilifi also experiences higher humidity throughout the year, which promotes the distribution of pathogens responsible for yellowing symptoms. On the other hand, Lamu's sampling sites are characterized by higher altitude and lower humidity, creating less favourable conditions for the microbes to spread and resulting in less severe symptoms (Ayugi et al., 2016; Dorestani & Aliabadi, 2017). An earlier research has observed the impact of temperature, relative humidity, rainfall, sun shining hour, and leaf wetness on the occurrence and severity of diseases in different pathosystems (Khan & Hossain, 2014). Moreover, the extent of land used for coconut cultivation may also play a role in the coconut's vulnerability to yellowing symptoms. As the coconut cultivation area grows, the risk of being susceptible to certain diseases also increases. Kilifi has the largest coconut cultivation area, followed by Kwale, and Lamu has the smallest coconut cultivation area, making it more vulnerable to yellowing symptoms (Afa-nocd, 2020).

The strong positive correlation observed implies that as the prevalence increases, so does severity. Correlation analysis clarifies relationships between the two variables, but it does not prove causation. A strong correlation does not always mean that one variable causes another; rather, it only means that they tend to move in simultaneously (Dorestani & Aliabadi, 2017). Another possible explanation for the high disease severity in Kilifi is that most of the symptoms were observed in old coconut plants, which are more susceptible to the disease. Most of the coconut plants in Kilifi were old compared to Lamu, which mainly consisted of younger plants. Moreover, according to Ngugi et al., (2002) severe epidemics in young plants can sometimes affect subsequent disease development hence the low disease severity levels observed in Lamu. The geographical locations, therefore, influence the prevalence and severity, providing vital information for researchers who want to

obtain data on the importance of yellowing diseases to coconut production in the coastal region. These studies relating surveys to yield loss need to be replicated in more geographical locations to be sensitive to the differences in complex constituents. According to research by Urashima et al., (2017), it has been observed that an entire field can potentially become contaminated by a single diseased plant.

5.1.2 Morphological Characterization of Bacterial and Fungal Isolates

In the hierarchical cluster analysis, the software selected representative samples to optimize visualization and interpretation by considering similarities in certain characteristics. According to the culture-dependent methods, numerous bacterial and fungal isolates were found in the samples. These methods have previously been used to characterize microbiota in yellowing diseased coconut plants, providing valuable insights into their identity, physiology, and potential ecological roles (Nadia et al., 2017; Ogugua & Salome, 2015).

Morphological and biochemical characteristics were used to determine the isolates and compared with known microbes associated with yellowing disease (positive controls). While morphological analysis observes and describes the physical properties of microbial cells, biochemical analysis looks at the ability of microbes to produce certain enzymes or use particular substrates, which can help differentiate the microbes (Gopireddy, 2011; Thomas et al., 2015). The ability to identify microorganisms and comprehend their roles in ecosystems makes these analyses valuable (Kim & Kim, 2021). A more thorough grasp of microbial diversity and ecology can be attained by merging morphological and biochemical data (Coughlan et al., 2015).

Visualization tools automatically limited the displayed isolates to produce a clearer and more interpretable clustergrams, effectively managing complexity in large datasets and ensuring efficient analysis to facilitate meaningful insights (Pasupathi et al., 2021). Consequently, not all isolates were included in the clustergram, reflecting the prioritization of representative data points for effective visualization and analysis (Li et

al., 2022). As a result, some bacterial isolates showed similarities to the positive controls, including *Erwinia psidii, Burkholderia nodosa, Leifsonia spp, Streptomyces fradiae,* and *Pantoea agglomerans* (**Figure 4.2**). These bacteria were also identified in a previous study by Nadia et al., (2017) in yellowing diseased coconuts. Among the bacterial isolates, *Streptomyces spp, Burkholderia spp, Leifsonia spp, Bacillus spp, Curtobacterium spp, Pseudomonas spp,* and *Enterobacter spp.* were identified through NGS analysis. For fungal isolates, morphological characteristics were used to characterize the isolates and compared with positive controls. Similarities were found between some isolates and *Phytophthora palmivora, Gibberella fujikuroi, Drechslera halodes, Ganoderma tornatum, Fusarium solani, Bipolaris incurvata,* and *Aspergillus nomius* (**Figure 4.3**). Previous studies by De Assis Costa et al., (2018) and Nadia et al., (2017) identified these fungi in yellowing diseased coconuts. The NGS analysis only confirmed the presence of *Fusarium spp, Bipolaris spp,* and *Mycosphaerella spp.* among the identified fungi. The results revealed similarities between isolates and known pathogens, providing valuable insights into the microbial composition of diseased coconut plants.

5.1.3 The Genetic Identity of Microbial Communities and Phytoplasma in Sampled Coconut Plants

The study identified 172 pure bacterial isolates and 109 pure fungal isolates using culture methods as compared to NGS, which identified 113,330 and 1,806 reads, respectively **(Appendix VIII).** Similar to what Coughlan et al., (2015) reported, this shows that culture methods provide approximately 0.1% to 10% of information on a particular sample's microbial diversity, which is insufficient for adequate analysis. The sequences collected for this study provide an overview of the yellowing diseased coconut microbiome that could not be detected using culture techniques. Amplicon sequencing of 16S rRNA gene on the Illumina MiSeq platform using NGS (bTEFAP) was initially described by Dowd et al., (2008) and has since been utilized in describing a wide range of microbes.

The alpha rarefaction was used to control the differences in sequencing depth across all samples, enabling direct comparison. In our case, a sampling depth of 25,000 was used

where the curves levelled off, indicating that the bacterial communities were reasonably well characterized with our sampling effort and that most microbial community diversities were captured (**Figure 4.6 & 4.7**). The rarefaction curves of OTUs also recorded different saturation levels and uneven curve distributions. Regarding counties, Kilifi exhibited the highest concentration, with Kwale following, and Lamu coming third. In terms of condition, there was a greater concentration of diseased samples compared to healthy ones. According to a survey by KCDA, on average, Lamu has recorded the highest yield of coconuts per tree, meaning challenges like plant pathogens are less faced (Alpex Consulting Africa Ltd, 2013).

The Kruskal-Wallis test results in Table 4.2 indicate no statistically significant differences in bacterial diversity based on the observed variables. This implies relatively consistent microbial ecology within the sampled populations across counties and conditions. Additionally, based on the alpha diversity boxplots, Kilifi exhibited the highest diversity in terms of richness and evenness, followed by Kwale, while Lamu showed the lowest diversity (**Figure 4.8**). These differences can be linked to variables that affect the growth and spread of microorganisms, such as humidity, human activities, and geographic location. Kilifi and Kwale have more humid climates, which foster an environment conducive to microbial growth. Aidoo et al., (2021) described that climate change can affect the distribution and abundance of plant pathogens by impacting host resistance and microbial interactions. Additionally, Dong et al., (2019) also hypothesized that geographic location significantly impacts the makeup of the phyllospheric community of plants. The higher occurrence of human activities in Kilifi and Kwale compared to Lamu may also contribute to the variations in microbial composition. According to Cavicchioli et al., (2019) and Gurr et al., (2016), human activities impact the widespread dispersal of microorganisms throughout different locations. On the other hand, bacterial diversity in the healthy samples was found to be less diverse than in symptomatic samples. This observation aligns with findings from Nadia et al., (2017), which similarly indicated that non-symptomatic plants exhibited a lower bacterial concentration.

The PCoA analysis indicated that samples within each county were clustered together, suggesting that the bacterial communities within each county are similar. Samples from Lamu were the most similar and consisted of lineages with a common evolutionary history since they were closely packed together compared to the others (**Figure 4.10**). Furthermore, samples from Lamu are not far from the origin compared to Kilifi and Kwale. This means that samples from Kilifi and Kwale are changing very fast compared to Lamu, which are changing slowly. For Kilifi and Kwale samples, though not closely packed together, showed a similar pattern in their clustering. This also means that as much as they were diverse, they also had similar evolutionary relationships. This disparity in samples from Kilifi and Kwale, shown by the PCoA plots, indicates fast changes in the relative abundance of bacterial communities. This suggests dysbiosis in the coconut plants and is known to cause stress and symptoms like leaf necrosis and death (Lei, 2020).

There was also an overlap of samples between Kilifi and Kwale, indicating that diseased coconut trees from the two counties could be colonized by the same type of bacteria. This aligns with a research by Nadia et al., (2017), who found that coconut plants displaying yellowing signs can carry comparable bacterial species irrespective of ecological location. However, in general, the beta diversity analyses showed that the variation in bacterial community composition was primarily driven by differences between the counties rather than within-county variation. Furthermore, the PCoA analysis also indicates that the healthy samples showed a closer clustering pattern with the Lamu samples, suggesting a strong similarity between the two. This aligns with findings of Hong et al., (2015), where some samples clustered with healthy samples. These results suggest that the microbial communities observed in diseased samples in Lamu, may represent either a transitional phase from a healthy state to widespread disease or the result of a distinct process of community selection associated with a specific localized disease condition.

PERMANOVA analysis showed that the three counties were significantly driving differences in the bacterial community profiles, indicating that the bacterial communities in each county are distinct from one another (**Figure 4.11**). The findings emphasize the importance of studying microbial communities at a regional level and suggest that even

slight geographic differences can significantly impact microbial community composition. Regarding the condition factor, it was observed that the differences in bacterial profiles were not primarily influenced by the two conditions. This implies that the bacterial communities observed in healthy coconut samples were also present in diseased samples, albeit in reduced proportions (**Figure 4.11**).

The taxonomic classification suggests that while the bacterial communities in the three counties share somewhat similar ecological niches, some specific bacterial taxa are still supported in particular niches. The compositions of bacteria in the samples were analyzed at phylum and genus levels. The higher abundance of Actinobacteria in all samples may indicate their adaptation to the environmental conditions in the study area. Moreover, Barka et al., (2016) confirmed that Actinobacteria can adapt to a variety of ecological environments depending on habitat and the prevailing climate conditions. Despite being predominantly found in soil (Lewin et al., 2016), in this study, Actinobacteria were isolated in significant quantities from leaves, indicating their presence in diverse environments. Previous studies that have assessed microbial communities on coconut plants have also shown the presence of Actinobacteria in high titers (Nadia et al., 2017). Actinobacteria includes harmful bacteria that cause plant diseases and can easily share genes with other bacteria through horizontal gene transfer, spreading their harmful traits (Lewin et al., 2016).

The most dominant genera in this study, *Streptomyce*s (a defining microbial taxon in Kilifi) and *Nonomuraea*, are also found in this phylum. These bacteria are renowned for producing bioactive metabolites that possess antimicrobial properties (Beaudoin et al., 2021; Sungthong & Nakaew, 2015). The abundance of *Streptomyces* and *Nonomuraea* in Kilifi and Kwale samples may indicate the prevalence of soil and rhizosphere-associated bacteria in these regions, as these genera are commonly found in soil environments (Barka et al., 2016; Sungthong & Nakaew, 2015). While these bacteria form mutualistic relationships with coconut plants and plants in general, protecting them against pathogens through the production of secondary metabolites and activation of the plant's immune system, it is important to note that they can pose some environmental concerns. If not

properly managed, the antimicrobial properties of these metabolites can disrupt natural microbial communities and potentially affect beneficial microorganisms (Isayenka & Beaudoin, 2022). Additionally, certain *Streptomyces* spp. can cause potato scab and produce thaxtomins, a family of phytotoxins, that produce compounds that are intimately involved in disease development in plants (Beaudoin et al., 2021; Isayenka & Beaudoin, 2022; Pandey & Gupta, 2020). Despite reduced microbial diversity in healthy coconut samples, *Streptomyces* and *Nonomuraea* genera continued to dominate, suggesting their potential significance in either suppressing diseases or preserving plant health. This aligns with a previous review by Beaudoin et al., (2021), highlighting *Streptomyces'* prevalence in healthy plant microbiomes. However, further investigation is needed to understand their specific functions and interactions. Another genus in Actinobacteria was *Pseudonocardia*, detected in all samples and a defining microbial taxon in Kilifi (**Figure 4.15**). It is a known antifungal commensal microorganism, and a higher abundance of this taxon might instead reflect the presence of fungal organisms that might be causing diseases in the coconut plant (Navarro-Martínez et al., 2017).

Proteobacteria was the next dominant phylum in our study, consistent with previous reports highlighting its abundance in plants (Nadia et al., 2017). Extending this knowledge to coconut trees, it has been documented that Alpha-, Beta-, and Gamma-proteobacteria are commonly present in high quantities in the coconut rhizosphere (Pandey & Gupta, 2020b). In our investigation, we observed the presence of *Burkholderia* and *Agrobacterium* genera, both associated with coconut plants exhibiting yellowing symptoms. While these bacteria are known to confer benefits to coconuts, they can be parasitic to other plant species. *Agrobacterium*, for instance, which was also a predominant microbial taxon in Kwale (**Table 4.2**), forms a parasitic relationship with plants, transferring its DNA (T-DNA) into the host plant's genome, leading to genetic modification. Although *Agrobacterium* is known to cause crown gall disease, no signs of the disease were observed in the coconut plants. This could be because the strain of *Agrobacterium* present in the samples might not be virulent enough to cause crown gall in coconuts (Gorshkov & Tsers, 2022). *Burkholderia*, on the other hand, has been

implicated in the yellowing of leguminous plants (Villarreal, 2017), severe seed-borne diseases in rice, wilting symptoms in various crops and also an important causal agent of leaf spots in orchid plants known to grow on various palm trees (Korir et al., 2017; Villarreal, 2017). These bacteria are known to induce plant diseases; for instance, phytopathogenic bacteria like *Burkholderia andropogonis* can infect more than 52 species of 15 families of unrelated monocotyledonous plants, with coconut palms being one of them (Elshafie & Camele, 2021; Nowak & Coenye, 2008). Another genus in Proteobacteria is *Sphingomonas*, which was detected in all samples. It is known to exist on most plants' aerial surfaces, though its pathogenicity has not been reported; it is closely related to the genus *Rhizomonas* that causes corky root disease of lettuce (Francis et al., 2014).

Other defining microbial taxa in Kwale, *Actinocatenispora*, and *Neorhizobium*, indicate their higher susceptibility in this county. These genera also play essential roles in plant-microbe interactions. *Actinocatenispora*, as an Actinobacteria, exhibits diverse metabolic capabilities and can contribute to plant growth promotion and disease suppression (Natsagdorj et al., 2021). The nitrogen-fixing bacteria *Neorhizobium*, on the other hand, creates symbiotic relationships with leguminous plants and gives them a crucial supply of nitrogen (Mousavi et al., 2014). These bacteria show mutualistic interactions between microbes and plants, which impact plant growth, nutrient uptake, and general plant health. It is noteworthy that Lamu did not exhibit any defining microbial taxa in contrast to the other counties. Interestingly, a survey conducted by the KCDA revealed that Lamu has a higher coconut yield per tree, implying a potentially lower incidence of plant pathogens in that region (Alpex Consulting Africa Ltd, 2013). The lower bacterial read counts in healthy samples compared to diseased ones raise questions about the impact of reduced diversity on coconut plant health signifying the presence of a more stable and resilient microbial community in healthy samples, better equipped to withstand pathogenic threats.

The prediction of categorical sample data (counties) was achieved without utilizing reference sequences. Instead, a machine learning-based approach, specifically the Random Forest algorithm, was employed to make predictions based on the observed taxa-

bar-plot patterns (Tonkovic et al., 2020). The classifier was trained using sequencing data to predict a county's susceptibility to specific bacteria, determined by its microbiome composition. This involved data clustering to identify prevalent bacteria in one county and those either absent or found in very low numbers in others, thereby establishing a sense of regional affiliation and enabling sample origin prediction, hence identifying defining microbial taxa of each county.

According to the results, each county had a unique defining microbial taxon, with specific OTUs that are more abundant in one county than others, making the specific counties more susceptible to the particular microbe. In addition to the defining microbial taxa previously discussed, the analysis also identified OTU 7 and OTU 12, representing *Nonomuraea* and *Pigmentiphaga*, respectively, as defining microbial taxa in Kilifi & Kwale but absent in Lamu. This suggests that these two counties are most susceptible to the two bacterial genera. For Lamu county, the frequencies were very low (<100); hence we couldn't necessarily place a bacterium to belong there specifically. This study used this classifier due to its high accuracy, fast prediction speed, endurance of noisy data and requires few tunable parameters (Deneke et al., 2017). This study also depicts the importance of considering both micro-average and macro-average metrics in classifier evaluation. While the micro-average provides a global perspective, the macro-average, by treating each class equally, highlights the classifier's performance in more challenging scenarios. In this case, the significantly higher AUC for macro-average underscores the classifier's ability to excel even when faced with class imbalances in the dataset (**Figure 4.16**).

The fungal communities exhibited similar patterns to those observed in the bacterial communities, as evidenced by the rarefaction curves of OTUs displaying varying levels of saturation and uneven distributions. When considering the geographical distribution across counties, Kilifi emerged with the highest concentration of fungal species, followed by Kwale, and then Lamu, indicating a gradient in fungal diversity across the study area. This variation in fungal richness and evenness among the counties reflects the diverse ecological conditions and microbial habitats present in each location (Aidoo et al., 2021;

Dong et al., 2019). There was a noticeable abundance of fungal species in the diseased samples compared to the healthy ones, indicating a potential association between disease state and fungal diversity. This observation aligns with previous studies suggesting that disease conditions can influence microbial community composition and diversity (Nadia et al., 2017). Kilifi exhibited the highest diversity in terms of both richness and evenness, followed by Kwale, while Lamu displayed the lowest diversity. This differential distribution of fungal diversity across counties underscores the influence of local environmental factors, agricultural practices, and host plant characteristics on shaping fungal communities (Gurr et al., 2016). On the other hand, Unweighted UniFrac analysis, did not reveal clear clustering patterns in the PCoA plot, suggesting that, unlike bacterial communities, fungal communities did not exhibit distinct separation based on the variables considered. Although some clustering tendencies were observed, particularly concerning geographical locations, the overall lack of clear clustering indicates a complex interplay of factors influencing fungal community structure and composition (Nadia et al., 2017).

Taxonomic analysis was performed at the phylum and genus level, using the UNITE reference database, revealing variation in fungal communities across the samples. Kilifi exhibited the highest abundance of sequences, having the most OTUs and reads, while Lamu had the least. Ascomycota's dominance and limited Basidiomycota representation indicate unique fungal composition in these regions (**Figure 4.18**). This is consistent with previous research on the most prevalent fungus populations in the CYD (Nadia et al., 2017). Ascomycota, the largest fungal phylum, is rich in plant pathogens with virulent genes contributing to their pathogenicity. (Abueleiwa et al., 2022; Panno et al., 2021). Ascomycota and Basidiomycota affect numerous horticultural and wild plants inhabiting roots, stems, and leaves while establishing substantial plant infections (Gonella et al., 2019; Tetz et al., 2023).

At the genus level, 17 genera were identified, showing variations in their compositions and proportions across the three counties. *Cyphellophora* was the most dominant genus, except in samples 1C, 3A, 3B, and 3D, where it was undetected (**Figure 4.19**). Since

Cyphellophora is known as a black yeast-like fungus, morphological characteristics that showed that most fungal isolates were black coincided with NGS data, indicating that most of the fungi belonged to this genus. *Devriesia*, the second most dominant genus, was present in all samples and even most prevalent in Lamu samples. *Cyphellophora* and *Devriesia* contain pathogens responsible for sooty blotch and flyspeck diseases in plants (Gao et al., 2015; Li et al., 2013). Other genera like *Bipolaris, Fusarium* and *Clonostachys*, known for causing significant leaf blights, root rots, and wilts in coconut and other plant species, were also present, although not dominant (De Assis Costa et al., 2018; Raja et al., 2006). Furthermore, Nadia et al., (2017) has reported the presence of these three fungal genera in yellowing diseased coconut plants. The findings shed light on the fungal diversity and abundance in the samples.

The profiling of microbial communities through 16S rRNA amplicon sequencing, specifically targeting the V4 region, has some limitations in accurately differentiating sequences to the species level. Instead, it can only reach the genus level (Glassing et al., 2015; Yoo et al., 2017). Additionally, there were uncertainty whether the leaf portions used were representative enough to capture all the available microbes.

Notably, phytoplasma strains were not detected by NGS, regardless of the presence of LYD symptoms in the coconut palms collected. Moreover, nested PCR also confirmed its absence since no bands were observed. These results provide valuable insights into the phytoplasma status of the coconut plants in the study area. Positive controls for the PCR were not included due to the limited availability of phytoplasma studies in the country, making it difficult to obtain archived phytoplasma from relevant authorities. The yellowing of the plant could therefore result from the other bacterial or fungal communities present. Furthermore, these microbial communities are known to affect and reduce phytoplasma titers (Nadia et al., 2017). Phytoplasmas is well known to be present at very low concentrations in the phloem of plants they infect hence can be difficult to detect them in coconut palms (Maejima et al., 2014). Similar results were also obtained by Daramcoum et al., (2018) in their study on the lethal yellowing disease in Ghana, where no phytoplasma was detected from samples taken from coconut trees at the onset of the

disease. Moreover, other related factors, for instance abiotic might have contributed to the yellowing-like symptoms seen in the coconut palms surveyed. The sampling exercise in all three counties was done in August 2021, a dry season in coastal Kenya. Furthermore, temperatures on the Kenyan coast are high year-round (averaging around 30°C) (Ayugi et al., 2016). This may have impacted the coconut palms' agronomic performance in the coastal counties.

5.2 Conclusions

1. In this study, we conducted an investigation into the prevalence and severity of yellowing disease affecting coconut palms, while also delving into the microbial communities inhabiting symptomatic and healthy leaves across three coastal counties. The findings reveal the widespread occurrence of coconut plants displaying symptoms of yellowing disease in the studied areas, with varying degrees of prevalence and severity observed, hence the null hypothesis stated for the first objective of this research is rejected.
2. The study findings also highlight the potential of morphological and biochemical characteristics as valuable tools in microbial identification, albeit with certain limitations. While these traditional methods offer insights, their efficacy may be influenced by growth conditions and media used, thus necessitating their integration with molecular techniques for comprehensive microbial identification. Despite these considerations, this study highlights the value of morphological and biochemical characterization in discerning culturable bacterial and fungal microbes from symptomatic coconut plants, leading to the rejection of the null hypothesis for the second objective of this study.
3. The use of high-throughput sequencing technique (NGS) in this study have yielded valuable insights into microbial diversity and distribution within the studied environments. NGS emerged as a powerful tool in identifying a broader range of microbial taxa, enriching our understanding of disease etiology and microbial community composition. While traditional culture methods confirmed the presence of known plant microbes associated with yellowing diseased coconut

palms, NGS enabled the detection of a wider array of microbial species, revealing regional variations in microbial communities. The exploration of machine learning techniques, specifically the Random Forest classifier, showcased their potential in enhancing microbial data analysis and disease management strategies, offering insights for early disease detection and targeted intervention measures. Thus, the rejection of the null hypothesis regarding the presence of microbial communities other than phytoplasma highlights the intricate microbial dynamics within coconut plants afflicted with yellowing disease symptoms along the Kenyan coast.

Overall, our study enhances the understanding of regional microbial ecologies. Although we did not find phytoplasma, other microbes may be responsible for the yellowing disease in coconut plants. This research aids in the development of strategic disease control measures and provides essential information to the KCDA for the preservation and sustainable use of Kenyan coconut germplasm.

5.3 Recommendations/Further Studies

- Consider sourcing coconut plantation seedlings from Lamu due to the relatively lower presence of pathogens compared to other counties, ensuring better-quality accessions.
- Given the identification of pathogens common to both coconut and other plants, it is advisable to extend existing control and mitigation strategies employed for other plants to coconut cultivation. This recommendation is particularly crucial as coconut plants are often neglected in disease management practices.
- Adoption of study findings by stakeholders, such as KCDA and KEPHIS to address challenges faced by coconut plants. By doing so, they can enhance and preserve coconut germplasm, ultimately benefiting the coconut industry.
- Studies into factors like agricultural practices, geographical location and human activities in more detail could offer valuable insights into the underlying mechanisms driving these differences in diversity and could have important

implications for understanding and managing microbial communities in these regions.

- Research on fungal ITS sequencing studies is warranted to thoroughly explore the fungal component and its potential contributions to the microbial ecosystem in future investigations.
- Short-gun metagenomic sequencing: With metagenomic sequencing, all the genetic material in a sample may be analyzed, not just selected target regions. A complete picture of the microbial community, including uncommon and unusual pathogens can be obtained.

REFERENCES

Abeysinghe, S., Abeysinghe, P. D., Kanatiwela-de Silva, C., Udagama, P., Warawichanee, K., Aljafar, N., Kawicha, P., & Dickinson, M. (2016). Refinement of the taxonomic structure of 16SrXI and 16SrXIV phytoplasmas of gramineous plants using multilocus sequence typing. *Plant Disease*, *100*(10), 2001–2010. https://doi.org/10.1094/PDIS-02-16-0244-RE

Abueleiwa, M. H. S., Harara, F. E. S., Al-Ghoul, M. M. K., Okasha, S. M., & Abu-Naser, S. S. (2022). Rule Based System for Diagnosing Bean Diseases and Treatment. *International Journal of Engineering and Information Systems (IJEAIS)*, *6*(5), 67–74.

Adkins, S., Foale, M., Bourdeix, R., Nguyen, Q., & Biddle, J. (2020). Coconut biotechnology: Towards the sustainability of the 'Tree of life.' In *Coconut Biotechnology: Towards the Sustainability of the "Tree of Life."* https://doi.org/10.1007/978-3-030-44988-9

AFA-NOCD. (2020). the Coconut Value Chain Status. *Agriculture and Food Authority (AFA)*, *November*, 2020.

Aidoo, O. F., Cunze, S., Guimapi, R. A., Arhin, L., Ablormeti, F. K., Tettey, E., Dampare, F., Afram, Y., Bonsu, O., Obeng, J., Lutuf, H., Dickinson, M., & Yankey, N. (2021). Lethal yellowing disease: insights from predicting potential distribution under different climate change scenarios. *Journal of Plant Diseases and Protection*, *128*(5), 1313–1325. https://doi.org/10.1007/s41348-021-00488-1

Al-Khayri, J. M., Jain, S. M., & Johnson, D. V. (2016). Advances in plant breeding strategies: Agronomic, abiotic and biotic stress traits. In *Advances in Plant Breeding Strategies: Agronomic, Abiotic and Biotic Stress Traits* (Vol. 2, Issue January 2016). https://doi.org/10.1007/978-3-319-22518-0

Aladdin. (2021). Types of culture media used in microbiology. *Www.Aladdin-E.Com*, *1*, 1–3. www.aladdin-e.com

Alexander, L. K., Lopes, B., Ricchetti-Masterson, K., & Yeatts, K. B. (2015). Second Edition of the ERIC Notebook: Cross-sectional Studies. *ERIC Notebook*, 1–5. https://sph.unc.edu/files/2015/07/nciph_ERIC8.pdf

Almeida, A., Mitchell, A. L., Tarkowska, A., & Finn, R. D. (2018). Benchmarking taxonomic assignments based on 16S rRNA gene profiling of the microbiota from commonly sampled environments. *GigaScience*, *7*(5), 1–10. https://doi.org/10.1093/gigascience/giy054

ALPEX CONSULTING AFRICA LTD. (2013). *Kenya Coconut Development Authority National Coconut Survey 2013 Final Draft Report*.

Alsohaili, S. A., & Bani-Hasan, B. M. (2018). Morphological and molecular identification of fungi isolated from different environmental sources in the northern eastern Desert of Jordan. *Jordan Journal of Biological Sciences*, *11*(3), 329–337.

Arocha-Rosete, Y., Konan Konan, J. L., Diallo, A. H., Allou, K., & Scott, J. A. (2014). Identification and molecular characterization of the phytoplasma associated with a lethal yellowing-type disease of coconut in Co'Ivoire. *Canadian Journal of Plant Pathology*, *36*(2), 141–150. https://doi.org/10.1080/07060661.2014.899275

Arumugam, T., & Hatta, M. A. M. (2022). Improving Coconut Using Modern Breeding Technologies: Challenges and Opportunities. *Plants*, *11*(24). https://doi.org/10.3390/plants11243414

Ayugi, B. O., Wang, W., & Chepkemoi, D. (2016). Analysis of Spatial and Temporal Patterns of Rainfall Variations over Kenya. *Environment and Earth Science*, *6*(11), 69–83.

Azaroual, S. E., Kasmi, Y., Aasfar, A., El Arroussi, H., Zeroual, Y., El Kadiri, Y., Zrhidri, A., Elfahime, E., Sefiani, A., & Meftah Kadmiri, I. (2022). Investigation of bacterial diversity using 16S rRNA sequencing and prediction of its functionalities in Moroccan phosphate mine ecosystem. *Scientific Reports*, *12*(1), 1–16. https://doi.org/10.1038/s41598-022-07765-5

Bae, S. Y., Lee, J., Jeong, J., Lim, C., & Choi, J. (2021). Effective data-balancing methods for class-imbalanced genotoxicity datasets using machine learning algorithms and molecular fingerprints. *Computational Toxicology*, *20*(July), 100178. https://doi.org/10.1016/j.comtox.2021.100178

Bailey, B. A., & Meinhardt, L. W. (2016). Cacao diseases: A history of old enemies and new encounters. In *Cacao Diseases: A History of Old Enemies and New Encounters* (Issue February). https://doi.org/10.1007/978-3-319-24789-2

Barka, E. A., Vatsa, P., Sanchez, L., Gaveau-Vaillant, N., Jacquard, C., Meier-Kolthoff, J. P., Klenk, H.-P., Clément, C., Ouhdouch, Y., & van Wezel, G. P. (2016). Correction for Barka et al., Taxonomy, Physiology, and Natural Products of Actinobacteria. *Microbiology and Molecular Biology Reviews*, *80*(4). https://doi.org/10.1128/mmbr.00044-16

Beaudoin, N., Isayenka, I., Ducharme, A., Massie, S., Gagnon, A., Hogue, R., Beaulieu, C., & Michaud, D. (2021). Habituation to thaxtomin a increases resistance to common scab in "russet burbank" potato. *PLoS ONE*, *16*(6 June 2021), 1–15. https://doi.org/10.1371/journal.pone.0253414

Bechem, E. T., & Afanga, Y. A. (2018). Morphological and molecular identification of fungi associated with corm rot and blight symptoms on plantain (*Musa paradisiaca*) in macro-propagators. *International Journal of Biological and Chemical Sciences*, *11*(6), 2793. https://doi.org/10.4314/ijbcs.v11i6.19

Bengtsson-Palme, J., Hartmann, M., Eriksson, K. M., Pal, C., Thorell, K., Larsson, D. G.

J., & Nilsson, R. H. (2015). metaxa2: Improved identification and taxonomic classification of small and large subunit rRNA in metagenomic data. *Molecular Ecology Resources*, *15*(6), 1403–1414. https://doi.org/10.1111/1755-0998.12399

Bertaccini, A. (2022). *Review and Phytoplasmas : When Bacteria Modify Plants Plants of the empire*. 1–20.

Bertrand, J. C., Caumette, P., Lebaron, P., Matheron, R., Normand, P., & Sime-Ngando, T. (2015). Environmental microbiology: Fundamentals and applications. In *Environmental Microbiology: Fundamentals and Applications*. https://doi.org/10.1007/978-94-017-9118-2

Bhargava, Balram; Tandon, N. (2015). Standard Operating Procedures for Fungal Identification and Detection of Antifungal Resistance. *Pengaruh Harga Diskon Dan Persepsi Produk Terhadap Nilai Belanja Serta Perilaku Pembelian Konsumen*, *7*(9), 27–44.

Bianco, P. A., Romanazzi, G., Mori, N., Myrie, W., & Bertaccini, A. (2019). Integrated management of phytoplasma diseases. *Phytoplasmas: Plant Pathogenic Bacteria - II: Transmission and Management of Phytoplasma - Associated Diseases*, 237–258. https://doi.org/10.1007/978-981-13-2832-9_11

Bila, J., Mondjana, A., Samils, B., & Högberg, N. (2015). High diversity, expanding populations and purifying selection in phytoplasmas causing coconut lethal yellowing in Mozambique. *Plant Pathology*, *64*(3), 597–604. https://doi.org/10.1111/ppa.12306

Bila, J., Persson, I., Mondjana, A., Manuel, L., Johansson, N., & Santos, L. (2016). EFFECT OF FARMING PRACTICES AND FARM HISTORY ON INCIDENCE OF COCONUT LETHAL YELLOWING IN MOZAMBIQUE The coconut palm (Cocos nucifera) is a major cash crop in the coastal regions of Mozambique , and contributes greatly to , income and food security of mi. *African Crop Science*, *24*(2),

167–178. https://doi.org/http://dx.doi.org/10.4314/acsj.v24i2.5

Blomme, G., Dita, M., Jacobsen, K. S., Vicente, L. P., Molina, A., Ocimati, W., Poussier, S., & Prior, P. (2017). Bacterial diseases of bananas and enset: Current state of knowledge and integrated approaches toward sustainable management. *Frontiers in Plant Science*, *8*(July), 1–25. https://doi.org/10.3389/fpls.2017.01290

Bock, C. H., Barbedo, J. G. A., Del Ponte, E. M., Bohnenkamp, D., & Mahlein, A.-K. (2020). From visual estimates to fully automated sensor-based measurements of plant disease severity: status and challenges for improving accuracy. *Phytopathology Research*, *2*(1). https://doi.org/10.1186/s42483-020-00049-8

Bodor, A., Bounedjoum, N., Vincze, G. E., Erdeiné Kis, Á., Laczi, K., Bende, G., Szilágyi, Á., Kovács, T., Perei, K., & Rákhely, G. (2020). Challenges of unculturable bacteria: environmental perspectives. *Reviews in Environmental Science and Biotechnology*, *19*(1), 1–22. https://doi.org/10.1007/s11157-020-09522-4

Bokulich, N. A., Dillon, M. R., Bolyen, E., Kaehler, B. D., Huttley, G. A., & Caporaso, J. G. (2018). Q2-Sample-Classifier: Machine-Learning Tools for Microbiome Classification and Regression. *Journal of Open Research Software*, *3*(30), 2–5. https://doi.org/10.21105/JOSS.00934

Bolyen, E., Rideout, J. R., Dillon, M. R., Bokulich, N. A., Abnet, C. C., Al-Ghalith, G. A., Alexander, H., Alm, E. J., Arumugam, M., Asnicar, F., Bai, Y., Bisanz, J. E., Bittinger, K., Brejnrod, A., Brislawn, C. J., Brown, C. T., Callahan, B. J., Caraballo-Rodríguez, A. M., Chase, J., … Caporaso, J. G. (2019). Reproducible, interactive, scalable and extensible microbiome data science using QIIME 2. *Nature Biotechnology*, *37*(8), 852–857. https://doi.org/10.1038/s41587-019-0209-9

Bonnet, M., Lagier, J. C., Raoult, D., & Khelaifia, S. (2020). Bacterial culture through selective and non-selective conditions: the evolution of culture media in clinical microbiology. *New Microbes and New Infections*, *34*, 100622.

https://doi.org/10.1016/j.nmni.2019.100622

Brandt, M. I., Trouche, B., Quintric, L., Günther, B., Wincker, P., Poulain, J., & Arnaud-Haond, S. (2021). Bioinformatic pipelines combining denoising and clustering tools allow for more comprehensive prokaryotic and eukaryotic metabarcoding. *Molecular Ecology Resources*, *21*(6), 1904–1921. https://doi.org/10.1111/1755-0998.13398

Brownhill, L., Njuguna, E. M., Bothi, K. L., Pelletier, B., Muhammad, L. W., & Hickey, G. M. (2016). Food security, gender and resilience: Improving smallholder and subsistence farming. In *Food Security, Gender and Resilience: Improving Smallholder and Subsistence Farming*. https://doi.org/10.4324/9781315745855

Buermans, H. P. J., & den Dunnen, J. T. (2014). Next generation sequencing technology: Advances and applications. *Biochimica et Biophysica Acta - Molecular Basis of Disease*, *1842*(10), 1932–1941. https://doi.org/10.1016/j.bbadis.2014.06.015

Buja, I., Sabella, E., Monteduro, A. G., Chiriacò, M. S., De Bellis, L., Luvisi, A., & Maruccio, G. (2021). Advances in plant disease detection and monitoring: From traditional assays to in-field diagnostics. *Sensors*, *21*(6), 1–22. https://doi.org/10.3390/s21062129

Bulgari, D., Quaglino, F., Bianco, P. A., & Casati, P. (2011). Preliminary results on endophytic bacterial community fluctuation during phytoplasma infection. *Bulletin of Insectology*, *64*(SUPPL. 1), 213–214.

Burdon, J. J., Thrall, P. H., & Ericson, L. (2006). The current and future dynamics of disease in plant communities. *Annual Review of Phytopathology*, *44*(November 2020), 19–39. https://doi.org/10.1146/annurev.phyto.43.040204.140238

Burns, D. T., Johnston, E. L., & Walker, M. J. (2020). Authenticity and the Potability of Coconut Water-A Critical Review. *Journal of AOAC International*, *103*(3), 800–806. https://doi.org/10.1093/jaocint/qsz008

Callahan, B. J., McMurdie, P. J., Rosen, M. J., Han, A. W., Johnson, A. J. A., & Holmes, S. P. (2016). DADA2: High-resolution sample inference from Illumina amplicon data. *Nature Methods*, *13*(7), 581–583. https://doi.org/10.1038/nmeth.3869

Cavicchioli, R., Ripple, W. J., Timmis, K. N., Azam, F., Bakken, L. R., Baylis, M., Behrenfeld, M. J., Boetius, A., Boyd, P. W., Classen, A. T., Crowther, T. W., Danovaro, R., Foreman, C. M., Huisman, J., Hutchins, D. A., Jansson, J. K., Karl, D. M., Koskella, B., Mark Welch, D. B., … Webster, N. S. (2019). Scientists' warning to humanity: microorganisms and climate change. *Nature Reviews Microbiology*, *17*(9), 569–586. https://doi.org/10.1038/s41579-019-0222-5

Chalupowicz, L., Dombrovsky, A., Gaba, V., Luria, N., Reuven, M., Beerman, A., Lachman, O., Dror, O., Nissan, G., & Manulis-Sasson, S. (2019). Diagnosis of plant diseases using the Nanopore sequencing platform. *Plant Pathology*, *68*(2), 229–238. https://doi.org/10.1111/ppa.12957

Charan, J., & Biswas, T. (2013). How to calculate sample size for different study designs in medical research? *Indian Journal of Psychological Medicine*, *35*(2), 121–126. https://doi.org/10.4103/0253-7176.116232

Chaudhary, N., Sharma, A. K., Agarwal, P., Gupta, A., & Sharma, V. K. (2015). 16S classifier: A tool for fast and accurate taxonomic classification of 16S rRNA hypervariable regions in metagenomic datasets. *PLoS ONE*, *10*(2), 1–13. https://doi.org/10.1371/journal.pone.0116106

Chiang, K. S., Liu, H. I., & Bock, C. H. (2017). *RESEARCH ARTICLE A discussion on disease severity index values . Part I : warning on inherent errors and suggestions to maximise accuracy*. *171*, 139–154. https://doi.org/10.1111/aab.12362

Chowdappa, P., Vinayaka, H., Chandrika, M., & ... (2018). Pest and disease free coconut. *Indian Coconut Journal*, *April*. https://www.cabdirect.org/cabdirect/abstract/20173102986

Chowdhury, M. S. M., Khairul Mazed, H. E. M., Rahman, M. H., Moonmoon, J. F., & Irin, I. J. (2015). Study on seedling diseases of jackfruit (*Artocarpus heterophyllus* L.) in Bangladesh. *International Journal of Applied Research*, *1*(4), 24–29. www.allresearchjournal.com

Compant, S., Brader, G., Muzammil, S., Sessitsch, A., Lebrihi, A., & Mathieu, F. (2013). Use of beneficial bacteria and their secondary metabolites to control grapevine pathogen diseases. *BioControl*, *58*(4), 435–455. https://doi.org/10.1007/s10526-012-9479-6

Coughlan, L. M., Cotter, P. D., Hill, C., Alvarez-ordóñez, A., Kelly, W. J., & Mora, D. (2015). *Biotechnological applications of functional metagenomics in the food and pharmaceutical industries*. *6*(June), 1–22. https://doi.org/10.3389/fmicb.2015.00672

D'Amore, R., Ijaz, U. Z., Schirmer, M., Kenny, J. G., Gregory, R., Darby, A. C., Shakya, M., Podar, M., Quince, C., & Hall, N. (2016). A comprehensive benchmarking study of protocols and sequencing platforms for 16S rRNA community profiling. *BMC Genomics*, *17*(1). https://doi.org/10.1186/s12864-015-2194-9

da Costa e Carvalho, R. R., de Souza, P. E., Warwick, D. R. N., Pozza, E. A., & de Carvalho Filho, J. L. S. (2013). Spatial and temporal analysis of stem bleeding disease in coconut palm in the state of sergipe, Brazil. *Anais Da Academia Brasileira de Ciencias*, *85*(4), 1567–1576. https://doi.org/10.1590/0001-37652013112412

Da Costa e Carvalho, R. R., Laranjeira, D., De Carvalho Filho, J. L. S., De Souza, P. E., Blank, A. F., Alves, P. B., De Jesus, H. C. R., & Warwick, D. R. N. (2013). In vitro activity of essential oils of Lippia sidoides and Lippia gracilis and their major chemical components against Thielaviopsis paradoxa, causal agent of stem bleeding in coconut palms. *Quimica Nova*, *36*(2), 241–244. https://doi.org/10.1590/S0100-40422013000200007

Danyo, G. (2011). Review of scientific research into the Cape Saint Paul Wilt Disease

(CSPWD) of coconut in Ghana. *African Journal of Agricultural Research*, *6*(19), 4567–4578. https://doi.org/10.5897/AJAR11.139

DARAMCOUM, W. A. M. P., KONAN, K. J.-L., YAO, S. D. M., YAIMA, A. R., KOFFI, E.-B. Z., YOBOUE, K., KOUASSI, K. M., KOUADJO, C. G., KOFFI, E., KOFFI, K. K. G., & N'GUETTA, A. S.-P. (2018). Molecular diagnosis of phytoplasma transmission from zygotic embryos to in vitro regenerated plants of coconut palm (Cocos nucifera L.). *African Journal of Biotechnology*, *17*(27), 862–869. https://doi.org/10.5897/ajb2018.16499

De Assis Costa, O. Y., Tupinambá, D. D., Bergmann, J. C., Barreto, C. C., & Quirino, B. F. (2018). Fungal diversity in oil palm leaves showing symptoms of Fatal Yellowing disease. *PLoS ONE*, *13*(1), 1–17. https://doi.org/10.1371/journal.pone.0191884

De Saeger, J., Park, J., Chung, H. S., Hernalsteens, J. P., Van Lijsebettens, M., Inzé, D., Van Montagu, M., & Depuydt, S. (2021). Agrobacterium strains and strain improvement: Present and outlook. *Biotechnology Advances*, *53*(December 2020). https://doi.org/10.1016/j.biotechadv.2020.107677

Decoin, V., Barbey, C., Bergeau, D., Latour, X., Feuilloley, M. G. J., Orange, N., & Merieau, A. (2014). A type VI secretion system is involved in Pseudomonas fluorescens bacterial competition. *PLoS ONE*, *9*(2). https://doi.org/10.1371/journal.pone.0089411

Degois, J., Clerc, F., Simon, X., Bontemps, C., Leblond, P., & Duquenne, P. (2017). First metagenomic survey of the microbial diversity in bioaerosols emitted in waste sorting plants. *Annals of Work Exposures and Health*, *61*(9), 1076–1086. https://doi.org/10.1093/annweh/wxx075

Delic, D. (2012). Polymerase Chain Reaction for Phytoplasmas Detection. *Polymerase Chain Reaction*, *148*. https://doi.org/10.5772/37728

Deneke, C., Rentzsch, R., & Renard, B. Y. (2017). PaPrBaG: A machine learning approach for the detection of novel pathogens from NGS data. *Scientific Reports*, *7*(July 2016), 1–13. https://doi.org/10.1038/srep39194

Dollet, M., Julia, J. F., Baillarguet, C. I. De, & Ta, A. (2014). Myndus spp, (Fulgoromorpha, Cixiidae) public enemy number one of the coconut palm, Cocos nucifera. *CIRAD-Symposia*, *1*, 29–30.

Dong, C. J., Wang, L. L., Li, Q., & Shang, Q. M. (2019). Bacterial communities in the rhizosphere, phyllosphere and endosphere of tomato plants. *PLoS ONE*, *14*(11), 1–17. https://doi.org/10.1371/journal.pone.0223847

Dorestani, A., & Aliabadi, S. (2017). Correlation, association, causation, and Granger causation in accounting research. *Academy of Accounting and Financial Studies Journal*, *21*(3), 1–13.

Dos Passos, E. M., Leivas, F. W. T., Teodoro, A. V., Da Silva, F. G., Talamini, V., & Dollet, M. (2019). Predation of Eggs of Lincus lobuliger Breddin (Hemiptera: Pentatomidae) on Coconut Trees by Hololepta (Leionota) Quadridentada (Olivier) (Coleoptera: Histeridae). *Florida Entomologist*, *102*(2), 425–427. https://doi.org/10.1653/024.102.0221

Dowd, S. E., Callaway, T. R., Wolcott, R. D., Sun, Y., McKeehan, T., Hagevoort, R. G., & Edrington, T. S. (2008). Evaluation of the bacterial diversity in the feces of cattle using 16S rDNA bacterial tag-encoded FLX amplicon pyrosequencing (bTEFAP). *BMC Microbiology*, *8*, 1–8. https://doi.org/10.1186/1471-2180-8-125

Dusfour, I., Vontas, J., David, J. P., Weetman, D., Fonseca, D. M., Corbel, V., Raghavendra, K., Coulibaly, M. B., Martins, A. J., Kasai, S., & Chandre, F. (2019). Management of insecticide resistance in the major Aedes vectors of arboviruses: Advances and challenges. *PLoS Neglected Tropical Diseases*, *13*(10), 1–22. https://doi.org/10.1371/journal.pntd.0007615

E, E. O., E, U. M., F, U. F., O, A. C., Ekhorutomwen, O. E., Udoh, M. E., Umaru, F. F., Aghayedo, C. O., & Iserhienrhien, A. (2019). NIGERIA. Developing molecular tools capable of identifying, characterizing and distinguishing phytoplasma strains responsible for the emerging lethal yellowing disease (LYD) of coconut in Nigeria. *International Journal of Biotechnology and Food Science*, *7*(4), 56–64. https://doi.org/10.33495/ijbfs

Edgar, R. C. (2018). Updating the 97% identity threshold for 16S ribosomal RNA OTUs. *Bioinformatics*, *34*(14), 2371–2375. https://doi.org/10.1093/bioinformatics/bty113

Elshafie, H. S., & Camele, I. (2021). An overview of metabolic activity, beneficial and pathogenic aspects of burkholderia spp. *Metabolites*, *11*(5). https://doi.org/10.3390/metabo11050321

Ezeonuegbu, B., Machido, D., & Yakubu, S. (2015). Resistance to some Heavy Metals among Fungal Flora of Raw Refinery Effluent. *Journal of Applied Sciences and Environmental Management*, *18*(4), 623. https://doi.org/10.4314/jasem.v18i4.10

Eziashi, E., & Omamor, I. (2010). Lethal yellowing disease of the coconut palms (Cocos nucifera L.): An overview of the crises. *African Journal of Biotechnology*, *9*(54), 9122–9127.

Fadiji, A. E., & Babalola, O. O. (2020). Metagenomics methods for the study of plant-associated microbial communities: A review. *Journal of Microbiological Methods*, *170*(January), 105860. https://doi.org/10.1016/j.mimet.2020.105860

Finyange, P., Muniu, F. K., Wachenje, D., & Kiponda, O. (2019). *Recommended Practices in Kenya*. 1–32.

Francis, I. M., Jochimsen, K. N., De Vos, P., & van Bruggen, A. H. C. (2014). Reclassification of rhizosphere bacteria including strains causing corky root of lettuce and proposal of Rhizorhapis suberifaciens gen. nov., comb. nov.,

Sphingobium mellinum sp. nov., Sphingobium xanthum sp. nov. and Rhizorhabdus argentea gen. nov., sp. . *International Journal of Systematic and Evolutionary Microbiology*, *64*(PART 4), 1340–1350. https://doi.org/10.1099/ijs.0.058909-0

Fukuda, K., Ogawa, M., Taniguchi, H., & Saito, M. (2016). Molecular Approaches to Studying Microbial Communities : Targeting the. *J. Uoeh*, *38*(3), 223–232.

Funke, H., Jehle, W., Kreis, A., Preiß, H., & Tan, G. (1993). CO2 processing technologies. *SAE Technical Papers*, *6*. https://doi.org/10.4271/932273

Gao, L., Ma, Y., Zhao, W., Wei, Z., Gleason, M. L., Chen, H., Hao, L., Sun, G., & Zhang, R. (2015). Three new species of Cyphellophora (chaetothyriales) associated with sooty blotch and flyspeck. *PLoS ONE*, *10*(9). https://doi.org/10.1371/journal.pone.0136857

Gedil, M., Ferguson, M., Girma, G., Gisel, A., Stavolone, L., & Rabbi, I. (2016). Perspectives on the Application of Next-generation Sequencing to the Improvement of Africa's Staple Food Crops. *Next Generation Sequencing - Advances, Applications and Challenges*. https://doi.org/10.5772/61665

Gilbert, J. A., & Dupont, C. L. (2011). Microbial metagenomics: Beyond the genome. *Annual Review of Marine Science*, *3*, 347–371. https://doi.org/10.1146/annurev-marine-120709-142811

Glassing, A., Dowd, S. E., Galandiuk, S., Davis, B., Jorden, J. R., & Chiodini, R. J. (2015). Changes in 16s RNA Gene Microbial Community Profiling by Concentration of Prokaryotic DNA. *Journal of Microbiological Methods*, *119*, 239–242. https://doi.org/10.1016/j.mimet.2015.11.001

Golinska, P., Wypij, M., Agarkar, G., Rathod, D., Dahm, H., & Rai, M. (2015). Endophytic actinobacteria of medicinal plants: Diversity and bioactivity. *Antonie van Leeuwenhoek, International Journal of General and Molecular Microbiology*,

108(2), 267–289. https://doi.org/10.1007/s10482-015-0502-7

Gonella, E., Musetti, R., Crotti, E., Martini, M., Casati, P., & Zchori-Fein, E. (2019). Microbe relationships with phytoplasmas in plants and insects. *Phytoplasmas: Plant Pathogenic Bacteria - II: Transmission and Management of Phytoplasma - Associated Diseases*, 207–235. https://doi.org/10.1007/978-981-13-2832-9_10

Goodwin, S., McPherson, J. D., & McCombie, W. R. (2016). Coming of age: Ten years of next-generation sequencing technologies. *Nature Reviews Genetics*, *17*(6), 333–351. https://doi.org/10.1038/nrg.2016.49

Gopireddy, V. R. (2011). Biochemical tests for the identification of bacteria. *International Journal of Pharmacy and Technology*, *3*(4), 1536–1555.

Gorshkov, V., & Tsers, I. (2022). Plant susceptible responses: the underestimated side of plant–pathogen interactions. *Biological Reviews*, *97*(1), 45–66. https://doi.org/10.1111/brv.12789

Gupta, A., Gopal, M., Thomas, G. V, Manikandan, V., Gajewski, J., Thomas, G., Seshagiri, S., Schuster, S. C., Rajesh, P., & Gupta, R. (2014). *Whole Genome Sequencing and Analysis of Plant Growth Promoting Bacteria Isolated from the Rhizosphere of Plantation Crops Coconut , Cocoa and Arecanut*. *9*(8). https://doi.org/10.1371/journal.pone.0104259

Gurr, G. M., Johnson, A. C., Ash, G. J., Wilson, B. A. L., Ero, M. M., Pilotti, C. A., Dewhurst, C. F., & You, M. S. (2016). Coconut lethal yellowing diseases: A phytoplasma threat to palms of global economic and social significance. *Frontiers in Plant Science*, *7*(OCTOBER2016), 1–21. https://doi.org/10.3389/fpls.2016.01521

Gürsoy, O., & Can, M. (2020). *Southeast Europe Journal of Soft Computing Available online : http://scjournal.ius.edu.ba Genomic Signal Processing Techniques for Taxonomy Prediction*. *9*(1).

Hardoim, P. R., van Overbeek, L. S., Berg, G., Pirttilä, A. M., Compant, S., Campisano, A., Döring, M., & Sessitsch, A. (2015). The Hidden World within Plants: Ecological and Evolutionary Considerations for Defining Functioning of Microbial Endophytes. *Microbiology and Molecular Biology Reviews*, *79*(3), 293–320. https://doi.org/10.1128/mmbr.00050-14

Harries, H. C., & Clement, C. R. (2014). Long-distance dispersal of the coconut palm by migration within the coral atoll ecosystem. *Annals of Botany*, *113*(4), 565–570. https://doi.org/10.1093/aob/mct293

Harris, J. L. (2000). Letter to the editor: Safe, low-distortion tape touch method for fungal slide mounts. *Journal of Clinical Microbiology*, *38*(12), 4683–4684. https://doi.org/10.1128/jcm.38.12.4683-4684.2000

Hartman, D. (2011). Perfecting Your Spread Plate Technique. *Journal of Microbiology & Biology Education*, *12*(2), 204–205. https://doi.org/10.1128/jmbe.v12i2.324

Hasnain, M., Munir, N., Abideen, Z., Zulfiqar, F., Koyro, H. W., El-Naggar, A., Caçador, I., Duarte, B., Rinklebe, J., & Yong, J. W. H. (2023). Biochar-plant interaction and detoxification strategies under abiotic stresses for achieving agricultural resilience: A critical review. *Ecotoxicology and Environmental Safety*, *249*(July 2022). https://doi.org/10.1016/j.ecoenv.2022.114408

Heya, H. M. (2022). *Characterization, Distribution and Risk Assessment of the Invasive Papaya Mealybug (Hemiptera: Psuedococcidae) in Kwale, Mombasa and Kilifi, Kenya*. http://ir.jkuat.ac.ke/handle/123456789/5774%0Ahttp://ir.jkuat.ac.ke/bitstream/handle/123456789/5774/Heya%2C Hellen Msigo- Msc Agric entomology-2022 IR.pdf?sequence=1&isAllowed=y

Hong, B. Y., Araujo, M. V. F., Strausbaugh, L. D., Terzi, E., Ioannidou, E., & Diaz, P. I. (2015). Microbiome profiles in periodontitis in relation to host and disease

characteristics. *PLoS ONE*, *10*(5), 1–14. https://doi.org/10.1371/journal.pone.0127077

Hu, T., Chitnis, N., Monos, D., & Dinh, A. (2021). Next-generation sequencing technologies: An overview. *Human Immunology*, *82*(11), 801–811. https://doi.org/10.1016/j.humimm.2021.02.012

Huang, L., & Wu, T. (2018). Novel neural network application for bacterial colony classification. *Theoretical Biology and Medical Modelling*, *15*(1), 1–16. https://doi.org/10.1186/s12976-018-0093-x

Huang, Y. Y., Matzke, A. J. M., & Matzke, M. (2013). Complete Sequence and Comparative Analysis of the Chloroplast Genome of Coconut Palm (Cocos nucifera). *PLoS ONE*, *8*(8), 1–12. https://doi.org/10.1371/journal.pone.0074736

Illumina Inc. (2013). Illumina Sequencing Technology - YouTube. *October 23*. https://www.illumina.com/documents/products/techspotlights/techspotlight_sequencing.pdf%0Ahttps://www.youtube.com/watch?v=womKfikWlxM

Isayenka, I., & Beaudoin, N. (2022). The Streptomyces scabiei Pathogenicity Factor Thaxtomin A Induces the Production of Phenolic Compounds in Potato Tubers. *Plants*, *11*(23). https://doi.org/10.3390/plants11233216

J.S. Warokka, J. S. W., P. Jones, P. J., & M.J. Dickinson, M. J. D. (2020). Detection of Phytoplasmas Associated With Kalimantan Wilt Disease of Coconut By the Polymerase Chain Reaction. *Jurnal Penelitian Tanaman Industri*, *12*(4), 154. https://doi.org/10.21082/jlittri.v12n4.2006.154-160

James, M. N., & Josephine, M. (2022). *Technological Innovation on Success of Coconut*.

Jaskowska, E., Butler, C., Preston, G., & Kelly, S. (2015). Phytomonas: Trypanosomatids Adapted to Plant Environments. *PLoS Pathogens*, *11*(1), 1–17.

https://doi.org/10.1371/journal.ppat.1004484

Jeong, J., Yun, K., Mun, S., Chung, W. H., Choi, S. Y., Nam, Y. do, Lim, M. Y., Hong, C. P., Park, C. H., Ahn, Y., & Han, K. (2021). The effect of taxonomic classification by full-length 16S rRNA sequencing with a synthetic long-read technology. *Scientific Reports*, *11*(1), 1–12. https://doi.org/10.1038/s41598-020-80826-9

Jiménez, R. R. (2021). Practical Metagenomics: microbiome tutorial with QIIME 2 [version 1; not peer reviewed]. *F1000Research*, *10*, 798.

Jovel, J., Patterson, J., Wang, W., Hotte, N., O'Keefe, S., Mitchel, T., Perry, T., Kao, D., Mason, A. L., Madsen, K. L., & Wong, G. K. S. (2016). Characterization of the gut microbiome using 16S or shotgun metagenomics. *Frontiers in Microbiology*, *7*(APR), 1–17. https://doi.org/10.3389/fmicb.2016.00459

Jufri, R. F. (2020). Microbial Isolation. *Journal La Lifesci*, *1*(1), 18–23. https://doi.org/10.37899/journallalifesci.v1i1.33

Kadere, T. T. (2021a). *a Survey on Coconut Production and Constraints Faced By Farmers Kilifi and Kwale Counties in Kenya*. *6*(1), 33–52.

Kadere, T. T. (2021b). Chemical Composition and Preservation of Mnazi and Its Distillate (Pyuwa). *European Journal of Nutrition & Food Safety*, *13*(1), 46–58. https://doi.org/10.9734/ejnfs/2021/v13i130347

Kandan, A., Bhaskaran, R., & Samiyappan, R. (2010). Ganoderma - a basal stem rot disease of coconut palm in south Asia and Asia pacific regions. *Archives of Phytopathology and Plant Protection*, *43*(15), 1445–1449. https://doi.org/10.1080/03235400802536527

Kandi, V. (2015). Bacterial Colony: First Report of Donut Colony Morphology among Diphtheroids Isolated in Blood. *Cureus*, *7*(11), 4–8.

https://doi.org/10.7759/cureus.374

Karun, A., & Niral, V. (2019). Coconut Genetic Resources. In *Conservation and Utilization of Horticultural Genetic Resources*. https://doi.org/10.1007/978-981-13-3669-0_8

Kashyap, N., Singh, S. K., Yadav, N., Singh, V. K., Kumari, M., Kumar, D., Shukla, L., Kaushalendra, Bhardwaj, N., & Kumar, A. (2023). Biocontrol Screening of Endophytes: Applications and Limitations. *Plants*, *12*(13), 2480. https://doi.org/10.3390/plants12132480

Khalfan, N. A. (2015). Adoption of improved technologies in coconut production by smallholder farmers in west district, Zanzibar. *Nhk技研*, *3*(2), 1–86.

Khan, M., & Hossain, I. (2014). Leaf spot disease of coconut seedling and its eco-friendly management. *Journal of the Bangladesh Agricultural University*, *11*(2), 199–208. https://doi.org/10.3329/jbau.v11i2.19894

Kim, S. O., & Kim, S. S. (2021). Bacterial pathogen detection by conventional culture-based and recent alternative (polymerase chain reaction, isothermal amplification, enzyme linked immunosorbent assay, bacteriophage amplification, and gold nanoparticle aggregation) methods in food samp. *Journal of Food Safety*, *41*(1), 1–12. https://doi.org/10.1111/jfs.12870

Korir, H., Mungai, N. W., Thuita, M., Hamba, Y., & Masso, C. (2017). Co-inoculation effect of rhizobia and plant growth promoting rhizobacteria on common bean growth in a low phosphorus soil. *Frontiers in Plant Science*, *8*(FEBRUARY). https://doi.org/10.3389/FPLS.2017.00141/FULL

Kornerup, A., & Wanscher, J. (1981). Methuen handbook of colour Fletcher. In *Fletcher & Son Ltd, Norwich*. England : Methuen. https://doi.org/LK - https://worldcat.org/title/855387030

Lagier, J. C., Edouard, S., Pagnier, I., Mediannikov, O., Drancourt, M., & Raoult, D. (2015). Current and past strategies for bacterial culture in clinical microbiology. *Clinical Microbiology Reviews*, *28*(1), 208–236. https://doi.org/10.1128/CMR.00110-14

Le Cocq, K., Gurr, S. J., Hirsch, P. R., & Mauchline, T. H. (2017). Exploitation of endophytes for sustainable agricultural intensification. *Molecular Plant Pathology*, *18*(3), 469–473. https://doi.org/10.1111/mpp.12483

Lee, I., Chalita, M., Ha, S. M., Na, S. I., Yoon, S. H., & Chun, J. (2017). ContEst16S: An algorithm that identifies contaminated prokaryotic genomes using 16S RNA gene sequences. *International Journal of Systematic and Evolutionary Microbiology*, *67*(6), 2053–2057. https://doi.org/10.1099/ijsem.0.001872

Lee, S. K., Lur, H. S., & Liu, C. Te. (2021). From lab to farm: Elucidating the beneficial roles of photosynthetic bacteria in sustainable agriculture. *Microorganisms*, *9*(12), 1–23. https://doi.org/10.3390/microorganisms9122453

Lei, L. (2020). Phyllosphere dysbiosis. *Nature Plants*, *6*(5), 434. https://doi.org/10.1038/s41477-020-0674-7

Lennon, J. T., Muscarella, M. E., Placella, S. A., & Lehmkuhl, B. K. (2018). How, when, and where relic DNA affects microbial diversity. *MBio*, *9*(3). https://doi.org/10.1128/mBio.00637-18

Lewin, G. R., Carlos, C., Chevrette, M. G., Horn, H. A., Mcdonald, B. R., Stankey, R. J., Fox, B. G., & Currie, C. R. (2016). *Evolution and Ecology of Actinobacteria and Their Bioenergy Applications*. https://doi.org/10.1146/annurev-micro-102215-095748

Lewis, E., Hudson, J. A., Cook, N., Barnes, J. D., & Haynes, E. (2020). Next-generation sequencing as a screening tool for foodborne pathogens in fresh produce. *Journal of*

Microbiological Methods, *171*, 105840. https://doi.org/10.1016/J.MIMET.2020.105840

Li, P., Luo, H., Ji, B., & Nielsen, J. (2022). Machine learning for data integration in human gut microbiome. *Microbial Cell Factories*, 1–16. https://doi.org/10.1186/s12934-022-01973-4

Li, T., Rezaeipanah, A., & Tag El Din, E. S. M. (2022). An ensemble agglomerative hierarchical clustering algorithm based on clusters clustering technique and the novel similarity measurement. *Journal of King Saud University - Computer and Information Sciences*, *34*(6), 3828–3842. https://doi.org/10.1016/j.jksuci.2022.04.010

Li, W., Xiao, Y., Wang, C., Dang, J., Chen, C., Gao, L., Batzer, J. C., Sun, G., & Gleason, M. L. (2013). A new species of Devriesia causing sooty blotch and flyspeck on Rubber Trees in China. *Mycological Progress*, *12*(4), 733–738. https://doi.org/10.1007/s11557-012-0885-z

Liland, K. H., Vinje, H., & Snipen, L. (2017). microclass: An R-package for 16S taxonomy classification. *BMC Bioinformatics*, *18*(1), 1–9. https://doi.org/10.1186/s12859-017-1583-2

Liofilchem. (2007). Motility Indole Urea Agar (M.I.U.). *Technical Sheet*, *1970*, 1–2. http://www.frilabo.pt/fcms/images/stories/610236_en_TS.pdf

Liu, K. L., & Wong, T. T. (2013). Naïve Bayesian classifiers with multinomial models for rRNA taxonomic assignment. *IEEE/ACM Transactions on Computational Biology and Bioinformatics / IEEE, ACM*, *10*(5), 1334–1339. https://doi.org/10.1109/tcbb.2013.114

Lozupone, C., Lladser, M. E., Knights, D., Stombaugh, J., & Knight, R. (2011). UniFrac: An effective distance metric for microbial community comparison. *ISME Journal*,

5(2), 169–172. https://doi.org/10.1038/ismej.2010.133

Maejima, K., Oshima, K., & Namba, S. (2014). Exploring the phytoplasmas, plant pathogenic bacteria. *Journal of General Plant Pathology*, *80*(3), 210–221. https://doi.org/10.1007/s10327-014-0512-8

Mahyao, A., Mourifie, I., Konan, K., Louis, J., & Diallo, H. (2016). *Socio-economic impact of the coconut lethal yellowing disease on Ivorian smallholder coconut farm families Baudoinia View project Yam agronomy View project*. *4*(9), 463–479. https://www.researchgate.net/publication/307881641

Manamgoda, D. S., Rossman, A. Y., Castlebury, L. A., Crous, P. W., Madrid, H., Chukeatirote, E., & Hyde, K. D. (2014). The genus Bipolaris. *Studies in Mycology*, *79*(1), 221–288. https://doi.org/10.1016/j.simyco.2014.10.002

Maurice, E. O., Muhammed, N., Stephen, M. G., Pascal, O. O., Francis, K. M., Emmanuel, M., & James, O. O. (2015). In-situ morphological characterization of coconut in the Coastal Lowlands of Kenya. *African Journal of Plant Science*, *9*(2), 65–74. https://doi.org/10.5897/ajps2014.1202

Mazivele, M. O. M., Nuaila, V., Durante, M., Colombo, M. M., & Taviani, E. (2018). Promising primers for detection of phytoplasma causing coconut lethal yellowing disease in Mozambique. *Phytoparasitica*, *46*(3), 301–308. https://doi.org/10.1007/s12600-018-0675-5

Mcdevitt, S. (2009). Methyl Red and Voges-Proskauer Test Protocols. *American Society for Microbiology*, *December 2009*, 1–9. www.asmscience.org

Michel, D., Franqueville, H. De, & Ducamp, M. (2012). Bud rot and other major diseases of coconut , a potential threat to oil palm. *Existing and Emerging Pests and Diseases of Oil Palm - Advances in Research and Management, December*, 13–14.

Miranda, F. M., Azevedo, V. A. C., Renard, B. Y., Piro, V. C., & Ramos, R. T. J. (2020). *HiTaC: Hierarchical Taxonomic Classification of Fungal ITS Sequences*. 1–8. https://doi.org/10.1101/2020.04.24.014852

Mizrahi-Man, O., Davenport, E. R., & Gilad, Y. (2013). Taxonomic Classification of Bacterial 16S rRNA Genes Using Short Sequencing Reads: Evaluation of Effective Study Designs. *PLoS ONE*, *8*(1), 18–23. https://doi.org/10.1371/journal.pone.0053608

Mousavi, S. A., Österman, J., Wahlberg, N., Nesme, X., Lavire, C., Vial, L., Paulin, L., de Lajudie, P., & Lindström, K. (2014). Phylogeny of the Rhizobium-Allorhizobium-Agrobacterium clade supports the delineation of Neorhizobium gen. nov. *Systematic and Applied Microbiology*, *37*(3), 208–215. https://doi.org/10.1016/j.syapm.2013.12.007

Mushtaq, S., Shafiq, M., Ashraf, T., Haider, M. S., Atta, S., Almaary, K. S., & Elshikh, M. S. (2022). Enumeration of citrus endophytic bacterial communities based on illumine metagenomics technique. *PLoS ONE*, *17*(4 April), 1–15. https://doi.org/10.1371/journal.pone.0263144

Naderali, N., Nejat, N., Vadamalai, G., Davis, R. E., Wei, W., Harrison, N. A., Kong, L., Kadir, J., Tan, Y. H., & Zhao, Y. (2017). 'Candidatus Phytoplasma wodyetiae', a new taxon associated with yellow decline disease of foxtail palm (Wodyetia bifurcata) in Malaysia. *International Journal of Systematic and Evolutionary Microbiology*, *67*(10), 3765–3772. https://doi.org/10.1099/ijsem.0.002187

Nadia, P. M.-L., Ahmed, H., Henry, S. T., Tacra, T. L., Julia, C., Pauline, W., Hortense, A. D., Jean, L. K. K., Keiko, Y., Wolfgang, M., James, S., & Yaima, A. R. (2017). Microbial diversity in leaves, trunk and rhizosphere of coconut palms (Cocos nucifera L.) associated with the coconut lethal yellowing phytoplasma in Grand-Lahou, Cte dIvoire. *African Journal of Biotechnology*, *16*(27), 1534–1550.

https://doi.org/10.5897/ajb2017.16006

Nadun, P. (2023). Science Journal of Gampaha Cocos nucifera L . (Coconut / Kapruka). *Science Journal of Gampaha*, *01*(February 2023), 9–16.

Naing, L., Nordin, R. Bin, Abdul Rahman, H., & Naing, Y. T. (2022). Sample size calculation for prevalence studies using Scalex and ScalaR calculators. *BMC Medical Research Methodology*, *22*(1), 209. https://doi.org/10.1186/s12874-022-01694-7

Nair, S., & Manimekalai, R. (2021). Phytoplasma diseases of plants: molecular diagnostics and way forward. *World Journal of Microbiology and Biotechnology*, *37*(6), 1–20. https://doi.org/10.1007/s11274-021-03061-y

Nair, S., Manimekalai, R., Ganga Raj, P., & Hegde, V. (2016). Loop mediated isothermal amplification (LAMP) assay for detection of coconut root wilt disease and arecanut yellow leaf disease phytoplasma. *World Journal of Microbiology and Biotechnology*, *32*(7). https://doi.org/10.1007/s11274-016-2078-4

Nampoothiri, K. U. K., Krishnakumar, V., Thampan, P. K., & Achuthan Nair, M. (2019). The coconut palm (Cocos nucifera L.) - Research and development perspectives. In *The Coconut Palm (Cocos nucifera L.) - Research and Development Perspectives*. https://doi.org/10.1007/978-981-13-2754-4

National Institute of Open Schooling. (2012). Bacterial Identification Tests. *National Institiute of Open Schooling*, 122–134.

Natsagdorj, O., Bekh-Ochir, D., Baljinova, T., Iizaka, Y., Fukumoto, A., Kato, F., Anzai, Y., & Javzan, B. (2021). Bioactive compounds and molecular diversity of endophytic actinobacteria isolated from desert plants. *IOP Conference Series: Earth and Environmental Science*, *908*(1), 3–8. https://doi.org/10.1088/1755-1315/908/1/012008

Navarro-Martínez, A., Corominas, N., Sainz de Baranda, C., Escudero-Jiménez, Á., Galán- Ros, J., Sáez- Nieto, J. A., & Solera, J. (2017). Pseudonocardia carboxydivorans in human cerebrospinal fluid: A case report in a patient with traumatic brain injury. *BMC Infectious Diseases*, *17*(1), 1–4. https://doi.org/10.1186/s12879-017-2538-y

Ngugi, H. K., King, S. B., Abayo, G. O., & Reddy, Y. V. R. (2002). Prevalence, incidence, and severity of sorghum diseases in western Kenya. *Plant Disease*, *86*(1), 65–70. https://doi.org/10.1094/PDIS.2002.86.1.65

Nikolaki, S., & Tsiamis, G. (2013). Microbial diversity in the era of omic technologies. *BioMed Research International*, *2013*. https://doi.org/10.1155/2013/958719

Nilsson, R. H., Larsson, K. H., Taylor, A. F. S., Bengtsson-Palme, J., Jeppesen, T. S., Schigel, D., Kennedy, P., Picard, K., Glöckner, F. O., Tedersoo, L., Saar, I., Kõljalg, U., & Abarenkov, K. (2019). The UNITE database for molecular identification of fungi: Handling dark taxa and parallel taxonomic classifications. *Nucleic Acids Research*, *47*(D1), D259–D264. https://doi.org/10.1093/nar/gky1022

Noble, T. J., Williams, B., Douglas, C. A., Giblot-Ducray, D., Mundree, S., & Young, A. J. (2022). Evaluating molecular diagnostic techniques for seed detection of Pseudomonas savastanoi pv. phaseolicola, causal agent of halo blight disease in mungbean (Vigna radiata). *Australasian Plant Pathology*, *51*(4), 453–459. https://doi.org/10.1007/s13313-022-00876-7

Nowak, J., & Coenye, T. (2008). *Diversity and occurrence of Burkholderia spp . in the natural environment*. https://doi.org/10.1111/j.1574-6976.2008.00113.x

OK, O., & SI, D. (2015). Culture- Dependent Characterization of Microbes associated with Oil Palm Kernel Borer, Pachymerus cardo in the Niger Delta. *Journal of Microbial & Biochemical Technology*, *08*(01), 10–15. https://doi.org/10.4172/1948-5948.1000255

Okereke, V. C., & Iwezor, S. C. (2015). *Farmers ' Awareness of the Existence of Crop Diseases in Etche and Ikwere Local Government Areas of Rivers State , Nigeria*. *2*(5), 135–139.

Osborne, N. G. (2008). Mycoplasma. In *Infectious Diseases in Obstetrics and Gynecology, Sixth Edition*. https://doi.org/10.5005/jp/books/12721_22

Oyoo, M. E. (2021). Improvement of Coconut Production in Kenyan Coast for Income Generation. *Kenya Policy Briefs*, *2*(2), 69–70.

Pacifico, D., Galetto, L., Rashidi, M., Abbà, S., Palmano, S., Firrao, G., Bosco, D., & Marzachì, C. (2015). Decreasing global transcript levels over time suggest that phytoplasma cells enter stationary phase during plant and insect colonization. *Applied and Environmental Microbiology*, *81*(7), 2591–2602. https://doi.org/10.1128/AEM.03096-14

Palinkas, L. A., Horwitz, S. M., Green, C. A., Wisdom, J. P., Duan, N., & Hoagwood, K. (2015). Purposeful Sampling for Qualitative Data Collection and Analysis in Mixed Method Implementation Research. *Administration and Policy in Mental Health and Mental Health Services Research*, *42*(5), 533–544. https://doi.org/10.1007/s10488-013-0528-y

Pandey, S., & Gupta, S. (2020a). Diversity analysis of ACC deaminase producing bacteria associated with rhizosphere of coconut tree (Cocos nucifera L.) grown in Lakshadweep islands of India and their ability to promote plant growth under saline conditions. *Journal of Biotechnology*, *324*(February), 183–197. https://doi.org/10.1016/j.jbiotec.2020.10.024

Pandey, S., & Gupta, S. (2020b). Diversity analysis of ACC deaminase producing bacteria associated with rhizosphere of coconut tree (Cocos nucifera L.) grown in Lakshadweep islands of India and their ability to promote plant growth under saline conditions. *Journal of Biotechnology*, *324*, 183–197.

https://doi.org/10.1016/j.jbiotec.2020.10.024

Panno, S., Davino, S., Caruso, A. G., Bertacca, S., Crnogorac, A., Mandić, A., Noris, E., & Matić, S. (2021). A review of the most common and economically important diseases that undermine the cultivation of tomato crop in the mediterranean basin. *Agronomy*, *11*(11), 1–45. https://doi.org/10.3390/agronomy11112188

Pasupathi, S., Shanmuganathan, V., Madasamy, K., Yesudhas, H. R., & Kim, M. (2021). Trend analysis using agglomerative hierarchical clustering approach for time series big data. *Journal of Supercomputing*, *77*(7), 6505–6524. https://doi.org/10.1007/s11227-020-03580-9

Pham, L. J. (2016). Coconut (Cocos nucifera). In *Industrial Oil Crops*. AOCS Press. Published by Elsevier Inc. All rights reserved. https://doi.org/10.1016/B978-1-893997-98-1.00009-9

Piombo, E., Abdelfattah, A., Droby, S., Wisniewski, M., Spadaro, D., & Schena, L. (2021). Metagenomics approaches for the detection and surveillance of emerging and recurrent plant pathogens. *Microorganisms*, *9*(1), 1–19. https://doi.org/10.3390/microorganisms9010188

Pole F.N., B. Nguma, & N. Mohammed. (2014). Status of Coconut Farming and the Associated Challenges in Kenya. *Cord*, *30*(2), 11. https://doi.org/10.37833/cord.v30i2.79

Popp, J., Pető, K., & Nagy, J. (2013). Pesticide productivity and food security. A review. *Agronomy for Sustainable Development*, *33*(1), 243–255. https://doi.org/10.1007/s13593-012-0105-x

Poretsky, R., Rodriguez-R, L. M., Luo, C., Tsementzi, D., & Konstantinidis, K. T. (2014). Strengths and limitations of 16S rRNA gene amplicon sequencing in revealing temporal microbial community dynamics. *PLoS ONE*, *9*(4).

https://doi.org/10.1371/journal.pone.0093827

Potdar, K., S., T., & D., C. (2017). A Comparative Study of Categorical Variable Encoding Techniques for Neural Network Classifiers. *International Journal of Computer Applications*, *175*(4), 7–9. https://doi.org/10.5120/ijca2017915495

Prades, A., Salum, U. N., & Pioch, D. (2016). OIL CROPS AND SUPPLY CHAIN IN ASIA New era for the coconut sector. What prospects for research? *Oilseeds & Fats, Crops and Lipids*, *23*(6), 4–7. https://www.ocl-journal.org/articles/ocl/pdf/2016/06/ocl160048s.pdf

R., M., V.P., S., Nair, S., Thomas, G. V., & V.K., B. (2014). Molecular characterization identifies 16SrXI-B group phytoplasma ('Candidatus Phytoplasma oryzae'-related strain) associated with root wilt disease of coconut in India. *Scientia Horticulturae*, *165*, 288–294. https://doi.org/10.1016/j.scienta.2013.11.031

Raja, P., Reddy, A. V. R., & Allam, U. S. (2006). First report of Alternaria tenuissima causing leaf spot and fruit rot on eggplant (Solanum melongena) in India. *Plant Pathology*, *55*(4), 579. https://doi.org/10.1111/j.1365-3059.2006.01379.x

Rajendhran, J., & Gunasekaran, P. (2011). Microbial phylogeny and diversity: Small subunit ribosomal RNA sequence analysis and beyond. *Microbiological Research*, *166*(2), 99–110. https://doi.org/10.1016/j.micres.2010.02.003

Rajesh, M. K., Jerard, B. A., Preethi, P., Thomas, R. J., Fayas, T. P., Rachana, K. E., & Karun, A. (2013). Development of a RAPD-derived SCAR marker associated with tall-type palm trait in coconut. *Scientia Horticulturae*, *150*, 312–316. https://doi.org/10.1016/j.scienta.2012.11.023

Rajesh, M. K., Jerard, B. A., Preethi, P., Thomas, R. J., & Karun, A. (2014). Application of RAPD markers in hybrid verification in coconut. *Crop Breeding and Applied Biotechnology*, *14*(1), 36–41. https://doi.org/10.1590/s1984-70332014000100006

Ramjegathesh, R., Karthikeyan, G., Rajendran, L., Johnson, I., Raguchander, T., & Samiyappan, R. (2012). Root (wilt) disease of coconut palms in South Asia - an overview. *Archives of Phytopathology and Plant Protection*, *45*(20), 2485–2493. https://doi.org/10.1080/03235408.2012.729772

Randriamihamison, N., Vialaneix, N., & Neuvial, P. (2021). Applicability and Interpretability of Ward's Hierarchical Agglomerative Clustering With or Without Contiguity Constraints. *Journal of Classification*, *38*(2), 363–389. https://doi.org/10.1007/s00357-020-09377-y

Rasam, D. V., Gokhale, N. B., Sawardekar, S. V., & Patil, D. M. (2016). Molecular characterisation of coconut (Cocos nucifera L.) varieties using ISSR and SSR markers. *Journal of Horticultural Science and Biotechnology*, *91*(4), 347–352. https://doi.org/10.1080/14620316.2016.1160544

Ray, M. R., & Sinha, D. (2012). *Metadata of the chapter that will be visualized online Chapter 7*. *938*, 147–158. https://doi.org/10.1007/978-1-62703-089-2

Resources, D., Type, R., Streak, T., Protocol, P., & Katz, D. S. (2012). *The Streak Plate Protocol The Streak Plate Protocol*. *March*, 1–10.

Resources, O. E., Petersen, J., & Mclaughlin, S. (2016). Laboratory Exercises in Microbiology : Discovering the Unseen World through Hands-On Investigation Dr . Susan McLaughlin. *Laboratory Excercises in Microbiology*, *1*(1), 19–31.

Reynolds, J. (2021). 8: Bacterial Colony Morphology - Biology LibreTexts. *LibreTexts Biology*, 3–8.

Ries, M., Ramaswami, U., Parini, R., Lindblad, B., Whybra, C., Willers, I., Gal, A., & Beck, M. (2003). The early clinical phenotype of Fabry disease: A study on 35 European children and adolescents. *European Journal of Pediatrics*, *162*(11), 767–772. https://doi.org/10.1007/s00431-003-1299-3

Santos, A., van Aerle, R., Barrientos, L., & Martinez-Urtaza, J. (2020). Computational methods for 16S metabarcoding studies using Nanopore sequencing data. *Computational and Structural Biotechnology Journal*, *18*, 296–305. https://doi.org/10.1016/j.csbj.2020.01.005

Sapra, R. L. (2021). How to Calculate an Adequate Sample Size? *How to Practice Academic Medicine and Publish from Developing Countries? A Practical Guide*, 81–93. https://doi.org/10.1007/978-981-16-5248-6_9

Savary, S., Ficke, A., Aubertot, J. N., & Hollier, C. (2012). Crop losses due to diseases and their implications for global food production losses and food security. *Food Security*, *4*(4), 519–537. https://doi.org/10.1007/s12571-012-0200-5

Serrano Cardona, L., & Muñoz Mata, E. (2013). Paraninfo Digital. *Early Human Development*, *83*(1), 1–11. https://doi.org/10.1016/j.earlhumdev.2006.05.022

Shao, T., Zhao, J. J., Liu, A., Long, X., & Rengel, Z. (2020). Effects of soil physicochemical properties on microbial communities in different ecological niches in coastal area. *Applied Soil Ecology*, *150*(December), 103486. https://doi.org/10.1016/j.apsoil.2019.103486

Sharma, P., & Sharma, S. (2016). *Paradigm Shift in Plant Disease Diagnostics: A Journey from Conventional Diagnostics to Nano-diagnostics*. 237–264. https://doi.org/10.1007/978-3-319-27312-9_11

Siddiqui, Y., Surendran, A., Paterson, R. R. M., Ali, A., & Ahmad, K. (2021). Current strategies and perspectives in detection and control of basal stem rot of oil palm. *Saudi Journal of Biological Sciences*, *28*(5), 2840–2849. https://doi.org/10.1016/j.sjbs.2021.02.016

Singh, P., Verma, A., & Alex, J. S. R. (2021). Disease and pest infection detection in coconut tree through deep learning techniques. *Computers and Electronics in*

Agriculture, *182*(January), 105986. https://doi.org/10.1016/j.compag.2021.105986

Slatko, B. E., Gardner, A. F., & Ausubel, F. M. (2018). Overview of Next-Generation Sequencing Technologies. *Current Protocols in Molecular Biology*, *122*(1), 1–11. https://doi.org/10.1002/cpmb.59

Smith, A., & Hussey, M. (2005). *American Society for Microbiology: Gram Stain Protocols*. *September 2005*, 1–9. www.asmscience.org

Snehalatharani, A., Maheswarappa, H. P., Devappa, V., & Malhotra, S. K. (2016). Status of coconut basal stem rot disease in India - A review. *Indian Journal of Agricultural Sciences*, *86*(12), 1519–1529.

Steen, A. D., Crits-Christoph, A., Carini, P., DeAngelis, K. M., Fierer, N., Lloyd, K. G., & Cameron Thrash, J. (2019). High proportions of bacteria and archaea across most biomes remain uncultured. *ISME Journal*, *13*(12), 3126–3130. https://doi.org/10.1038/s41396-019-0484-y

Stoler, N., & Nekrutenko, A. (2021). Sequencing error profiles of Illumina sequencing instruments. *NAR Genomics and Bioinformatics*, *3*(1), 1–9. https://doi.org/10.1093/nargab/lqab019

Su, D., Chen, S., Zhou, W., Yang, J., Luo, Z., Zhang, Z., Tian, Y., Dong, Q., Shen, X., Wei, S., Tong, J., & Cui, X. (2022). Comparative Analysis of the Microbial Community Structures Between Healthy and Anthracnose-Infected Strawberry Rhizosphere Soils Using Illumina Sequencing Technology in Yunnan Province, Southwest of China. *Frontiers in Microbiology*, *13*(May). https://doi.org/10.3389/fmicb.2022.881450

Sungthong, R., & Nakaew, N. (2015). The genus Nonomuraea: A review of a rare actinomycete taxon for novel metabolites. *Journal of Basic Microbiology*, *55*(5), 554–565. https://doi.org/10.1002/jobm.201300691

Tanno, K., Maejima, K., Miyazaki, A., Koinuma, H., Iwabuchi, N., Kitazawa, Y., Nijo, T., Hashimoto, M., Yamaji, Y., & Namba, S. (2018). Comprehensive screening of antimicrobials to control phytoplasma diseases using an in vitro plant–phytoplasma co-culture system. *Microbiology (United Kingdom)*, *164*(8), 1048–1058. https://doi.org/10.1099/mic.0.000681

Tedersoo, L., Bahram, M., Zinger, L., Nilsson, R. H., Kennedy, P. G., Yang, T., Anslan, S., & Mikryukov, V. (2022). Best practices in metabarcoding of fungi: From experimental design to results. *Molecular Ecology*, *31*(10), 2769–2795. https://doi.org/10.1111/mec.16460

Tetz, V., Kardava, K., Krasnov, K., Vecherkovskaya, M., & Tetz, G. (2023). Antifungal activity of a novel synthetic polymer M451 against phytopathogens. *Frontiers in Microbiology*, *14*(March). https://doi.org/10.3389/fmicb.2023.1176428

Thomas, P., Sekhar, A. C., Upreti, R., Mujawar, M. M., & Pasha, S. S. (2015). Optimization of single plate-serial dilution spotting (SP-SDS) with sample anchoring as an assured method for bacterial and yeast cfu enumeration and single colony isolation from diverse samples. *Biotechnology Reports*, *8*, 45–55. https://doi.org/10.1016/j.btre.2015.08.003

Thomas, R. J., Shareefa, M., & Nair, R. V. (2019). Varietal resistance in coconut. In *The Coconut Palm (Cocos nucifera L.) - Research and Development Perspectives*. https://doi.org/10.1007/978-981-13-2754-4_5

Tonkovic, P., Kalajdziski, S., Zdravevski, E., Lameski, P., Corizzo, R., Pires, I. M., Garcia, N. M., Loncar-Turukalo, T., & Trajkovik, V. (2020). Literature on applied machine learning in metagenomic classification: A scoping review. *Biology*, *9*(12), 1–25. https://doi.org/10.3390/biology9120453

Top, P. P., & Huanglongbing, C. (2014). Vigilancia Epidemiológica y Estatus Actual del Amarillamiento Letal del Cocotero, Punta Morada de la Papa y Huanglongbing de

los Cítricos (HLB) en México. *Revista Mexicana de Fitopatología*, *32*(2), 120–131.

Trivellone, V., & Dietrich, C. H. (2021). Evolutionary Diversification in Insect Vector-Phytoplasma-Plant Associations. *Annals of the Entomological Society of America*, *114*(2), 137–150. https://doi.org/10.1093/aesa/saaa048

Trivellone, V., Wei, W., Filippin, L., & Dietrich, C. H. (2021). Screening potential insect vectors in a museum biorepository reveals undiscovered diversity of plant pathogens in natural areas. *Ecology and Evolution*, *11*(11), 6493–6503. https://doi.org/10.1002/ece3.7502

Urashima, A. S., Silva, M. F., Correa, J. J., Moraes, M. C., Singh, A. V., Smith, E. C., & Sainz, M. B. (2017). Prevalence and severity of ratoon stunt in commercial Brazilian sugarcane fields. *Plant Disease*, *101*(5), 815–821. https://doi.org/10.1094/PDIS-07-16-1030-RE

Usaid. (2013). *USAID Country Profile: Property Rights and Resource Governance Dominican Republic*. 1–40. http://www.usaidlandtenure.net/sites/default/files/country-profiles/full-reports/USAID_Land_Tenure_Dominican_Republic_Profile.pdf

Vadamalai, G., Thanarajoo, S. S., Joseph, H., Kong, L. L., & Randles, J. W. (2017). Coconut Cadang-Cadang Viroid and Coconut Tinangaja Viroid. In *Viroids and Satellites*. Elsevier Inc. https://doi.org/10.1016/B978-0-12-801498-1.00025-5

Venugopal, A., A, R. K., & Joseph, D. (2017). World Journal of Pharmaceutical Sciences Cocos Nucifera: It's Pharmacological Activities. *Pharmacological Activities. World J Pharm Sci*, *5*(8), 195–200. http://www.wjpsonline.org/

Verma, S. K., Jasrotia, R. S., Iquebal, M. A., Jaiswal, S., Angadi, U. B., Rai, A., & Kumar, D. (2017). Deciphering genes associated with root wilt disease of coconut and development of its transcriptomic database (CnTDB). *Physiological and Molecular*

Plant Pathology, *100*, 255–263. https://doi.org/10.1016/j.pmpp.2017.03.011

Větrovský, T., & Baldrian, P. (2013). The Variability of the 16S rRNA Gene in Bacterial Genomes and Its Consequences for Bacterial Community Analyses. *PLoS ONE*, *8*(2), 1–10. https://doi.org/10.1371/journal.pone.0057923

Villarreal, A. W. (2017). *Chiapas , Mexico , exhibit stress tolerance and growth*. *September*. https://doi.org/10.1016/j.ram.2017.04.009

Wang, X., & Cheng, Z. (2020). Cross-Sectional Studies: Strengths, Weaknesses, and Recommendations. *Chest*, *158*(1), S65–S71. https://doi.org/10.1016/j.chest.2020.03.012

Watanabe, T. (2010). Identification of Fungi. *Pictorial Atlas of Soil and Seed Fungi*, 9–11. https://doi.org/10.1201/ebk1439804193-c3

Wei, W., Trivellone, V., Dietrich, C. H., Zhao, Y., Bottner-parker, K. D., & Ivanauskas, A. (2021). Identification of phytoplasmas representing multiple new genetic lineages from phloem-feeding leafhoppers highlights the diversity of phytoplasmas and their potential vectors. *Pathogens*, *10*(3), 1–17. https://doi.org/10.3390/pathogens10030352

Whitfield-Cargile, C. M., Cohen, N. D., Suchodolski, J., Chaffin, M. K., McQueen, C. M., Arnold, C. E., Dowd, S. E., & Blodgett, G. P. (2015). Composition and diversity of the fecal microbiome and inferred fecal metagenome does not predict subsequent pneumonia caused by rhodococcus equi in foals. *PLoS ONE*, *10*(8), 1–19. https://doi.org/10.1371/journal.pone.0136586

Wijerathna, Y. M. A. M. (2015). Application of biotechnology in coconut (Cocos nucifera L.): Sri Lanka. *Plant Tissue Culture and Biotechnology*, *25*(1), 99–102. https://doi.org/10.3329/ptcb.v25i1.24130

Wu, Y. H., Cheong, L. C., Meon, S., Lau, W. H., Kong, L. L., Joseph, H., & Vadamalai, G. (2013). Characterization of Coconut cadang-cadang viroid variants from oil palm affected by orange spotting disease in Malaysia. *Archives of Virology*, *158*(6), 1407–1410. https://doi.org/10.1007/s00705-013-1624-8

Yoo, K., Lee, T. K., Choi, E. J., Yang, J., Shukla, S. K., Hwang, S. il, & Park, J. (2017). Molecular approaches for the detection and monitoring of microbial communities in bioaerosols: A review. *Journal of Environmental Sciences (China)*, *51*, 234–247. https://doi.org/10.1016/j.jes.2016.07.002

Yoon, S. H., Ha, S. M., Kwon, S., Lim, J., Kim, Y., Seo, H., & Chun, J. (2017). Introducing EzBioCloud: A taxonomically united database of 16S rRNA gene sequences and whole-genome assemblies. *International Journal of Systematic and Evolutionary Microbiology*, *67*(5), 1613–1617. https://doi.org/10.1099/ijsem.0.001755

Zaynab, M., Fatima, M., Sharif, Y., Zafar, M. H., Ali, H., & Khan, K. A. (2019). Role of primary metabolites in plant defense against pathogens. *Microbial Pathogenesis*, *137*, 103728. https://doi.org/10.1016/j.micpath.2019.103728

Zhang, J., Kobert, K., Flouri, T., & Stamatakis, A. (2014). PEAR: A fast and accurate Illumina Paired-End reAd mergeR. *Bioinformatics*, *30*(5), 614–620. https://doi.org/10.1093/bioinformatics/btt593

Zhou, G., Yin, H., Chen, F., Wang, Y., Gao, Q., Yang, F., He, C., Zhang, L., & Wan, Y. (2022). The genome of Areca catechu provides insights into sex determination of monoecious plants. *New Phytologist*, *236*(6), 2327–2343. https://doi.org/10.1111/nph.18471

Zhou, L., Yarra, R., & Cao, H. (2020). SSR based association mapping analysis for fatty acid content in coconut flesh and exploration of the elite alleles in Cocos nucifera L. *Current Plant Biology*, *21*(February), 100141.

https://doi.org/10.1016/j.cpb.2020.100141

APPENDICES

Appendix I: GPS Coordinates of Sampled Sites and Surveillance Exercise in Kwale

Sample ID	Latitude	Longitude	X symptomatic plants/20 plants	Prevalence /20 plants (%)
KW01Di	S04^{0}08.049'	E039^{0}37.497'	4	20
KW02Cii	S04^{0}08.445'	E039^{0}37.218'	3	15
KW03Di	S04^{0}33.397'	E039^{0}07.954'	4	20
KW04Biii	S04^{0}33.381'	E039^{0}08.310'	2	10
KW05Ai	S04^{0}34.260'	E039^{0}08.881'	1	5
KW06Cii	S04^{0}34.268'	E039^{0}08.907'	3	15
KW07Aii	S04^{0}34.780'	E039^{0}09.310'	1	5
KW08Biii	S04^{0}33.381'	E039^{0}09.334'	2	10
KW09Ci	S04^{0}38.910'	E039^{0}11.533'	3	15
KW10Bii	S04^{0}38.882'	E039^{0}11.569'	2	10
KW11Dii	S04^{0}38.872'	E039^{0}11.557'	4	20
KW12E	S04^{0}39.065'	E039^{0}11.658'	-	-
KW13Ciii	S04^{0}39.058'	E039^{0}11.021'	3	15
KW14Di	S04^{0}39.126'	E039^{0}11.671'	4	20
KW15E	S04^{0}39.117'	E039^{0}11.665'	-	-
KW16Ci	S04^{0}39.124'	E039^{0}11.652'	3	15
KW17Diii	S04^{0}39.144'	E039^{0}11.647'	4	20
KW18Di	S04^{0}39.174'	E039^{0}11.632'	4	20
KW19Cii	S04^{0}39.191'	E039^{0}11.650'	3	15
KW20Ciii	S04^{0}39.190'	E039^{0}11.655'	3	15
KW21E	S04^{0}31.943'	E039^{0}08.917'	-	-
			53	
			(18 symptomatic samples x 20**) 360 surveyed plants**	53/360*100 = **14.72**

Appendix II: GPS coordinates of Sampled Sites and Surveillance Exercise in Kilifi

Sample ID	Latitude	Longitude	X symptomatic plants/20 plants	Prevalence/20 plants (%)
KL01Cii	S04^{0}29.876'	E039^{0}12.541'	3	15
KL02Diii	S04^{0}29.852'	E039^{0}12.538'	4	20
KL03Ai	S04^{0}29.834'	E039^{0}12.563'	1	5
KL04Cii	S04^{0}30.607'	E039^{0}16.983'	3	15
KL05Dii	S04^{0}30.601'	E039^{0}16.989'	4	20
KL06Ciii	S04^{0}28.594'	E039^{0}27.529'	3	15
KL07Di	S04^{0}28.613'	E039^{0}27.544'	4	20
KL08Diii	S04^{0}28.611'	E039^{0}27.553'	4	20
KL09Dii	S04^{0}27.501'	E039^{0}28.971'	4	20
KL10Ciii	S04^{0}23.675'	E039^{0}29.093'	3	15
KL11Dii	S04^{0}23.669'	E039^{0}29.085'	4	10
KL12Biii	S04^{0}23.662'	E039^{0}29.067'	2	10
KL13E	S04^{0}23.659'	E039^{0}29.068'	-	-
KL14Ci	S04^{0}21.307'	E039^{0}32.097'	3	5
KL15Diii	S04^{0}21.285'	E039^{0}32.106'	4	10
KL16E	S04^{0}01.400'	E039^{0}36.817'	-	-
KL17Di	S04^{0}01.406'	E039^{0}36.729'	3	15
KL18Dii	S03^{0}54.276'	E039^{0}48.824'	4	20
KL19E	S03^{0}54.284'	E039^{0}48.846'	-	-
KL20Dii	S03^{0}54.258'	E039^{0}44.846'	4	5
KL21Ciii	S03^{0}54.272'	E039^{0}44.806'	3	15
			60	
			(18 symptomatic samples x 20**) 360 surveyed plants**	60/360*100 = **16.67**

Appendix III: GPS Coordinates of Sampled Sites and Surveillance Exercise in Lamu

Sample ID	Latitude	Longitude	X symptomatic plants/20 plants	Prevalence/20 plants (%)
LA01Cii	S03^{0}54.307'	E039^{0}48.846'	3	15
LA02Di	S03^{0}53.837'	E039^{0}45.850'	4	10
LA03Dii	S03^{0}53.831'	E039^{0}45.580'	4	20
LA04Ai	S03^{0}53.802'	E039^{0}45.596'	1	5
LA05Ci	S03^{0}53.798'	E039^{0}45.599'	3	5
LA06Diii	S03^{0}53.710'	E039^{0}45.627'	4	20
LA07E	S03^{0}53.706'	E039^{0}45.609'	-	-
LA08Biii	S03^{0}53.781'	E039^{0}45.558'	2	10
LA09Ciii	S03^{0}53.775'	E039^{0}45.550'	3	15
LA10Ai	S03^{0}53.798'	E039^{0}45.539'	1	5
LA11Biii:	2°25'46.3"S	40°43'14.2"E	2	10
LA12Ci	2°25'51.6"S	40°43'19.8"E	3	15
LA13Bii	2°25'48.6"S	40°43'21.8"E	2	10
LA14Ci	2°26'09.9"S	40°42'55.4"E	3	15
LA15Ai	2°25'09.9"S	40°42'49.4"E	1	5
LA16Bi	2°25'16.0"S	40°42'58.1"E	2	10
LA17Dii	2°25'20.6"S	40°43'06.4"E	4	20
LA18Dii	2°25'47.6"S	40°42'37.8"E	4	20
LA19Cii	2°26'34.4"S	40°43'30.4"E	3	15
LA20E	2°26'34.9"S	40°43'55.3"E	-	-
LA21E	S03^{0}53.798'	E039^{0}45.539'	-	-
			49	
			(18 symptomatic samples x 20**) 360 surveyed plants**	49/360*100 = **13.61**

Key

Prevalence	X symptomatic plants/20 plants	Severity	% of plant with symptoms	County code	County name
A	1	i - mild	<10	KW	Kwale
B	2	ii - moderate	10-50	KL	Kilifi
C	3	iii - severe	>50	LA	Lamu
D	4				
E	Healthy control				

Appendix IV: Calculation of Severity for LY Symptomatic Plants

Disease Score	**Disease Grade**	**No. of disease ratings**				**Total ratings**			
		Kwale	**Kilifi**	**Lamu**	**Overall**	**Kwale**	**Kilifi**	**Lamu**	**Overall**
Mild	1	7	4	8	19	7	4	8	19
Moderate	2	6	7	6	19	12	14	12	38
Severe	3	5	7	4	16	15	21	12	48
		Σ=18	**Σ=18**	**Σ=18**	**Σ=54**	**Σ=34**	**Σ=39**	**Σ=32**	**Σ=105**

$$\textbf{Severity} = \left[\frac{\sum \text{Total ratings}}{\sum \text{No. of disease ratings} \times \text{maximum disease grade}}\right] \times 100\%$$

Appendix V: Colony Morphology and Microscopic Characteristics of Bacterial Isolates and Positive Controls

Sample ID	Form	Elevation	Margin	Size	Colour	Surface	Opacity	Gram Staining	Cell Shape
KW01Di (1)	Circular	Umbonate	Entire	Medium	Cream	Glistening	Opaque	-ve	Rods
KW01Di (2a)	Irregular	Umbonate	Curled	Medium	Cream	Glistening	Translucent	+ve	Cocci
KW01Di (2b)	Irregular	Raised	Curled	Medium	Cream	Glistening	Translucent	+ve	Rods
KW01Di (2c)	Circular	Convex	Entire	Large	Colourless	Glistening	Translucent	+ve	Cocci
KW01Di (3)	Spreading	Flat	Entire	Small	Cream	Glistening	Translucent	+ve	Rods
KW01Di (4)	Irregular	Umbonate	Undulate	Small	Cream	Rough	Translucent	+ve	Rods
KW01Di (5a)	Circular	Flat	Entire	Large	Cream	Rough	Translucent	+ve	Rods
KW01Di (5b)	Irregular	Flat	Undulate	Medium	Cream	Rough	Translucent	+ve	Rods
KW02Cii (1)	Irregular	Umbonate	Entire	Large	Yellow	Rough	Translucent	+ve	Rods
KW02Cii (2a)	Irregular	Umbonate	Undulate	Medium	Yellow	Rough	Opaque	-ve	Rods
KW02Cii (2b)	Irregular	Umbonate	Undulate	Small	Yellow	Rough	Translucent	+ve	Rods
KW03Di (1)	Irregular	Raised	Curled	Small	White	Rough	Translucent	-ve	Rods
KW03Di (2)	Irregular	Raised	Undulate	Large	Cream	Rough	Transparent	+ve	Cocci
KW04Biii (1)	Circular	Raised	Entire	Medium	Cream	Rough	Opaque	+ve	Rods
KW04Biii (2)	Irregular	Umbonate	Undulate	Medium	Cream	Rough	Opaque	+ve	Rods
KW04Biii (3)	Rhizoid	Crateriform	Entire	Small	Cream	Rough	Translucent	+ve	Rods
KW04Biii (4)	Circular	Raised	Entire	Small	Cream	Rough	Opaque	-ve	Rods
KW04Biii (5)	Irregular	Umbonate	Undulate	Medium	Cream	Glistening	Opaque	-ve	Rods
KW05Ai (1)	Irregular	Umbonate	Undulate	Medium	Cream	Rough	Opaque	-ve	Rods
KW05Ai (2a)	Circular	Raised	Entire	Small	White	Rough	Translucent	+ve	Rods
KW05Ai (2b)	Rhizoid	Flat	Entire	Small	Yellow	Rough	Translucent	+ve	Rods
KW06Cii (1)	Circular	Crateriform	Entire	Pinpoint	Cream	Rough	Translucent	+ve	Rods
KW06Cii (2)	Circular	Crateriform	Entire	Pinpoint	White	Rough	Translucent	+ve	Rods
KW07Aii (1)	Circular	Raised	Curled	Medium	Cream	Glistening	Translucent	+ve	Rods

KW07Aii (2)	Rhizoid	Flat	Entire	Small	Cream	Rough	Translucent	+ve	Rods
KW07Aii (3a)	Circular	Raised	Entire	Small	Cream	Glistening	Translucent	+ve	Rods
KW07Aii (3b)	Circular	Raised	Curled	Medium	Cream	Glistening	Translucent	+ve	Rods
KW08Biii (1)	Irregular	Umbonate	Undulate	Medium	Cream	Rough	Translucent	+ve	Rods
KW08Biii (2)	Irregular	Umbonate	Undulate	Medium	Cream	Rough	Translucent	+ve	Rods
KW08Biii (3)	Irregular	Umbonate	Undulate	Medium	Cream	Rough	Translucent	+ve	Rods
KW09Ci (1)	Circular	Raised	Entire	Medium	Cream	Glistening	Opaque	-ve	Rods
KW09Ci (2)	Circular	Raised	Entire	Medium	Cream	Glistening	Translucent	+ve	Rods
KW09Ci (3)	Rhizoid	Flat	Entire	Small	Yellow	Rough	Opaque	-ve	Rods
KW09Ci (4)	Filamentous	Flat	Filiform	Small	Yellow	Rough	Translucent	+ve	Rods
KW10Bii (1)	Circular	Crateriform	Entire	Small	Cream	Rough	Opaque	-ve	Rods
KW10Bii (2)	Filamentous	Crateriform	Entire	Small	Cream	Rough	Opaque	+ve	Rods
KW11Dii (1a)	Circular	Crateriform	Entire	Small	Cream	Rough	Opaque	+ve	Rods
KW11Dii (1b)	Circular	Crateriform	Entire	Small	Yellow	Glistening	Translucent	+ve	Rods
KW12E	Irregular	Flat	Lobate	Large	Yellow	Rough	Translucent	+ve	Rods
KW13Ciii	Circular	Crateriform	Entire	Small	Cream	Rough	Opaque	-ve	Cocci
KW14Di (1)	Circular	Raised	Entire	Small	Colourless	Glistening	Translucent	+ve	Rods
KW14Di (2)	Circular	Raised	Entire	Small	Cream	Glistening	Translucent	+ve	Rods
KW15E	Irregular	Umbonate	Entire	Medium	Cream	Rough	Opaque	+ve	Cocci
KW16Ci (1)	Irregular	Umbonate	Undulate	Medium	Cream	Rough	Opaque	+ve	Rods
KW16Ci (2)	Irregular	Umbonate	Undulate	Medium	Cream	Rough	Opaque	+ve	Rods
KW17Diii	Circular	Convex	Entire	Small	Yellow	Glistening	Translucent	+ve	Rods
KW18Di (1)	Irregular	Raised	Lobate	Small	Yellow	Glistening	Translucent	+ve	Rods
KW18Di (2)	Circular	Flat	Entire	Medium	Yellow	Glistening	Translucent	+ve	Cocci
KW19Cii (1)	Irregular	Umbonate	Undulate	Medium	Cream	Rough	Opaque	+ve	Rods
KW19Cii (2)	Circular	Raised	Entire	Large	Cream	Rough	Opaque	+ve	Cocci
KW20Ciii (1)	Circular	Raised	Entire	Small	Cream	Rough	Opaque	+ve	Rods

KW20Ciii (2)	Irregular	Raised	Undulate	Small	White	Rough	Opaque	+ve	Cocci
KW21E	Spreading	Flat	Entire	Small	Cream	Glistening	Translucent	-ve	Cocci
KL01Cii (1)	Rhizoid	Flat	Entire	Small	Cream	Rough	Opaque	+ve	Rods
KL01Cii (2)	Circular	Umbonate	Entire	Small	Yellow	Glistening	Transparent	+ve	Rods
KL01Cii (3)	Circular	Raised	Entire	Small	Colourless	Glistening	Transparent	-ve	Rods
KL01Cii (4)	Rhizoid	Raised	Entire	Small	Yellow	Glistening	Opaque	-ve	Rods
KL02Diii (1)	Irregular	Flat	Undulate	Medium	Cream	Glistening	Opaque	+ve	Rods
KL02Diii (2)	Irregular	Umbonate	Undulate	Small	Cream	Rough	Opaque	+ve	Rods
KL02Diii (3)	Irregular	Umbonate	Undulate	Large	Cream	Rough	Translucent	+ve	Vibrio
KL03Ai (1a)	Circular	Raised	Entire	Small	Colourless	Glistening	Transparent	+ve	Rods
KL03Ai (1b)	Circular	Raised	Entire	Small	Colourless	Glistening	Transparent	+ve	Rods
KL03Ai (1c)	Filamentous	Flat	Filiform	Small	Cream	Rough	Transparent	+ve	Rods
KL03Ai (2)	Circular	Raised	Entire	Small	Colourless	Glistening	Transparent	+ve	Rods
KL04Cii (1)	Circular	Flat	Entire	Small	Yellow	Smooth	Transparent	+ve	Cocci
KL04Cii (2a)	Circular	Raised	Entire	Small	White	Glistening	Translucent	+ve	Rods
KL04Cii (2b)	Irregular	Raised	Curled	Large	White	Rough	Translucent	+ve	Cocci
KL04Cii (3)	Circular	Raised	Entire	Small	Cream	Rough	Translucent	+ve	Rods
KL04Cii (4)	Rhizoid	Crateriform	Entire	Medium	Yellow	Rough	Translucent	+ve	Rods
KL05Dii (1)	Circular	Umbonate	Entire	Small	Cream	Glistening	Translucent	+ve	Cocci
KL05Dii (2)	Circular	Crateriform	Entire	Small	Yellow	Glistening	Translucent	+ve	Rods
KL05Dii (3)	Irregular	Umbonate	Undulate	Medium	Cream	Rough	Opaque	-ve	Rods
KL06Ciii (1a)	Circular	Raised	Entire	Small	Cream	Rough	Translucent	+ve	Cocci
KL06Ciii (1b)	Irregular	Flat	Entire	Small	Cream	Rough	Translucent	+ve	Rods
KL06Ciii (2a)	Circular	Raised	Curled	Medium	Cream	Glistening	Translucent	+ve	Cocci
KL06Ciii (2b)	Irregular	Raised	Undulate	Medium	White	Rough	Translucent	+ve	Cocci
KL06Ciii (3a)	Irregular	Flat	Undulate	Medium	White	Rough	Translucent	-ve	Rods

KL06Ciii (3b)	Filamentous	Raised	Filiform	Small	Cream	Rough	Transparent	+ve	Rods
KL07Di (1)	Irregular	Umbonate	Undulate	Medium	White	Glistening	Translucent	+ve	Rods
KL07Di (2)	Rhizoid	Crateriform	Entire	Small	Yellow	Rough	Translucent	+ve	Rods
KL07Di (3)	Circular	Raised	Entire	Small	Yellow	Rough	Translucent	+ve	Rods
KL07Di (4)	Irregular	Umbonate	Undulate	Small	Cream	Glistening	Translucent	+ve	Rods
KL08Diii (1)	Irregular	Raised	Curled	Small	Cream	Glistening	Translucent	+ve	Rods
KL08Diii (2)	Irregular	Raised	Curled	Medium	Cream	Glistening	Translucent	+ve	Rods
KL08Diii (3a)	Rhizoid	Raised	Entire	Small	Yellow	Rough	Translucent	+ve	Rods
KL08Diii (3b)	Rhizoid	Flat	Entire	Small	Yellow	Rough	Translucent	+ve	Rods
KL09Dii (1)	Circular	Raised	Entire	Medium	Cream	Glistening	Translucent	+ve	Rods
KL09Dii (2)	Irregular	Crateriform	Lobate	Large	Colourless	Glistening	Transparent	+ve	Rods
KL09Dii (3)	Circular	Raised	Entire	Small	Yellow	Rough	Translucent	+ve	Rods
KL10Ciii (1)	Irregular	Umbonate	Undulate	Medium	Cream	Rough	Opaque	+ve	Spiral
KL10Ciii (2)	Irregular	Umbonate	Undulate	Medium	Cream	Glistening	Translucent	+ve	Spiral
KL10Ciii (3)	Irregular	Umbonate	Undulate	Medium	Cream	Rough	Opaque	+ve	Rods
KL11Dii (1)	Irregular	Umbonate	Undulate	Medium	Cream	Glistening	Translucent	+ve	Rods
KL11Dii (2)	Circular	Raised	Entire	Small	Orange	Glistening	Transparent	+ve	Cocci
KL11Dii (3)	Circular	Raised	Entire	Small	Cream	Rough	Translucent	+ve	Cocci
KL11Dii (4)	Circular	Raised	Curled	Medium	Cream	Glistening	Translucent	+ve	Cocci
KL12Biii (1)	Irregular	Umbonate	Undulate	Large	Cream	Rough	Translucent	+ve	Rods
KL12Biii (2)	Circular	Flat	Entire	Small	White	Glistening	Translucent	+ve	Rods
KL13E	Filamentous	Flat	Filiform	Medium	Colourless	Rough	Opaque	+ve	Rods
KL14Ci (1)	Circular	Raised	Entire	Medium	Yellow	Glistening	Translucent	-ve	Rods
KL14Ci (2)	Irregular	Flat	Entire	Small	Yellow	Glistening	Transparent	-ve	Rods
KL14Ci (3)	Circular	Raised	Entire	Small	Yellow	Glistening	Translucent	+ve	Rods
KL14Ci (4)	Circular	Raised	Entire	Small	Cream	Glistening	Transparent	+ve	Rods
KL15Diii (1)	Circular	Umbonate	Entire	Small	Yellow	Rough	Transparent	+ve	Rods

KL15Diii (2)	Circular	Crateriform	Entire	Pinpoint	Yellow	Glistening	Translucent	+ve	Rods
KL15Diii (3a)	Circular	Raised	Entire	Small	Yellow	Glistening	Translucent	-ve	Cocci
KL15Diii (3b)	Circular	Crateriform	Entire	Small	Yellow	Glistening	Translucent	-ve	Cocci
KL15Diii (4a)	Circular	Flat	Entire	Small	Cream	Rough	Translucent	-ve	Rods
KL15Diii (4b)	Circular	Raised	Entire	Small	Colourless	Rough	Translucent	+ve	Rods
KL16E (1)	Irregular	Umbonate	Undulate	Medium	White	Glistening	Translucent	+ve	Rods
KL16E (2)	Irregular	Umbonate	Undulate	Medium	White	Rough	Opaque	+ve	Rods
KL16E (3)	Irregular	Flat	Undulate	Large	Cream	Rough	Opaque	+ve	Rods
KL17Di (1)	Irregular	Flat	Entire	Small	Cream	Glistening	Transparent	+ve	Cocci
KL17Di (2)	Circular	Raised	Entire	Medium	Cream	Glistening	Transparent	-ve	Rods
KL17Di (3)	Irregular	Flat	Lobate	Small	White	Glistening	Transparent	+ve	Rods
KL17Di (4)	Circular	Raised	Entire	Small	Orange	Glistening	Transparent	+ve	Cocci
KL18Dii (1)	Irregular	Raised	Undulate	Medium	White	Rough	Opaque	-ve	Rods
KL18Dii (2)	Circular	Umbonate	Entire	Small	Cream	Glistening	Translucent	+ve	Cocci
KL18Dii (3)	Circular	Flat	Entire	Small	Yellow	Glistening	Transparent	+ve	Rods
KL19E	Circular	Raised	Entire	Small	White	Glistening	Transparent	+ve	Rods
KL20Dii (1)	Irregular	Flat	Undulate	Large	Cream	Glistening	Translucent	-ve	Rods
KL20Dii (2)	Irregular	Umbonate	Undulate	Medium	White	Rough	Opaque	+ve	Cocci
KL20Dii (3)	Irregular	Flat	Undulate	Large	Cream	Rough	Translucent	+ve	Rods
KL21Ciii (1)	Irregular	Raised	Curled	Large	White	Glistening	Translucent	+ve	Rods
KL21Ciii (2)	Irregular	Flat	Undulate	Small	Yellow	Glistening	Opaque	+ve	Rods
KL21Ciii (3)	Irregular	Raised	Curled	Medium	White	Glistening	Translucent	+ve	Cocci
LA01Cii	Irregular	Flat	Undulate	Small	Yellow	Glistening	Opaque	+ve	Cocci
LA02Di (1)	Irregular	Umbonate	Undulate	Medium	Colourless	Glistening	Translucent	+ve	Cocci
LA02Di (2)	Rhizoid	Flat	Entire	Small	Yellow	Rough	Translucent	+ve	Rods
LA03Dii (1)	Circular	Raised	Entire	Medium	Cream	Rough	Opaque	-ve	Rods
LA03Dii (2)	Circular	Umbonate	Entire	Small	White	Rough	Opaque	-ve	Rods
LA04Ai (1)	Circular	Raised	Entire	Medium	Colourless	Rough	Translucent	+ve	Rods
LA04Ai (2)	Circular	Raised	Entire	Medium	Colourless	Rough	Translucent	+ve	Rods

LA05Ci	Irregular	Umbonate	Undulate	Medium	White	Rough	Translucent	+ve	Rods
LA06Diii (1)	Circular	Raised	Entire	Medium	Colourless	Rough	Translucent	+ve	Rods
LA06Diii (2)	Circular	Raised	Entire	Small	Cream	Rough	Translucent	+ve	Rods
LA07E	Circular	Raised	Entire	Medium	Colourless	Rough	Translucent	+ve	Rods
LA08Biii (1)	Circular	Raised	Entire	Small	Cream	Glistening	Translucent	+ve	Rods
LA08Biii (2)	Circular	Raised	Entire	Medium	Cream	Rough	Translucent	+ve	Rods
LA09Ciii (1)	Circular	Raised	Entire	Small	Yellow	Glistening	Transparent	+ve	Rods
LA09Ciii (2)	Circular	Raised	Entire	Medium	Cream	Rough	Translucent	+ve	Rods
LA10Ai (1)	Circular	Raised	Entire	Small	Cream	Rough	Translucent	+ve	Rods
LA10Ai (2)	Circular	Raised	Entire	Small	Cream	Rough	Translucent	+ve	Rods
LA11Biii:	Circular	Crateriform	Entire	Small	Cream	Rough	Opaque	+ve	Rods
LA12Ci	Circular	Flat	Entire	Small	Cream	Rough	Translucent	+ve	Rods
LA13Bii (1a)	Circular	Raised	Entire	Medium	Cream	Rough	Translucent	+ve	Rods
LA13Bii (1b)	Irregular	Umbonate	Undulate	Medium	Cream	Glistening	Translucent	+ve	Rods
LA13Bii (2)	Irregular	Umbonate	Undulate	Small	Yellow	Rough	Translucent	+ve	Rods
LA13Bii (3)	Irregular	Umbonate	Undulate	Medium	Cream	Rough	Translucent	+ve	Rods
LA13Bii (4)	Irregular	Flat	Undulate	Small	White	Rough	Translucent	+ve	Cocci
LA14Ci (1)	Circular	Raised	Entire	Small	Yellow	Glistening	Opaque	-ve	Cocci
LA14Ci (2)	Circular	Umbonate	Entire	Small	Yellow	Glistening	Translucent	+ve	Rods
LA14Ci (3)	Irregular	Umbonate	Undulate	Medium	Cream	Glistening	Translucent	+ve	Rods
LA14Ci (4)	Irregular	Umbonate	Undulate	Small	White	Glistening	Translucent	+ve	Rods
LA14Ci (5)	Irregular	Umbonate	Undulate	Small	White	Glistening	Translucent	+ve	Rods
LA15Ai (1)	Irregular	Umbonate	Undulate	Medium	Cream	Rough	Opaque	+ve	Rods
LA15Ai (2)	Rhizoid	Crateriform	Entire	Small	Yellow	Rough	Translucent	+ve	Cocci
LA15Ai (3)	Circular	Crateriform	Entire	Small	Yellow	Rough	Translucent	+ve	Rods
LA15Ai (4)	Circular	Raised	Entire	Small	White	Glistening	Opaque	+ve	Rods
LA16Bi (1a)	Rhizoid	Flat	Entire	Small	Yellow	Rough	Translucent	+ve	Cocci
LA16Bi (1b)	Rhizoid	Flat	Entire	Small	Yellow	Rough	Translucent	-ve	Rods
LA16Bi (2a)	Circular	Raised	Entire	Medium	White	Rough	Translucent	+ve	Rods

LA16Bi (2b)	Circular	Crateriform	Entire	Small	Yellow	Rough	Translucent	+ve	Rods
LA17Dii	Circular	Flat	Entire	Medium	Cream	Rough	Translucent	+ve	Rods
LA18Dii	Circular	Raised	Entire	Medium	Cream	Rough	Translucent	+ve	Rods
LA19Cii (1)	Circular	Raised	Entire	Small	Orange	Glistening	Translucent	+ve	Rods
LA19Cii (2)	Circular	Flat	Entire	Pinpoint	Colourless	Glistening	Translucent	+ve	Rods
LA19Cii (3a)	Circular	Raised	Entire	Small	Yellow	Glistening	Translucent	+ve	Rods
LA19Cii (3b)	Circular	Flat	Entire	Small	Yellow	Rough	Opaque	-ve	Rods
LA19Cii (4)	Irregular	Umbonate	Undulate	Medium	Cream	Rough	Translucent	+ve	Cocci
LA20E	Rhizoid	Raised	Undulate	Small	White	Glistening	Translucent	+ve	Rods
LA21E	Irregular	Umbonate	Undulate	Medium	Cream	Glistening	Translucent	+ve	Rods
Agrobacterium tumefaciens	Circular	Convex	Entire	Small	White	Glistening	Translucent	-ve	Rods
Bacillus aquimaris	Circular	Raised	Entire	Medium	Orange	Glistening	Translucent	+ve	Rods
Bacillus cereus	Irregular	Raised	Lobate	Large	White	Smooth	Opaque	+ve	Rods
Bacillus subtilis	Irregular	Flat	Lobate	Large	Cream	Glistening	Opaque	+ve	Rods
Burkholderia cepacia	Circular	Convex	Entire	Medium	Yellow	Glistening	Opaque	-ve	Rods
Curtobacterium flaccumfaciens	Circular	Convex	Entire	Small	Yellow	Smooth	Opaque	-ve	Rods
Erwinia tracheiphila	Circular	Convex	Entire	Small	White	Glistening	Translucent	-ve	Rods
Erwinia psidii	Circular	Convex	Entire	Small	White	Glistening	Translucent	-ve	Rods
Leifsonia sp.	Circular	Raised	Entire	Medium	Yellow	Smooth	Opaque	+ve	Rods
Pseudomonas aureginosa	Irregular	Flat	Undulate	Medium	White	Smooth	Opaque	-ve	Rods
Serratia odorifera	Circular	Convex	Entire	Medium	White	Smooth	Opaque	-ve	Rods

Streptomyces fradiae	Filamentous	Flat	Filiform	Small	White	Glistening	Opaque	+ve	Cocci

Appendix VI: Colony Morphology and Microscopic Characteristics of Fungal Isolates and Positive Controls

Sample ID	**Top colour**	**Bottom colour**	**Appearance**	**Surface**	**Mycelium**	**Form**	**Elevation**	**Margin**	**Hyphae**	**Spore**
KW01Di	Grey	Black	Fluffy	Dry	Thick	Circular	Raised	Entire	Septate	-
KW02Cii	White	Yellow	Cottony	Dry	Thick	Circular	Convex	Curled	Septate	-
KW03Di	Black	Black	Fluffy	Dry	Thick	Circular	Raised	Entire	Septate	-
KW04Biii (1)	Grey	Black	Fluffy	Dry	Thick	Circular	Raised	Entire	Septate	-
KW04Biii (2)	Black	Black	Fluffy	Dry	Thick	Circular	Raised	Entire	Septate	-
KW05Ai	Grey	Red	Wavy	Dry	Thick	Circular	Raised	Entire	Septate	+
KW06Cii (1)	Grey	Black	Fluffy	Dry	Thick	Circular	Raised	Entire	Aseptate	-
KW06Cii (2)	Grey	Black	Fluffy	Dry	Thick	Circular	Raised	Entire	Aseptate	-
KW07Aiii	Brown	Brown	Wavy	Dry	Thin	Irregular	Flat	Undulate	Aseptate	+
KW08Biii (1)	Grey	Black	Fluffy	Dry	Thick	Circular	Raised	Entire	Septate	-
KW08Biii (2)	Grey	Black	Fluffy	Dry	Thick	Circular	Raised	Entire	Septate	-
KW09Ci	White	Yellow	Fluffy	Dry	Thick	Irregular	Raised	Undulate	Septate	+
KW10Bii (1)	White	White	Fluffy	Dry	Thick	Circular	Raised	Entire	Septate	+
KW10Bii (2)	Brown	Brown	Fluffy	Dry	Thick	Circular	Raised	Entire	Septate	-
KW11Dii (1)	Grey	Black	Fluffy	Dry	Thick	Circular	Raised	Entire	Septate	-
KW11Dii (2)	Grey	Black	Fluffy	Dry	Thick	Circular	Raised	Entire	Septate	-
KW12E	Black	Black	Fluffy	Dry	Thick	Circular	Flat	Entire	Septate	-
KW13Ciii (1)	Grey	Black	Fluffy	Dry	Thick	Circular	Raised	Entire	Septate	-
KW13Ciii (2)	Grey	Black	Fluffy	Dry	Thick	Circular	Raised	Entire	Septate	+

KW14Di (1)	Grey	Black	Fluffy	Dry	Thick	Circular	Raised	Entire	Septate	+
KW14Di (2)	Orange	Yellow	Fluffy	Dry	Thick	Circular	Raised	Entire	Septate	-
KW14Di (3)	Green	Yellow	Wavy	Dry	Thick	Circular	Flat	Entire	Aseptate	-
KW15E	Green	Yellow	Fluffy	Dry	Thin	Circular	Flat	Entire	Aseptate	-
KW16Ci (1)	Grey	Black	Fluffy	Dry	Thick	Circular	Raised	Entire	Septate	+
KW16Ci (2)	Grey	Black	Fluffy	Dry	Thick	Circular	Raised	Entire	Septate	+
KW17Diii (1)	Black	Black	Fluffy	Dry	Thick	Circular	Raised	Entire	Septate	-
KW17Diii (2)	Black	Black	Fluffy	Dry	Thick	Circular	Raised	Entire	Septate	+
KW17Diii (3)	Grey	Brown	Fluffy	Dry	Thick	Circular	Raised	Entire	Septate	+
KW18Di (1)	Grey	Green	Fluffy	Dry	Thick	Circular	Raised	Entire	Aseptate	-
KW18Di (2)	Grey	Green	Fluffy	Dry	Thin	Irregular	Raised	Undulate	Aseptate	-
KW19Cii (1)	Lilac	Purple	Fluffy	Dry	Thick	Circular	Raised	Entire	Septate	-
KW19Cii (2)	Grey	Black	Rough	Dry	Thick	Irregular	Raised	Undulate	Septate	+
KW20Ciii (1)	Grey	Black	Fluffy	Dry	Thick	Circular	Raised	Entire	Septate	-
KW20Ciii (2)	White	Brown	Cottony	Wrinkled	Thick	Irregular	Flat	Undulate	Septate	+
KW21E	Grey	Brown	Fluffy	Dry	Thick	Circular	Raised	Entire	Septate	-
KL01Cii (1)	Black	Black	Fluffy	Dry	Thick	Circular	Raised	Entire	Septate	-
KL01Cii (2)	Grey	Black	Fluffy	Dry	Thick	Circular	Raised	Entire	Septate	-
KL01Cii (3)	Grey	Black	Fluffy	Dry	Thick	Circular	Raised	Entire	Pseudoseptate	-
KL01Cii (4)	Purple	White	Fluffy	Dry	Thick	Circular	Raised	Entire	Septate	+
KL02Diii (1)	Green	Brown	Velvety	Wrinkled	Thick	Circular	Flat	Entire	Septate	-
KL02Diii (2)	Grey	Black	Fluffy	Dry	Thick	Circular	Raised	Entire	Septate	-
KL03Ai (1)	Purple	Purple	Cottony	Dry	Thin	Circular	Raised	Entire	Pseudoseptate	+
KL03Ai (2)	Grey	Black	Fluffy	Dry	Thick	Circular	Raised	Entire	Septate	-

KL03Ai (3)	Grey	Black	Fluffy	Dry	Thick	Circular	Raised	Entire	Septate	-
KL04Cii (1)	Yellow	Brown	Cottony	Wrinkled	Thick	Irregular	Convex	Undulate	Aseptate	-
KL04Cii (2)	Grey	Black	Fluffy	Dry	Thick	Circular	Raised	Entire	Septate	-
KL05Dii (1)	Grey	Brown	Fluffy	Dry	Thick	Circular	Raised	Entire	Septate	-
KL05Dii (2)	Grey	Black	Fluffy	Dry	Thick	Circular	Raised	Entire	Septate	-
KL06Ciii (1)	Grey	Black	Fluffy	Dry	Thick	Circular	Raised	Entire	Septate	-
KL06Ciii (2)	Purple	Yellow	Fluffy	Dry	Thick	Circular	Raised	Entire	Aseptate	-
KL06Ciii (3)	Grey	Black	Fluffy	Dry	Thick	Circular	Raised	Entire	Aseptate	-
KL07Di (1)	White	Yellow	Cottony	Dry	Thick	Circular	Convex	Curled	Septate	-
KL07Di (2)	Black	Black	Fluffy	Dry	Thick	Circular	Raised	Entire	Septate	-
KL08Diii (1)	Green	Cream	Fluffy	Dry	Thick	Circular	Raised	Entire	Pseudos eptate	-
KL08Diii (2)	Brown	Brown	Velvety	Wrinkled	Thin	Circular	Flat	Entire	Septate	+
KL09Dii (1)	Brown	Cream	Fluffy	Dry	Very thin	Circular	Flat	Entire	Aseptate	-
KL09Dii (2)	Grey	Black	Fluffy	Dry	Thick	Circular	Raised	Entire	Septate	-
KL09Dii (3)	White	Yellow	Fluffy	Dry	Thick	Irregular	Convex	Undulate	Septate	+
KL10Ciii	Grey	Black	Fluffy	Dry	Thick	Circular	Raised	Entire	Septate	-
KL11Dii	Green	Orange	Velvety	Dry	Thick	Irregular	Raised	Undulate	Aseptate	-
KL12Biii (1)	White	Brown	Fluffy	Dry	Thick	Circular	Raised	Entire	Septate	-
KL12Biii (2)	White	Yellow	Cottony	Concentr ic rings	Thick	Circular	Raised	Curled	Aseptate	+
KL13E	Green	Brown	Less fluffy	Wrinkled	Thin	Circular	Flat	Entire	Septate	-
KL14Ci	White	Yellow	Wavy	Dry	Thin	Irregular	Flat	Undulate	Septate	+
KL15Diii (1)	Brown	Red	Less fluffy	Wrinkled	Thin	Circular	Flat	Entire	Septate	-
KL15Diii (2)	Green	Green	Less fluffy	Wrinkled	Thick	Circular	Flat	Entire	Septate	-
KL15Diii (3)	Green	Brown	Velvety	Wrinkled	Thin	Circular	Flat	Entire	Septate	+

KL16E	Grey	Brown	Fluffy	Dry	Thick	Circular	Raised	Entire	Septate	-
KL17Di (1)	Grey	Black	Fluffy	Dry	Thin	Circular	Flat	Entire	Aseptate	-
KL17Di (2)	Grey	Black	Fluffy	Dry	Thick	Circular	Raised	Entire	Aseptate	-
KL18Dii (1)	Grey	Black	Velvety	Dry	Thick	Circular	Raised	Entire	Septate	+
KL18Dii (2)	Grey	Black	Fluffy	Dry	Thick	Circular	Raised	Entire	Septate	-
KL19E	Black	Black	Fluffy	Dry	Thick	Circular	Raised	Entire	Septate	-
KL20Dii (1)	Cream	Red	Fluffy	Dry	Thick	Circular	Raised	Entire	Pseudoseptate	+
KL20Dii (2)	Orange	Orange	Fluffy	Dry	Thick	Circular	Raised	Entire	Pseudoseptate	-
KL21Ciii (1)	Brown	Brown	Velvety	Wrinkled	Thin	Circular	Flat	Entire	Septate	+
KL21Ciii (2)	Orange	Yellow	Fluffy	Dry	Thick	Circular	Raised	Entire	Septate	-
LA01Cii	Grey	Black	Fluffy	Dry	Thick	Circular	Raised	Entire	Septate	-
LA02Di (1)	Grey	Black	Fluffy	Dry	Thick	Circular	Raised	Entire	Septate	-
LA02Di (2)	White	Yellow	Cottony	Dry	Thick	Circular	Raised	Entire	Septate	-
LA03Dii	White	Yellow	Fluffy	Dry	Thick	Circular	Raised	Entire	Pseudoseptate	-
LA04Ai (1)	Black	Black	Fluffy	Dry	Thick	Circular	Raised	Entire	Aseptate	-
LA04Ai (2)	Grey	Black	Fluffy	Dry	Thick	Circular	Raised	Entire	Aseptate	-
LA05Ci (1)	Grey	Black	Fluffy	Dry	Thick	Circular	Raised	Entire	Septate	-
LA05Ci (2)	Grey	Black	Fluffy	Dry	Thick	Circular	Raised	Entire	Septate	-
LA06Diii (1)	Pink	Grey	Fluffy	Dry	Thick	Circular	Raised	Entire	Aseptate	-
LA06Diii (2)	Brown	Brown	Rough	Dry	Thin	Irregular	Raised	Undulate	Aseptate	+
LA07E	Green	Black	Fluffy	Dry	Thick	Circular	Raised	Entire	Aseptate	+
LA08Biii (1)	Green	Cream	Fluffy	Dry	Thin	Circular	Flat	Entire	Pseudoseptate	-

LA08Biii (2)	Green	Cream	Fluffy	Dry	Thin	Circular	Flat	Entire	Pseudoseptate	-
LA09Ciii (1)	White	Red	Cottony	Dry	Thick	Circular	Convex	Entire	Aseptate	-
LA09Ciii (2)	White	Grey	Fluffy	Dry	Thick	Circular	Raised	Entire	Aseptate	-
LA10Ai	Grey	Black	Fluffy	Dry	Thick	Circular	Raised	Entire	Pseudoseptate	-
LA11Biii	Purple	Yellow	Fluffy	Dry	Thick	Circular	Flat	Entire	Aseptate	-
LA12Ci	Grey	Black	Fluffy	Dry	Thick	Circular	Raised	Entire	Aseptate	-
LA13Bii (1)	Grey	Black	Fluffy	Dry	Thick	Circular	Raised	Entire	Septate	+
LA13Bii (2)	Grey	Black	Fluffy	Dry	Thick	Circular	Raised	Entire	Septate	-
LA14Ci (1)	Black	Green	Fluffy	Dry	Thin	Circular	Flat	Entire	Septate	-
LA14Ci (2)	Green	Brown	Velvety	Wrinkled	Thin	Irregular	Flat	Entire	Septate	+
LA15Ai (1)	White	Yellow	Fluffy	Dry	Thin	Irregular	Raised	Undulate	Septate	-
LA15Ai (2)	Grey	Black	Fluffy	Dry	Thick	Circular	Raised	Entire	Septate	-
LA16Bi (1)	White	Yellow	Fluffy	Dry	Thick	Circular	Raised	Entire	Septate	-
LA16Bi (2)	Grey	Brown	Fluffy	Dry	Thick	Circular	Raised	Entire	Septate	-
LA17Dii	Green	Green	Velvety	Wrinkled	Thin	Circular	Flat	Entire	Septate	+
LA18Dii	Grey	Brown	Fluffy	Dry	Thick	Circular	Raised	Entire	Septate	+
LA19Cii (1)	Brown	Brown	Velvety	Wrinkled	Thick	Irregular	Flat	Undulate	Aseptate	+
LA19Cii (2)	Black	White	Fluffy	Dry	Thick	Circular	Raised	Entire	Aseptate	-
LA20E	Green	Green	Cottony	Concentric rings	Thin	Irregular	Flat	Entire	Septate	+
LA21E	Green	Brown	Velvety	Wrinkled	Thin	Irregular	Flat	Entire	Septate	+
Aspergillus niger	Brown	Grey	Cottony	Dry	Thick	Circular	Umbonate	Entire	Septate	+
Aspergillus nomius	Green	Cream	Less fluffy	Concentric rings	Thin	Circular	Flat	Entire	Septate	+

Cunninghamella bainieri	White	Grey	Cottony	Dry	Thick	Circular	Flat	Entire	Aseptate	-
Drechslera gigantea	Grey	Grey	Cottony	Concentric rings	Thick	Circular	Flat	Entire	Aseptate	-
Drechslera halodes	Black	Black	Fluffy	Dry	Thick	Circular	Flat	Entire	Pseudoseptate	-
Exophiala alcalophila	Brown	Black	Mucoid	Moist	Thick	Circular	Convex	Entire	Aseptate	-
Fusarium solani	Cream	Green	Cottony	Dry	Thick	Circular	Raised	Entire	Septate	-
Ganoderma tornatum	Red	Red	Fluffy	Concentric rings	Thick	Circular	Convex	Entire	Aseptate	-
Gibberella fujikuroi	White	Pink	Fluffy	Dry	Thick	Circular	Crateriform	Entire	Septate	+
Marasmiellus cocophilus	White	Yellow	Cottony	Dry	Thick	Circular	Raised	Entire	Septate	-
Mycosphaerella parkiiaffinis	Grey	Black	Fluffy	Dry	Thick	Irregular	Raised	Undulate	Septate	+
Penicillium citreosulfuratum	Yellow	Yellow	Cottony	Wrinkled	Thick	Circular	Raised	Entire	Septate	+
Penicillium daleae	White	Brown	Cottony	Wrinkled	Thick	Circular	Convex	Entire	Septate	+
Phytophthora palmivora	Green	Green	Fluffy	Dry	Thick	Irregular	Raised	Undulate	Septate	+
Rhizoctonia solani	Orange	Orange	Mucoid	Moist	Thin	Circular	Raised	Entire	Septate	-
Trichoderma helicum	Green	Green	Cottony	Moist	Thin	Irregular	Flat	Entire	Septate	+

Appendix VII: Biochemical Characterization of Bacterial Isolates

Sample ID	Methyl Red	Citrate	Catalase	Motility	Indole	Urease	Glucose	Sucrose	Lactose	H_2S	CO_2	Oxidase
KW01Di (1)	-	+	+	+	-	-	+	-	-	-	-	+
KW01Di (2a)	-	+	+	+	-	-	+	+	+	-	-	-
KW01Di (2b)	+	+	+	+	+	-	+	-	-	+	-	+
KW01Di (2c)	+	+	-	-	-	-	+	-	-	-	-	+
KW01Di (3)	-	+	+	-	-	-	+	-	-	-	-	-
KW01Di (4)	+	+	+	-	-	-	-	-	-	-	-	-
KW01Di (5a)	-	+	+	-	-	+	-	-	-	-	-	-
KW01Di (5b)	-	+	+	-	-	+	+	-	-	-	-	+
KW02Cii (1)	-	+	-	-	+	+	+	-	-	-	-	-
KW02Cii (2a)	+	+	+	+	-	-	+	+	+	-	-	+
KW02Cii (2b)	+	+	+	+	-	-	+	+	+	-	-	+
KW03Di (1)	-	+	-	-	-	-	+	-	-	-	-	+
KW03Di (2)	-	+	-	-	-	-	+	-	-	-	-	+
KW04Biii (1)	+	+	+	-	+	+	+	-	-	-	-	-
KW04Biii (2)	+	+	+	+	-	-	+	+	+	-	-	-
KW04Biii (3)	-	+	-	-	-	+	+	-	-	-	-	-
KW04Biii (4)	-	+	+	-	-	-	+	+	+	-	-	+
KW04Biii (5)	+	+	+	-	-	+	+	+	+	-	-	-
KW05Ai (1)	-	+	+	-	-	-	+	+	+	-	-	+
KW05Ai (2a)	-	+	+	-	-	-	+	-	-	-	-	+
KW05Ai (2b)	-	+	+	-	-	-	+	-	-	-	-	-
KW06Cii (1)	-	+	+	-	-	-	+	-	-	-	-	+
KW06Cii (2)	-	+	+	-	-	-	+	-	-	-	-	+
KW07Aii (1)	-	-	+	+	-	-	+	+	+	-	-	-
KW07Aii (2)	-	+	+	-	-	-	+	-	-	-	-	+
KW07Aii (3a)	-	+	+	+	-	-	+	-	-	+	-	+
KW07Aii (3b)	-	-	+	+	-	-	+	+	+	-	-	-

KW08Biii (1)	-	+	+	-	-	-	+	-	-	-	-	+
KW08Biii (2)	-	+	+	-	-	-	+	-	-	-	-	+
KW08Biii (3)	-	+	+	-	-	-	+	-	-	-	-	+
KW09Ci (1)	-	+	+	+	+	-	+	+	+	-	-	-
KW09Ci (2)	-	+	+	-	-	-	+	-	-	+	-	+
KW09Ci (3)	-	+	-	-	-	+	+	+	+	-	-	+
KW09Ci (4)	-	+	+	+	-	-	+	-	-	-	-	+
KW10Bii (1)	+	+	+	-	-	-	+	-	-	-	-	+
KW10Bii (2)	+	+	-	+	-	-	+	-	-	-	-	+
KW11Dii (1a)	-	+	+	+	-	+	-	-	-	-	-	+
KW11Dii (1b)	-	+	-	-	-	+	+	-	-	-	-	+
KW12E	-	+	-	-	-	+	+	-	-	-	-	-
KW13Ciii	-	+	+	-	-	+	+	-	-	-	-	+
KW14Di (1)	-	+	+	+	-	-	+	-	-	+	-	+
KW14Di (2)	+	-	+	+	-	+	+	+	+	-	-	+
KW15E	+	-	+	+	-	-	+	+	+	-	-	+
KW16Ci (1)	+	-	+	+	-	-	+	+	+	-	-	+
KW16Ci (2)	-	-	+	+	-	-	+	-	-	+	-	-
KW17Diii	+	+	+	-	-	-	+	-	-	-	-	+
KW18Di (1)	+	+	+	-	+	-	+	-	-	-	-	+
KW18Di (2)	+	+	+	+	+	+	+	-	-	+	-	+
KW19Cii (1)	-	+	+	-	-	-	+	-	-	-	-	+
KW19Cii (2)	-	+	+	-	-	-	+	-	-	-	-	+
KW20Ciii (1)	+	-	+	+	-	-	+	+	+	-	-	+
KW20Ciii (2)	-	+	+	-	-	-	+	-	-	-	-	+
KW21E	-	+	+	-	-	-	+	-	-	-	-	-
KL01Cii (1)	-	+	+	+	-	-	+	+	+	-	-	+
KL01Cii (2)	-	+	+	-	-	-	+	+	+	-	-	+
KL01Cii (3)	-	+	+	-	-	+	+	-	-	-	-	+
KL01Cii (4)	+	+	+	-	-	-	-	-	-	-	-	-
KL02Diii (1)	-	+	+	-	-	-	+	-	-	-	-	+
KL02Diii (2)	-	+	-	-	-	+	+	+	+	-	-	-

KL02Diii (3)	+	+	+	-	-	-	-	-	-	-	-	-
KL03Ai (1a)	-	+	+	-	-	+	+	-	-	-	-	+
KL03Ai (1b)	-	+	+	-	-	+	+	-	-	-	-	+
KL03Ai (1c)	-	+	+	-	-	+	+	-	-	-	-	+
KL03Ai (2)	-	+	+	-	-	+	+	-	-	-	-	+
KL04Cii (1)	+	+	+	+	-	+	+	-	-	+	-	+
KL04Cii (2a)	-	+	+	-	-	-	+	-	-	-	-	-
KL04Cii (3)	-	+	+	-	-	+	+	-	-	-	-	-
KL04Cii (4)	-	+	-	-	-	+	+	+	+	-	-	+
KL05Dii (1)	+	-	+	+	-	-	+	+	+	-	-	+
KL05Dii (2)	-	+	+	-	-	+	+	-	-	-	-	+
KL05Dii (3)	-	+	+	-	-	-	+	-	-	-	-	+
KL06Ciii (1a)	-	+	+	-	-	-	+	-	-	-	-	-
KL06Ciii (1b)	-	+	+	-	-	+	+	-	-	-	-	+
KL06Ciii (2a)	-	+	+	-	-	+	+	-	-	-	-	+
KL06Ciii (2b)	+	-	+	-	-	+	+	-	-	-	-	+
KL06Ciii (3a)	-	+	+	+	-	-	+	-	-	-	-	+
KL06Ciii (3b)	-	-	+	-	-	+	+	-	-	-	-	-
KL07Di (1)	-	+	+	-	-	-	+	-	-	-	-	+
KL07Di (2)	-	+	-	-	-	+	+	-	-	-	-	-
KL07Di (3)	-	+	+	-	-	+	+	+	+	-	-	-
KL07Di (4)	-	-	+	+	-	-	+	-	-	-	-	-
KL08Diii (1)	-	+	+	+	-	-	+	+	+	-	-	+
KL08Diii (2)	-	+	+	+	-	-	+	+	+	-	-	+
KL08Diii (3a)	+	+	+	-	-	-	-	-	-	-	-	-
KL08Diii (3b)	-	+	-	-	-	+	+	+	+	-	-	+
KL09Dii (1)	-	+	+	-	-	-	+	+	+	-	-	-
KL09Dii (2)	-	+	+	-	-	+	+	+	+	-	-	+
KL09Dii (3)	-	-	+	+	-	-	+	+	+	-	-	-
KL10Ciii (1)	-	+	+	+	-	-	+	-	-	-	-	+
KL10Ciii (2)	-	+	+	-	-	-	-	-	-	-	-	-
KL10Ciii (3)	+	-	+	+	-	-	+	+	+	-	-	+

KL11Dii (1)	-	-	+	+	-	-	+	-	-	-	-	-
KL11Dii (2)	-	+	+	-	-	+	+	-	-	-	-	-
KL11Dii (3)	-	+	+	-	-	-	+	-	-	-	-	+
KL11Dii (4)	+	-	-	-	-	-	+	-	-	-	-	+
KL12Biii (1)	+	+	+	-	-	-	-	-	-	-	-	-
KL12Biii (2)	-	+	+	+	-	-	+	-	-	-	-	-
KL13E	-	+	+	+	-	-	+	-	-	-	-	+
KL14Ci (1)	-	+	+	-	-	+	+	-	-	-	-	+
KL14Ci (2)	-	+	+	+	-	-	+	-	-	-	-	+
KL14Ci (3)	+	+	+	+	-	+	+	-	-	+	-	-
KL14Ci (4)	-	+	+	+	-	-	+	-	-	-	-	+
KL15Diii (1)	+	+	+	-	-	-	-	-	-	-	-	+
KL15Diii (2)	-	+	+	-	-	+	+	-	-	-	-	+
KL15Diii (3a)	-	+	+	-	-	+	+	+	+	-	-	+
KL15Diii (3b)	-	+	+	-	-	+	+	-	-	-	-	+
KL15Diii (4a)	-	+	+	-	-	+	-	-	-	-	-	-
KL15Diii (4b)	-	+	+	-	-	+	-	-	-	-	-	-
KL16E (1)	+	+	+	-	-	-	-	-	-	-	-	-
KL16E (2)	+	+	+	-	-	-	-	-	-	-	-	-
KL16E (3)	+	-	-	+	-	-	+	+	+	-	-	-
KL17Di (1)	-	-	+	+	-	-	+	-	-	-	-	-
KL17Di (2)	-	+	+	+	-	-	+	-	-	-	-	+
KL17Di (3)	-	+	+	-	-	+	+	-	-	-	-	-
KL17Di (4)	+	-	-	-	-	-	+	-	-	-	-	-
KL18Dii (1)	+	+	+	-	-	-	+	-	-	-	-	+
KL18Dii (2)	+	+	+	+	-	+	+	-	-	-	-	+
KL18Dii (3)	-	+	+	-	-	-	+	-	-	-	-	-
KL19E	-	+	+	-	-	+	+	-	-	-	-	+
KL20Dii (1)	+	-	-	+	-	-	+	+	+	-	-	+
KL20Dii (2)	+	-	+	+	-	-	+	+	+	-	-	-
KL20Dii (3)	+	+	+	+	-	-	+	+	+	-	-	+
KL21Ciii (1)	-	+	+	+	-	-	+	+	+	-	-	+

KL21Ciii (2)	-	+	+	-	-	-	+	+	+	-	-	-
KL21Ciii (3)	-	+	+	+	-	-	+	+	+	-	-	+
LA01Cii	-	-	+	-	-	+	+	-	-	-	-	-
LA02Di (1)	+	-	-	+	-	+	+	-	-	+	-	-
LA02Di (2)	+	+	+	-	-	+	+	-	-	-	-	+
LA03Dii (1)	+	+	+	-	+	+	+	-	-	-	-	-
LA03Dii (2)	+	+	+	+	-	-	+	-	-	-	-	+
LA04Ai (1)	+	-	+	+	-	-	+	+	+	-	-	+
LA04Ai (2)	+	+	-	-	-	-	+	-	-	-	-	+
LA05Ci	-	+	+	-	-	+	+	-	-	-	-	+
LA06Diii (1)	-	+	+	-	-	+	+	-	-	-	-	+
LA06Diii (2)	-	+	+	-	-	+	+	-	-	-	-	+
LA07E	+	+	+	-	+	+	+	-	-	-	-	+
LA08Biii (1)	-	+	+	+	-	-	+	-	-	-	-	+
LA08Biii (2)	+	+	+	-	+	+	+	-	-	-	-	-
LA09Ciii (1)	+	+	+	-	+	+	+	-	-	-	-	-
LA09Ciii (2)	+	+	+	-	-	+	+	-	-	-	-	-
LA10Ai (1)	+	-	+	+	-	-	+	+	+	-	-	+
LA10Ai (2)	+	+	+	-	+	+	+	-	-	-	-	-
LA11Biii:	-	+	-	-	-	+	+	-	-	-	-	-
LA12Ci	-	+	+	-	-	+	-	-	-	-	-	-
LA13Bii (1a)	+	+	+	-	+	+	+	-	-	-	-	-
LA13Bii (1b)	-	-	+	+	-	-	+	-	-	+	-	-
LA13Bii (2)	-	+	+	-	-	+	+	-	-	-	-	+
LA13Bii (3)	+	+	+	+	-	-	+	-	-	-	-	+
LA13Bii (4)	-	+	+	-	-	+	+	-	-	-	-	+
LA14Ci (1)	-	+	+	+	+	-	+	+	+	-	-	-
LA14Ci (2)	+	+	+	-	-	-	-	-	-	-	-	+
LA14Ci (3)	+	+	+	-	-	-	-	-	-	-	-	-
LA14Ci (4)	+	+	+	-	-	-	-	-	-	-	-	-
LA14Ci (5)	-	+	+	-	-	-	+	-	-	-	-	+
LA15Ai (1)	-	-	+	+	-	-	+	+	+	-	-	-

LA15Ai (2)	-	-	-	-	-	+	+	-	-	-	-	-
LA15Ai (3)	-	-	-	-	-	+	+	-	-	-	-	-
LA15Ai (4)	-	-	-	-	-	+	+	-	-	-	-	-
LA16Bi (1a)	+	+	+	-	-	+	+	-	-	-	-	+
LA16Bi (1b)	+	+	+	-	-	+	+	-	-	-	-	+
LA16Bi (2a)	-	+	+	-	-	-	+	-	-	-	-	-
LA16Bi (2b)	-	+	+	-	-	-	+	-	-	-	-	+
LA17Dii	-	+	+	-	-	+	-	-	-	-	-	-
LA18Dii	+	+	+	-	+	+	+	-	-	-	-	-
LA19Cii (1)	-	-	+	-	-	-	-	-	-	+	-	+
LA19Cii (2)	+	+	+	+	-	+	+	-	-	+	-	+
LA19Cii (3a)	-	+	+	+	-	-	+	-	-	-	-	+
LA19Cii (3b)	-	+	+	-	-	+	+	-	-	-	-	+
LA19Cii (4)	+	-	+	+	-	-	+	+	+	-	-	+
LA20E	+	-	-	+	-	-	+	+	+	-	-	-
LA21E	+	+	+	-	-	-	-	-	-	-	-	-
Bacillus cereus	-	+	+	+	-	+	+	+	+	-	-	+
Burkholderia anthina	-	-	+	+	+	-	-	-	-	-	-	+
Burkholderia cepacia	+	+	+	+	+	-	-	-	-	-	-	+
Chryseobacterium shigense	-	+	+	-	+	+	-	-	-	-	-	-
Erwinia tracheiphila	+	-	+	+	-	-	+	+	-	-	-	-
Enterobacter hormaechei	-	+	+	+	-	+	+	+	+	-	-	-
Leifsonia sp	+	-	+	+	-	-	+	+	-	-	-	-
Ralstonia solanacearum	+	+	+	+	-	-	-	-	-	-	+	+
Pantoea dispersa	-	+	+	+	-	-	+	-	-	-	-	-

Staphylococcus aureus	+	+	+	-	-	+	+	+	+	-	-	-
Streptomyces fradiae	-	+	+	-	-	+	+	+	+	+	-	+

Appendix VIII: Bacterial OTU Table Showing Relative Abundance

https://bsppjournals.onlinelibrary.wiley.com/action/downloadSupplement?doi=10.1111%2Fppa.13856&file=ppa13856-sup-0006-TableS1.docx

Appendix IX: Taxonomic representation of Bacterial OTUs

https://bsppjournals.onlinelibrary.wiley.com/action/downloadSupplement?doi=10.1111%2Fppa.13856&file=ppa13856-sup-0007-TableS2.docx

Appendix X: Fungal OTU Table Showing Relative Abundance

	Kwale					Kilifi					Lamu				
#OTU ID	**1A**	**1B**	**1C**	**1D**	**1E**	**2A**	**2B**	**2C**	**2D**	**2E**	**3A**	**3B**	**3C**	**3D**	**3E**
OTU_1	1	10	0	21	1	258	24	36	13	5	0	0	0	0	1
OTU_2	0	0	1	7	0	123	82	1	1	0	0	0	0	0	0
OTU_3	1	2	9	6	0	157	9	12	0	1	18	2	1	0	1
OTU_4	0	0	12	34	0	88	0	0	7	0	0	0	0	0	0
OTU_5	0	0	0	0	0	96	4	1	12	4	0	0	0	0	0
OTU_6	5	4	10	34	4	13	18	2	0	0	0	0	0	0	0
OTU_7	0	0	0	0	0	53	0	0	6	0	0	0	0	0	0
OTU_8	2	0	0	0	1	9	0	1	0	0	46	1	1	5	0
OTU_9	1	0	3	2	0	17	0	2	34	4	0	0	0	0	0
OTU_10	3	4	0	33	2	4	2	4	0	0	0	0	0	0	0
OTU_11	4	0	0	1	1	12	1	2	0	0	25	1	3	6	0
OTU_12	0	0	0	1	0	28	0	3	0	0	0	0	0	0	0
OTU_13	1	0	0	2	0	5	1	8	0	1	0	0	1	0	1
OTU_14	0	0	0	0	0	7	2	3	3	0	0	0	0	0	0
OTU_15	2	1	0	0	0	13	0	6	0	2	2	0	0	0	0
OTU_16	0	1	0	0	0	12	2	1	0	0	0	0	0	0	0
OTU_17	3	0	0	0	3	4	3	5	0	1	1	3	1	3	0
OTU_18	0	0	0	3	0	18	10	0	0	1	0	0	0	0	0
OTU_19	7	0	0	0	1	24	0	1	0	0	8	0	0	0	0
OTU_20	1	1	1	0	0	10	0	1	0	0	0	0	0	0	0
OTU_21	0	1	6	0	0	0	1	0	0	0	4	0	0	0	0
OTU_22	0	0	0	1	0	2	0	1	8	1	0	0	0	0	0
OTU_23	0	0	0	0	0	8	5	0	0	0	0	0	0	0	0
OTU_24	0	0	0	0	0	19	0	0	0	0	0	0	0	0	0
OTU_25	0	2	1	0	0	0	0	0	0	0	16	0	2	2	2
OTU_26	6	1	2	2	1	5	1	1	0	1	0	0	0	0	0
OTU_27	16	0	0	0	0	0	0	0	0	0	0	0	0	0	0
OTU_28	0	0	1	0	0	2	0	3	11	0	0	0	0	0	0

Appendix XI: Taxonomic representation of Fungal OTUs

OTU ID	Taxonomy
OTU_1	k__fungi;p__ascomycota;c__eurotiomycetes;o__chaetothyriales;f__cyphellophoraceae;g__cyphellophora
OTU_2	k__fungi;p__ascomycota;c__dothideomycetes;o__pleosporales;f__testudinaceae;g__lepidosphaeria
OTU_3	k__fungi;p__ascomycota;c__dothideomycetes;o__mycosphaerellales;f__teratosphaeriaceae;g__devriesia
OTU_4	k__fungi;p__ascomycota;c__sordariomycetes;o__hypocreales;f__bionectriaceae;g__clonostachys
OTU_5	k__fungi;p__ascomycota;c__dothideomycetes;o__pleosporales;f__pleosporaceae;g__bipolaris
OTU_6	k__fungi;p__ascomycota;c__dothideomycetes;o__capnodiales;f__capnodiaceae;g__microxyphium
OTU_7	k__fungi;p__ascomycota;c__dothideomycetes;o__pleosporales;f__shiraiaceae;g__shiraia
OTU_8	k__fungi;p__ascomycota;c__dothideomycetes;o__mycosphaerellales;f__teratosphaeriaceae;g__devriesia
OTU_9	k__fungi;p__ascomycota;c__sordariomycetes;o__hypocreales;f__nectriaceae;g__fusarium
OTU_10	k__fungi;p__ascomycota;c__sordariomycetes;o__hypocreales;f__ophiocordycipitaceae;g__tolypocladium
OTU_11	k__fungi;p__ascomycota;c__dothideomycetes;o__mycosphaerellales;f__teratosphaeriaceae;g__devriesia
OTU_12	k__fungi;p__ascomycota;c__sordariomycetes;o__hypocreales;f__ascomycota;g__acremonium
OTU_13	k__fungi;p__ascomycota;c__eurotiomycetes;o__chaetothyriales;f__cyphellophoraceae;g__cyphellophora
OTU_14	k__fungi;p__ascomycota;c__eurotiomycetes;o__chaetothyriales;f__cyphellophoraceae;g__cyphellophora
OTU_15	k__fungi;p__ascomycota;c__dothideomycetes;o__mycosphaerellales;f__mycosphaerellaceae;g__stenella
OTU_16	k__fungi;p__ascomycota;c__dothideomycetes;o__pleosporales;f__testudinaceae;g__lepidosphaeria
OTU_17	k__fungi;p__basidiomycota;c__tremellomycetes;o__tremellales;f__tremellaceae;g__tremella
OTU_18	k__fungi;p__ascomycota;c__dothideomycetes;o__pleosporales;f__testudinaceae;g__lepidosphaeria
OTU_19	k__fungi;p__ascomycota;c__dothideomycetes;o__mycosphaerellales;f__teratosphaeriaceae;g__devriesia
OTU_20	k__fungi;p__ascomycota;c__dothideomycetes;o__mycosphaerellales;f__teratosphaeriaceae;g__devriesia

OTU_21	k__fungi;p__ascomycota;c__sordariomycetes;o__xylariales;f__amphisphaeriaceae;g__amphisphaeria
OTU_22	k__fungi;p__ascomycota;c__sordariomycetes;o__sordariomycetes;f__thyridiaceae;g__thyridium
OTU_23	k__fungi;p__ascomycota;c__sordariomycetes;o__hypocreales;f__ophiocordycipitaceae;g__polycephalomyces
OTU_24	k__fungi;p__ascomycota;c__sordariomycetes;o__hypocreales;f__ascomycota;g__acremonium
OTU_25	k__fungi;p__ascomycota;c__dothideomycetes;o__mycosphaerellales;f__neodevriesiaceae;g__tripospermum
OTU_26	k__fungi;p__ascomycota;c__dothideomycetes;o__botryosphaeriales;f__botryosphaeriaceae;g__lasiodiplodia
OTU_27	k__fungi;p__ascomycota;c__sordariomycetes;o__hypocreales;f__bionectriaceae;g__clonostachys
OTU_28	k__fungi;p__ascomycota;c__sordariomycetes;o__hypocreales;f__ascomycota;g__acremonium

Appendix XII: Hierarchical Clustergram of Morphological and Biochemical Relationship among the Bacterial and Fungal Isolates

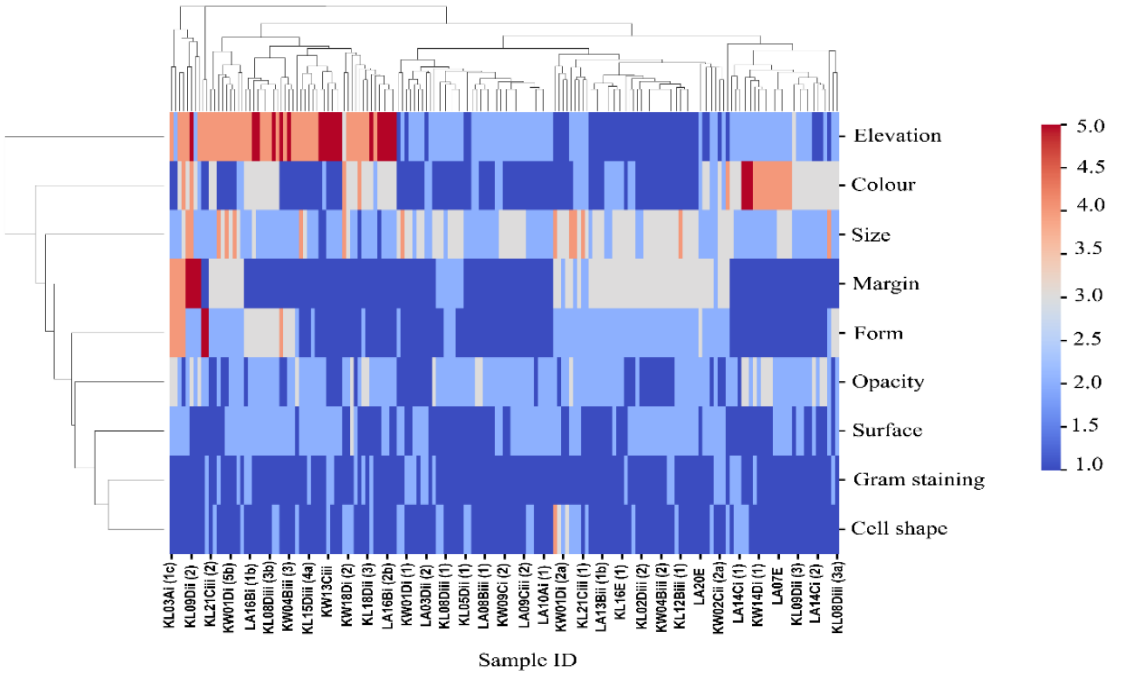

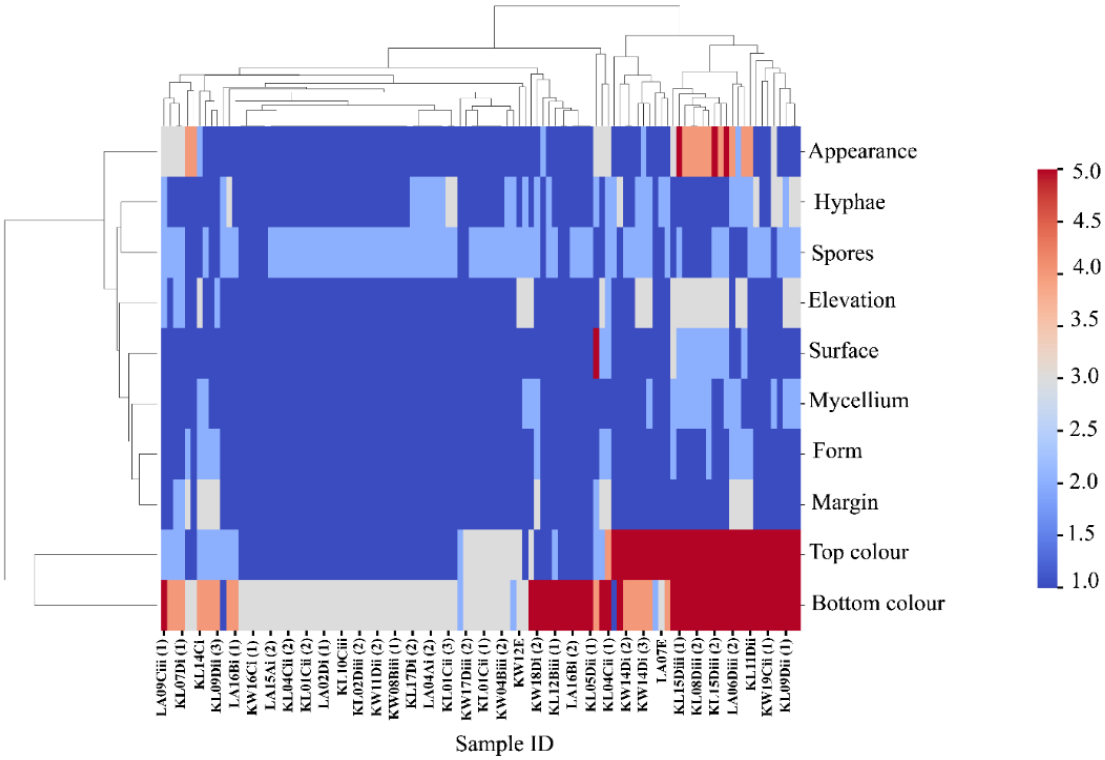

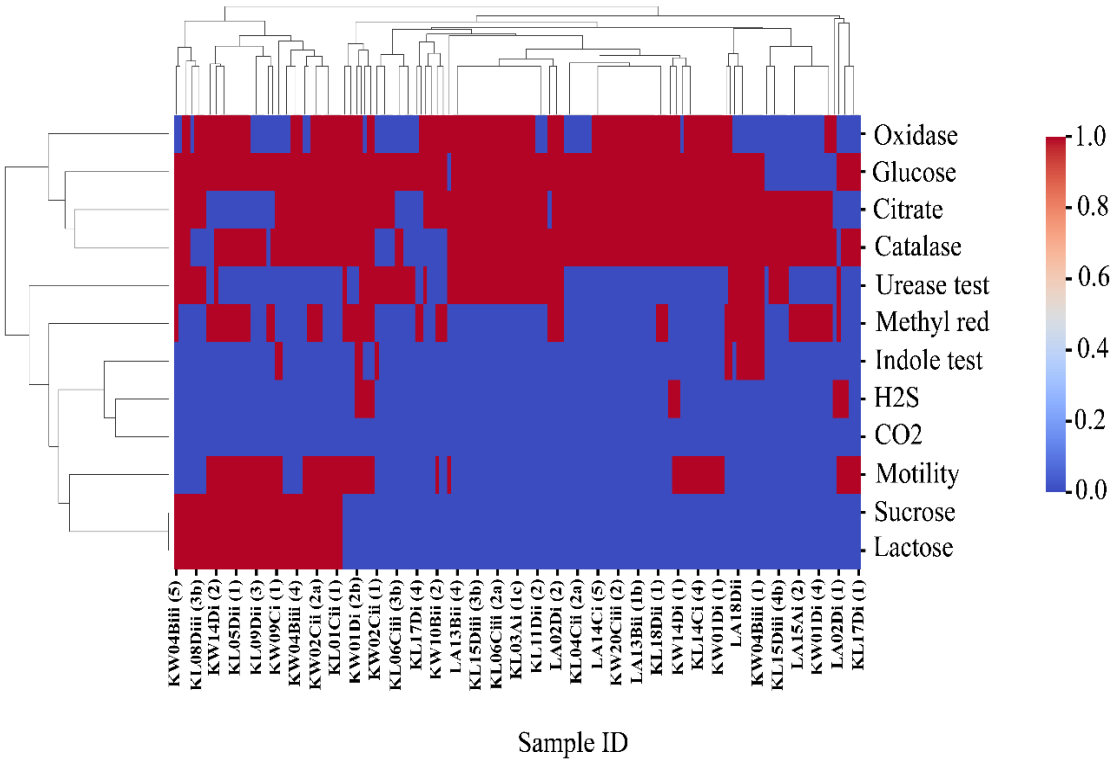
Oxidase
Glucose
Citrate
Catalase
Urease test
Methyl red
Indole test
H2S
CO2
Motility
Sucrose
Lactose
1.0
0.8
0.6
0.4
0.2
0.0
KW04Biii (5)
KL08Diii (3b)
KW14Di (2)
KL05Dii (1)
KL09Dii (3)
KW09Ci (1)
KW04Biii (4)
KW02Cii (2a)
KL01Cii (1)
KW01Di (2b)
KW02Cii (1)
KL06Ciii (3b)
KL17Di (4)
KW10Bii (2)
LA13Bii (4)
KL15Diii (3b)
KL06Cii (2a)
KL03Ai (1c)
KL11Dii (2)
LA02Di (2)
KL04Cii (2a)
LA14Ci (5)
KW20Ciii (2)
LA13Bii (1b)
KL18Dii (1)
KW14Di (1)
KL14Ci (4)
KW01Di (1)
LA18Dii
KW04Biii (1)
KL15Diii (4b)
LA15Ai (2)
KW01Di (4)
LA02Di (1)
KL17Di (1)
Sample ID